

## TABLE OF CONTENTS

<b>Course Catalog</b> .....	<b>3</b>
<b>Textbook</b> .....	<b>3</b>
<b>References</b> .....	<b>3</b>
Books.....	3
<b>Instructor</b> .....	<b>3</b>
<b>Prerequisites</b> .....	<b>3</b>
<b>Background in linear algebra, signal analysis, random processes, digital signal processing and wireless communication systems.</b> .....	<b>3</b>
<b>Topics Covered</b> .....	<b>3</b>
<b>Evaluation</b> .....	<b>4</b>
<b>I. Filter Banks in Digital Communications</b> .....	<b>5</b>
<b>I.1. Signal Processing Role in Communications</b> .....	<b>5</b>
<b>I.2. The Communication Channel</b> .....	<b>5</b>
<b>I.3. Power Allocation and Water Filling</b> .....	<b>7</b>
I.3.A. Project .....	10
<b>I.4. Multi-Rate Signal Processing</b> .....	<b>10</b>
I.4.A. Upsampling.....	10
I.4.B. Interpolation.....	13
I.4.C. Downsampling.....	14
I.4.D. Decimation .....	17
I.4.E. Interleaving.....	18
I.4.F. Deinterleaving.....	18
<b>I.5. The Digital Transmultiplexer</b> .....	<b>19</b>
I.5.A. Transmultiplexer .....	19
I.5.B. Frequency Responses of Transmitting Filters.....	21
<b>I.6. Discrete Multitone Modulation (DMT)</b> .....	<b>21</b>
<b>I.7. Biorthogonality and Perfect DMT Systems</b> .....	<b>22</b>
<b>I.8. Orthonormal DMT Systems and DFT Filter Banks</b> .....	<b>25</b>
<b>I.9. Filter Bank Multicarrier Modulation</b> .....	<b>32</b>
<b>II. Multicarrier Modulation</b> .....	<b>44</b>
<b>II.1. Introduction</b> .....	<b>44</b>

I: Filter Banks in Digital Communications

<b>II.2. Single-Carrier Transmission .....</b>	<b>45</b>
<b>II.3. Nyquist Criterion .....</b>	<b>47</b>
<b>II.4. Wireless Single-Carrier Transmission.....</b>	<b>47</b>
<b>II.5. Multi-Carrier Transmission .....</b>	<b>48</b>
<b>II.6. Orthogonal Frequency Division Multiplexing.....</b>	<b>49</b>
II.6.A. Cyclic Prefix.....	49
<b>II.7. Effect of Multipath Channel on OFDM Symbols .....</b>	<b>52</b>
II.7.A. Cyclic Prefix (CP) .....	54
<b>II.8. OFDMA: Multiple Access Extension of OFDM .....</b>	<b>58</b>
<b>II.9. MC-CDMA .....</b>	<b>59</b>
II.9.A. Signal Structure .....	59
II.9.B. Downlink Signal .....	60
II.9.C. Uplink Signal .....	61
II.9.D. Spreading Techniques .....	62
<b>II.10. MC-DS-CDMA .....</b>	<b>64</b>
II.10.A. Signal Structure .....	64

## SYLLABUS

### Course Catalog

3 Credit hours (3 h lectures). Filter banks in wireless communications. Multicarrier modulation techniques. Multiple-input multiple-output systems. Additional topics.

### Textbook

Several books and journal articles.

### References

#### BOOKS

1. P. P. Vaidyanathan, *Multirate Systems and Filter Banks*, Prentice-Hall, 1993
2. Yong Soo Cho, Jaekwon Kim, Won Young Yang and Chung G. Kang, *MIMO-OFDM Wireless Communications with Matlab*, Wiley, 2010
3. Volker Kühn, *Wireless Communications over MIMO Channels*, John Wiley & Sons, 2006
4. Fa-Long Luo and Charlie (Jianzhong) Zhang (Editors), *Signal Processing for 5G: Algorithms and Implementations*, John Wiley & Sons, 2016
5. A. B. Gershman and N. D. Sidiropoulos (Editors), *Space-Time Processing for MIMO Communications*, John Wiley & Sons, 2005

### Instructor

Instructor: Dr. Mohammad M. Banat

Email Address: [banat@just.edu.jo](mailto:banat@just.edu.jo)

### Prerequisites

Background in linear algebra, signal analysis, random processes, digital signal processing and wireless communication systems.

### Topics Covered

Week	Topics
1-5	Filter Banks in Wireless Communications
6-7	Multicarrier Modulation
8-9	Filter Bank Multicarrier Modulation
10-12	MIMO Systems
13-14	Multiuser Systems
15-16	Adaptive Modulation

I: Filter Banks in Digital Communications

**Evaluation**

<b>Assessment Tool</b>	<b>Expected Due Date</b>	<b>Weight</b>
Mid-Term Exam	8 May 2022	25%
Term Project Report	19 May 2022	15%
Presentations	26 May 2022	10%
Final Exam	According to the university final examination schedule	50%

\*\*\*

## **I. FILTER BANKS IN DIGITAL COMMUNICATIONS**

### ***1.1. Signal Processing Role in Communications***

With more and more users desiring to share communication channels, efficient use of channel bandwidth gains importance. For example, telephone lines which were originally intended to carry low-bandwidth speech signals, are today used to carry several megabits of data per second. On a wireless communication channel in particular, a large number of users need to share the medium to send and receive information-bearing signals. The channel bandwidth may sometimes appear to be insufficient to carry signals at high bit rates. It has been demonstrated in many modern systems and applications that digital signal processing (DSP) techniques can be used to allow channels with limited bandwidths to carry signals at high bit rates.

Communications and DSP are two closely related fields that are the subject of extensive current research interest. DSP provides tools for the modeling, analysis, design and optimization of communication systems. Such tools have allowed the introduction of sophisticated communication systems that meet the most demanding user and operator requirements. Virtually error-free transmission of information, elegant design and compact size, power- and bandwidth-efficient operation, low cost, and so on, are just a few examples of current user and operator demands on communication systems and devices.

The use of DSP tools in communications is too wide-spread to cite comprehensively here. A few indicative system examples include multicarrier modulation (MCM) systems, multiple-input multiple-output (MIMO) systems and code-division multiple access (CDMA) systems. On a more general level, DSP is used in source and channel coding, signal design and modulation, channel modeling, prediction, estimation, tracking and equalization, and in receiver design, optimization and implementation.

Filter banks are DSP subsystems with flexible and versatile structures that allow them to be used in a wide variety of signal processing applications. Filter banks were originally proposed for applications in speech compression. Filter banks have been used for the compression of image, video, and audio signals. More recently filter banks have been used in digital communication systems in many forms including:

- Transmultiplexing
- Precoding
- Channel equalization
- Fractionally spaced equalization
- Discrete multi-tone (DMT) modulation and MCM

### ***1.2. The Communication Channel***

Communication channels introduce linear and nonlinear distortions, random noise components, fading and interference. Reliable transmission of information at high rate under such unfavorable conditions has been possible because of fundamental contributions from many disciplines such as information theory, signal processing, linear system theory, and mathematics.

I: Filter Banks in Digital Communications

The simplest communication channel can be modeled as a linear time invariant system with transfer function  $C(z)$  followed by an additive Gaussian noise (AWGN) source  $e(n)$ . This is illustrated in Figure I.1.

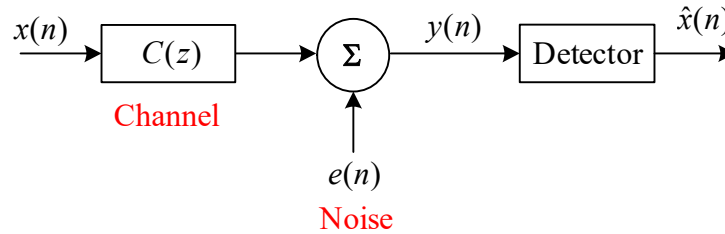


Figure I.1: Communication system

We adopt baseband equivalent signal and system models. This is why in a digital communication system each sample  $x(n)$  is assumed to come from a fixed finite set of generally complex values. Usually, the set of values represent all the possible signal constellation points of the lowpass representation of a modulated signal. For example, in the PAM signal constellation in Figure I.2, the set of possible signal values consists of the eight values  $\{\pm d, \pm 3d, \pm 5d, \pm 7d\}$ .

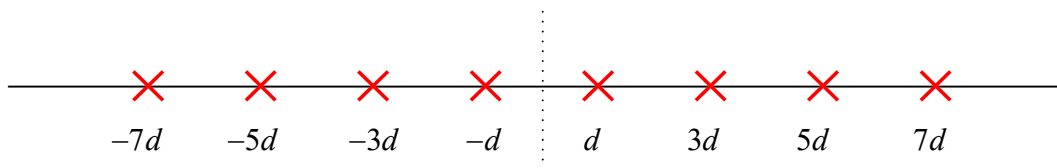


Figure I.2: Antipodal PAM signal constellation

See also Figure I.3 for a 16-point QAM signal constellation with complex possible signal values from the set  $\{\pm d \pm jd, \pm d \pm j3d, \pm 3d \pm jd, \pm 3d \pm j3d\}$ .

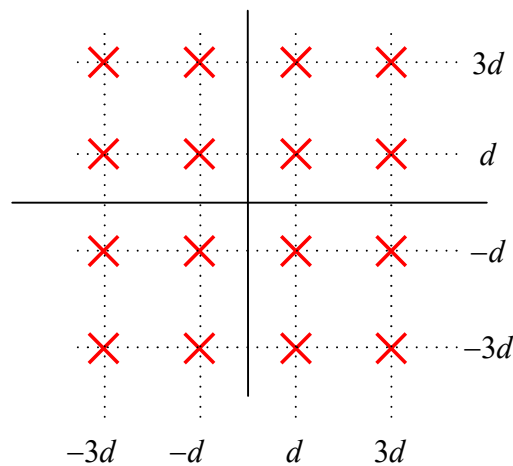


Figure I.3: Square QAM signal constellation

If each symbol  $x(n)$  is a  $b$ -bit number and there are  $f_s$  symbols per second, then the bit rate is  $R = bf_s$  bits per second. The received signal  $y(n)$  is a noisy and distorted version of  $x(n)$ . The

I: Filter Banks in Digital Communications

estimated value  $\hat{x}(n)$  belongs to the same constellation that  $x(n)$  came from. There is a nonzero probability of error  $P_e$  in this detection because of the noise  $e(n)$  and the intersymbol interference caused by the channel  $C(z)$ . The acceptable value of  $P_e$  depends on the application.

A wireless channel is a randomly time varying one, and a single  $C(z)$  cannot be used to represent it successfully. However, a common practice in this regard is to use short-term transfer functions to represent the channel over periods of time where the channel can be considered not to vary considerably.

**I.3. Power Allocation and Water Filling**

The transmitted signal power  $P_x$  is proportional to the mean square value of  $x(n)$ . Assume that  $x(n)$  is a wide sense stationary (WSS) random process with a power spectral density  $S_x(e^{j\omega})$ . The total signal power is given by:

$$P_x = \frac{1}{2\pi} \int_{-\pi}^{\pi} S_x(e^{j\omega}) d\omega \quad (I.1)$$

Note that  $S_x(e^{j\omega})$  is periodic in  $\omega$  with a period of  $2\pi$ . The error probability  $P_e$  depends on the transmitted power  $P_x$ , and on the bit rate  $R$ . For fixed power, the error probability increases with the bit rate  $R$ . For a fixed bit rate  $R$ , the error probability decreases with increasing the power  $P_x$ .

The power spectrum of  $x(n)$  shows how its power is distributed over frequency. By carefully shaping  $S_x(e^{j\omega})$ , we can increase the achievable bit rate (for fixed error probability and transmitted power). To see how this is achieved, note that the error probability is a decreasing function of the signal-to-noise ratio (SNR). The SNR  $\gamma_x$  is generally given by

$$\gamma_x = C_0 \frac{\mathcal{E}_x}{\sigma_q^2} \quad (I.2)$$

where  $\mathcal{E}_x$  is the signal average symbol (or bit) energy,  $\sigma_q^2$  is the noise variance at the receive filter output and  $C_0$  is a proportionality constant. Let the average symbol energy be written in terms of the average power  $P_x$ , the bit duration  $T$  and the bit rate  $R$  as follows:

$$\begin{aligned} \mathcal{E}_x &= P_x T \\ &= \frac{P_x}{R} \end{aligned} \quad (I.3)$$

Substituting (I.3) into (I.2) yields the following expression for the SNR

I: Filter Banks in Digital Communications

$$\gamma_x = C_0 \frac{P_x}{\sigma_q^2 R} \quad (I.4)$$

Note that the SNR is proportional to the power bit rate ratio. In other words, the SNR does not change if both the power and the bit rate are scaled by the same factor. Consequently, the error probability does not change if both the power and the bit rate are scaled by the same factor.

Note that when  $P_e$  is equal to a fixed value  $P_{e0}$ ,  $\gamma_x$  is equal to a fixed value, say  $\gamma_{x0}$ . When this is the case, we have, based on (I.4), the condition

$$\frac{P_x}{R\sigma_q^2} = \frac{\gamma_{x0}}{C_0} \quad (I.5)$$

When, in addition to fixing  $P_e$ , the signal power  $P_x$  is also fixed, it can be easily seen from (I.5) that the symbol rate is inversely proportional to  $\sigma_q^2$ . This means that we can increase the bit rate when  $\sigma_q^2$  is small, while still achieving the same  $P_e$  by the transmitting the same  $P_x$ . Furthermore, note that from the second line in (I.3), the signal power and the bit rate can be increased in the same proportion while keeping  $\mathcal{E}_x$  fixed, and hence, keeping  $P_e$  fixed for the same  $\sigma_q^2$ . Now, consider the following two cases:

- Case 1: Let  $\sigma_q^2 = \sigma_{q0}^2$ , where  $\sigma_{q0}^2$  is some fixed value. For a given  $P_e$ , we should have from (I.5):

$$\frac{P_x}{R} = \gamma_{x0} \sigma_{q0}^2 \quad (I.6)$$

- Case 2: Now let  $\sigma_q^2 = \xi \sigma_{q0}^2$ , where  $\xi$  is a positive constant. If the same  $P_e$  above is to be achieved, we should have

$$\frac{P_x}{R} = \gamma_{x0} \xi \sigma_{q0}^2 \quad (I.7)$$

When  $\xi < 1$ , the power-rate ratio in (I.7) is smaller than that in (I.6), meaning that for the same  $P_x$  the bit rate is larger.

The idea of shaping  $S_x(e^{j\omega})$  is to “pour” more power (and increase the bit rate) in the regions where the channel gain is larger and the noise spectrum is smaller.

If the transfer function of the channel  $C(z)$  is known, then the detector can equalize it by using a filter with a transfer function  $1/C(z)$ . This is illustrated in Figure I.4.

I: Filter Banks in Digital Communications

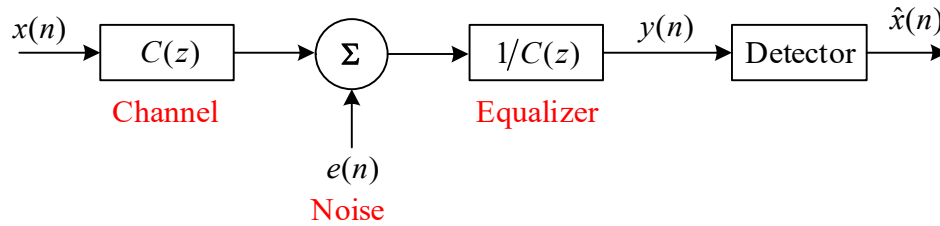


Figure I.4: Communication Channel

This is called the ideal equalizer. It is also known as the zero-forcing equalizer. In practice,  $1/C(z)$  can be approximated with a stable (possibly FIR) filter.

The effective noise  $q(n)$  seen by the receiver, i.e., the noise component of  $y(n)$ , is  $e(n)$  filtered by  $1/C(z)$ . The power spectral density of  $q(n)$  is given by:

$$S_q(e^{j\omega}) = S_e(e^{j\omega}) \frac{1}{|C(e^{j\omega})|^2} \quad (I.8)$$

In frequency regions where  $S_q(e^{j\omega})$  is small, we should allocate more power. The optimal power distribution  $S_x(e^{j\omega})$  is given by:

$$S_x(e^{j\omega}) = \begin{cases} \lambda - S_q(e^{j\omega}), & S_q(e^{j\omega}) \leq \lambda \\ 0, & \text{otherwise} \end{cases} \quad (I.9)$$

where  $\lambda$  is a constant. The choice of  $\lambda$  depends on the total available power  $P$ . Figure I.5 illustrates a typical power allocation process according to (I.9).

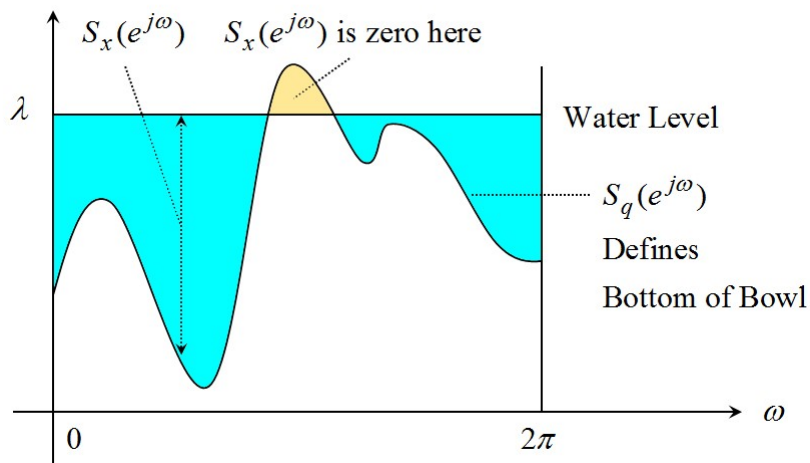


Figure I.5: Optimal water filling strategy

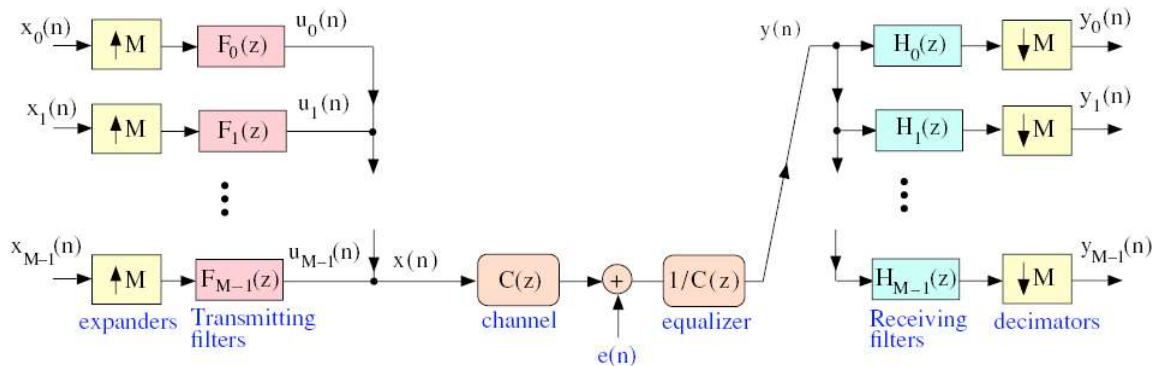
For fixed total power  $P$  and fixed channel, the capacity  $C$  is the maximum rate at which information can be transmitted with arbitrarily small error probability. Note that  $x(n)$  is user

I: Filter Banks in Digital Communications

generated data. A clever way to approximate optimal power allocation would be to divide the channel bandwidth into several subbands and transmit in each subband channel separately. This already suggests a resemblance to frequency division multiplexing, but the main difference now is that the different subband channels carry different parts of a single input stream.

**I.3.A. PROJECT**

Consider a binary sequence  $s(n)$  of equally probable zeros and ones. The sequence is partitioned into 8-bit blocks. Each block is subdivided into three groups of lengths 3, 2, 3 bits respectively. A signal  $x_k(n)$  is generated from the bits representing group  $k$ . Let  $x_0(n)$  be an 8-PSK signal,  $x_1(n)$  be a 4-PAM signal, and  $x_2(n)$  be an 8-QAM signal. Let the signals  $x_0(n)$ ,  $x_1(n)$ ,  $x_2(n)$  be processed by the system below ( $M = 3$ ) in which  $F_0(z)$ ,  $F_1(z)$ ,  $F_2(z)$  have uniform non-overlapping frequency responses that cover the frequency range  $[0, 2\pi]$ . Let  $e(n)$  be AWGN with a flat PSD equal to  $\sigma^2$ . Let the discrete-time channel impulse response over a short period of time be given by:  $c(n) = \delta(n) - 0.5\delta(n-1)$ .



- Use the water filling strategy (approximately) to assign relative powers to  $x_0(n)$ ,  $x_1(n)$ ,  $x_2(n)$ . Assume enough power is available.
- Sketch the three signal space constellations.

**I.4. Multi-Rate Signal Processing**

In a multi-rate system, signals are processed at different sampling rates. Multi-rate signal processing techniques have been in use for many years. The use of multiple sampling rates offers many advantages, such as reduced computational complexity for a given task, reduced transmission rate (in bits per second), and/or reduced storage requirement, depending on the application.

**I.4.A. UPSAMPLING**

The  $M$ -fold upsampler, shown in the block diagram in Figure I.6, merely inserts  $M - 1$  zeros between adjacent samples, as demonstrated in Figure I.7 for  $M = 3$ .

I: Filter Banks in Digital Communications

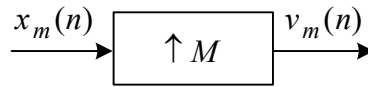


Figure I.6: Upsampler

The input and output signals of the upsampler are shown in Figure I.7.

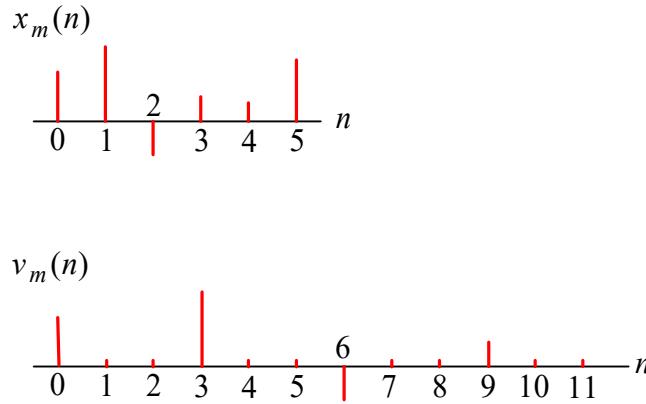


Figure I.7: Upsampling with  $M = 3$

Note that for generating samples of  $v_m(n)$ , two zeros are inserted between each two successive samples of  $x_m(n)$ . The output and input of the upsampler are related by:

$$v_m(n) = \begin{cases} x_m\left(\frac{n}{M}\right), & \frac{n}{M} \in \mathbb{Z} \\ 0, & \text{otherwise} \end{cases} \quad (\text{I.10})$$

$$V_m(z) = X_m(z^M) \quad (\text{I.11})$$

$$V_m(e^{j\omega}) = X_m(e^{j\omega M}) \quad (\text{I.12})$$

Note that upsampling generates  $M$  “squeezed” copies of  $X_m(e^{j\omega})$  in the region  $0 \leq \omega < 2\pi$ . This is illustrated in Figure I.8.

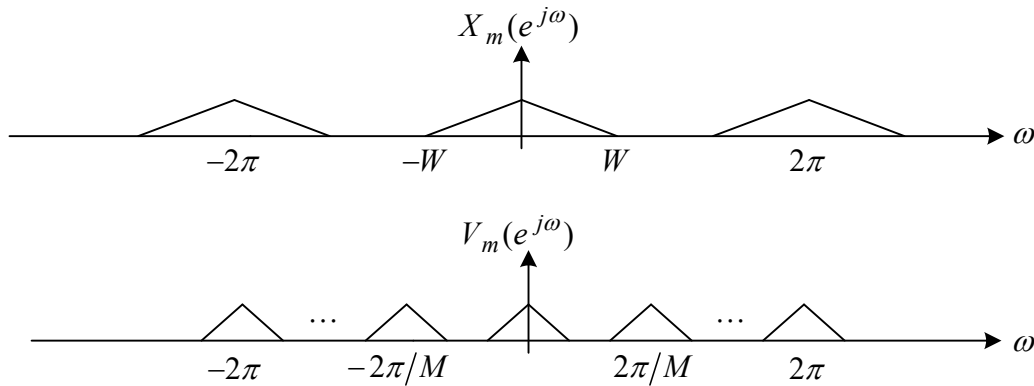


Figure I.8

I: Filter Banks in Digital Communications

When  $x_m(n)$  is a WSS random signal, then the autocorrelation function of the upsampled signal is given by

$$\begin{aligned} \varphi_{v_m}(n, k) &= \mathbb{E} \left[ v_m^*(n) v_m(n+k) \right] \\ &= \begin{cases} \mathbb{E} \left[ x_m^* \left( \frac{n}{M} \right) x_m \left( \frac{n}{M} + \frac{k}{M} \right) \right], & \frac{n}{M}, \frac{k}{M} \in \mathbb{Z} \\ 0, & \text{otherwise} \end{cases} \end{aligned} \quad (\text{I.13})$$

The last result means that  $\varphi_{v_m}(n, k)$  is a periodic function of  $n$  with period  $M$ . This is true because for all values of  $n$  that are separated by multiples of  $M$  while these values of  $n$  are not multiples of  $M$  themselves,  $\varphi_{v_m}(n, k)$  is zero. Additionally, for all values of  $n$  that are separated by multiples of  $M$  while these values of  $n$  are themselves multiples of  $M$ ,  $\varphi_{v_m}(n, k)$  is equal to an upsampled version of  $\varphi_{x_m}(k)$ . Thus,  $v_m(n)$  is a cyclo-stationary random process. Note that setting  $k = 0$  in (I.13) reveals that the variance of  $v_m(n)$  is a periodic function of  $n$  with period  $M$ .

To determine the upsampler output power spectral density, we first have to determine the time-averaged autocorrelation function. To do this we perform averaging over the fundamental period  $0 \leq n \leq M-1$ :

$$\bar{\varphi}_{v_m}(k) = \frac{1}{M} \sum_{n=0}^{M-1} \varphi_{v_m}(n, k) \quad (\text{I.14})$$

Obviously, the summation in (I.14) contains one non-zero term (at  $n = 0$ ). This gives rise to

$$\begin{aligned} \bar{\varphi}_{v_m}(k) &= \frac{1}{M} \varphi_{v_m}(0, k) \\ &= \frac{1}{M} \left[ \varphi_{x_m}(k) \right]^{\uparrow M} \end{aligned} \quad (\text{I.15})$$

Therefore, the average power spectral density of the upsampler output is

$$S_{v_m}(e^{j\omega}) = \frac{1}{M} S_{x_m}(e^{j\omega M}) \quad (\text{I.16})$$

Integrating over  $-\pi \leq \omega < \pi$  yields

$$P_{v_m} = \frac{P_{x_m}}{M} \quad (\text{I.17})$$

and

I: Filter Banks in Digital Communications

$$\begin{aligned}\sigma_{v_m}^2 &= P_{v_m} \\ &= \frac{P_{x_m}}{M} \\ &= \frac{\sigma_{x_m}^2}{M}\end{aligned}\tag{I.18}$$

**I.4.B. INTERPOLATION**

An interpolator is an upsampler (denoted by  $\uparrow M$ ), followed by an interpolation filter  $f_m(n)$  (FIR with length  $L$ ). Let the input be  $x_m(n)$ , the upsampler output be  $v_m(n)$  and the interpolation filter output be  $u_m(n)$ . This process is shown in Figure I.9.

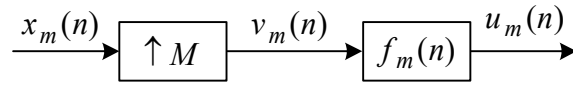


Figure I.9: Interpolation

The interpolator output can be expressed as

$$\begin{aligned}u_m(n) &= \sum_{i=0}^{L-1} f_m(i)v_m(n-i) \\ &= \sum_{\substack{i=0 \\ (n-i)/M \in \mathbb{Z}}}^{L-1} f_m(i)x_m((n-i)/M)\end{aligned}\tag{I.19}$$

$$\begin{aligned}U_m(z) &= V_m(z)F_m(z) \\ &= X_m(z^M)F_m(z)\end{aligned}\tag{I.20}$$

When  $x_m(n)$  is a WSS random process,

$$\begin{aligned}S_{u_m}(e^{j\omega}) &= S_{v_m}(e^{j\omega})|F_m(e^{j\omega})|^2 \\ &= \frac{1}{M}S_{x_m}(e^{j\omega M})|F_m(e^{j\omega})|^2\end{aligned}\tag{I.21}$$

Taking the inverse DTFT of both sides of (I.21), the autocorrelation function of  $u_m(n)$  is given by

$$\begin{aligned}\bar{\varphi}_{u_m}(k) &= \bar{\varphi}_{v_m}(k) * f_m(k) * f_m^*(-k) \\ &= \frac{1}{M}[\bar{\varphi}_{x_m}(k)]^{\uparrow M} * f_m(k) * f_m^*(-k) \\ &= \gamma_{x_m}(k) * \phi_{f_m}(k)\end{aligned}\tag{I.22}$$

where

I: Filter Banks in Digital Communications

$$\gamma_{x_m}(k) = \frac{1}{M} \left[ \varphi_{x_m}(k) \right]^{\uparrow M} \quad (I.23)$$

and

$$\phi_{f_m}(k) = f_m(k) * f_m^*(-k) \quad (I.24)$$

The time correlation function  $\phi_{f_m}(k)$  of  $f_m(k)$  is equal to

$$\phi_{f_m}(k) = \sum_{l=0}^{L-1} f_m(l) f_m^*(l+k) \quad (I.25)$$

This is a finite-duration sequence that is non-zero only when  $-(L-1) \leq k \leq L-1$ . Hence, (I.22) becomes

$$\bar{\varphi}_{u_m}(k) = \sum_{i=-(L-1)}^{L-1} \phi_{f_m}(i) \gamma_{x_m}(k-i) \quad (I.26)$$

The average power in  $u_m(n)$  is equal to

$$\begin{aligned} P_{u_m} &= \bar{\varphi}_{u_m}(0) \\ &= \sum_{i=-(L-1)}^{L-1} \phi_{f_m}(i) \gamma_{x_m}(-i) \end{aligned} \quad (I.27)$$

Since  $\gamma_{x_m}(k)$  is an upsampled autocorrelation function, the non-zero terms in the summation in (I.27) are those for which  $i$  is an integer multiple of  $M$ . For the special case when  $L = M$ , the only such term is  $i = 0$ , and hence,

$$\begin{aligned} P_{u_m} &= \phi_{f_m}(0) \gamma_{x_m}(0) \\ &= \frac{1}{M} \phi_{f_m}(0) \varphi_{x_m}(0) \\ &= \frac{P_{x_m}}{M} \end{aligned} \quad (I.28)$$

**I.4.C. DOWNSAMPLING**

The  $M$ -fold downsampler is shown in the block diagram in Figure I.10. Only a subset of input samples are retained.

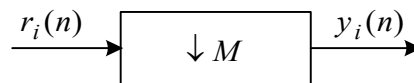


Figure I.10: Downsampling

The downsampling operation is illustrated in Figure I.11 for the  $M = 3$  case.

I: Filter Banks in Digital Communications

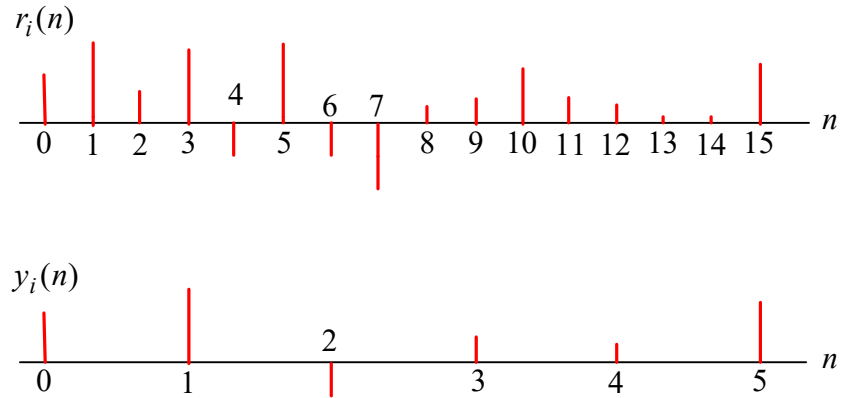


Figure I.11: Downsampling with  $M = 3$

Note that the samples automatically get renumbered so that  $y_i(1) = r_i(3)$ ,  $y_i(2) = r_i(6)$  and so forth.

The output and input of the downsampler are related by:

$$y_i(n) = r_i(Mn) \quad (I.29)$$

**Exercise I.1**

Show that

$$Y_i(z) = \frac{1}{M} \sum_{m=0}^{M-1} R_i(z^{1/M} e^{-j2\pi m/M}) \quad (I.30)$$

$$Y_i(e^{j\omega}) = \frac{1}{M} \sum_{m=0}^{M-1} R_i\left(e^{j\frac{\omega}{M}} W_M^{-m}\right) \quad (I.31)$$

where

$$W_M = e^{j\frac{2\pi}{M}} \quad (I.32)$$

Therefore,

$$Y_i(e^{j\omega}) = \frac{1}{M} \sum_{m=0}^{M-1} R_i\left(e^{j\frac{\omega-2\pi m}{M}}\right) \quad (I.33)$$

Note that in the frequency domain, the output spectrum consists of  $M$  shifted replicas of the input spectrum expanded by the factor  $M$ . Note also that stretching  $R_k(e^{j\omega})$  by a factor of  $M$  can cause aliasing.

I: Filter Banks in Digital Communications

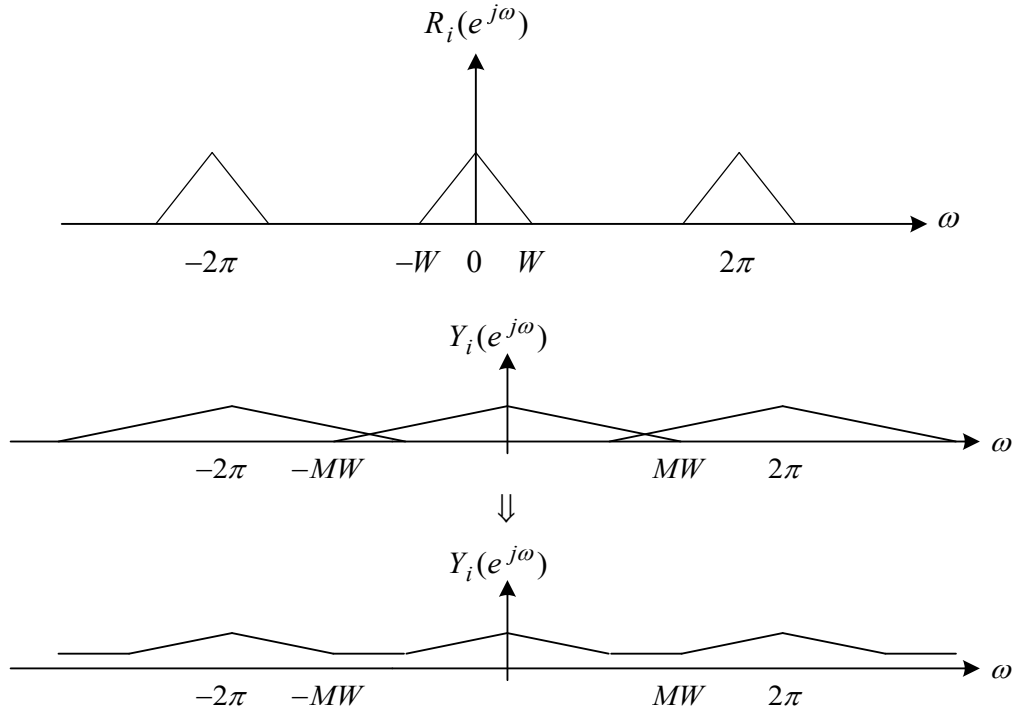


Figure I.12

Exercise I.2

Determine the conditions on  $R_k(e^{j\omega})$  to avoid aliasing due to downsampling.

When  $r_i(n)$  is a WSS random signal, then the autocorrelation function of the downsampled signal is given by

$$\begin{aligned}
 \varphi_{y_i}(k) &= E \left[ y_i^*(n) y_i(n+k) \right] \\
 &= E \left[ r_i^*(Mn) r_i(Mn + Mk) \right] \\
 &= \varphi_{r_i}(Mk)
 \end{aligned}
 \tag{I.34}$$

Therefore, the output power spectral density is related to the input output spectral by

$$S_{y_i}(e^{j\omega}) = \frac{1}{M} \sum_{m=0}^{M-1} S_{r_i} \left( e^{j\frac{\omega}{M}} W_M^{-m} \right)
 \tag{I.35}$$

Substituting for  $W_M$  from (I.32) yields

$$S_{y_i}(e^{j\omega}) = \frac{1}{M} \sum_{m=0}^{M-1} S_{r_i} \left( e^{j\frac{\omega - 2\pi m}{M}} \right)
 \tag{I.36}$$

I: Filter Banks in Digital Communications

Given that  $r_i(n)$  is bandlimited such that downsampling does not result in aliasing, the output power is equal to

$$P_{y_i} = \frac{1}{M} \sum_{m=0}^{M-1} \frac{1}{2\pi} \int_{-\pi}^{\pi} S_{r_i} \left( e^{j\frac{\omega}{M}} W_M^{-m} \right) d\omega \quad (\text{I.37})$$

The  $M$  power spectrum terms inside the summation in (I.37) are non-overlapping, and when integrated over  $-\pi \leq \omega < \pi$ , each one of them integrates to  $P_{r_i}$ . Therefore,

$$P_{y_i} = P_{r_i} \quad (\text{I.38})$$

Given that  $r_i(n)$ , and consequently  $y_i(n)$ , is zero-mean, then

$$\begin{aligned} \sigma_{y_i}^2 &= P_{y_i} \\ &= P_{r_i} \\ &= \sigma_{r_i}^2 \end{aligned} \quad (\text{I.39})$$

**I.4.D. DECIMATION**

A decimator is an anti-aliasing filter  $h_i(n)$  (FIR with length  $L$ ), followed by a downsampler (denoted by  $\downarrow M$ ). This process is shown in Figure I.13.

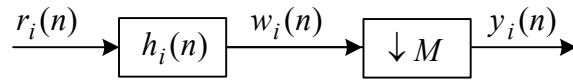


Figure I.13: Decimation

Letting the input be  $r_i(n)$ , the anti-aliasing filter output be  $w_i(n)$ , and the downsampler output be  $y_i(n)$ , then

$$\begin{aligned} w_i(n) &= r_i(n) * h_i(n) \\ &= \sum_{l=0}^{L-1} h_i(l) r_i(n-l) \end{aligned} \quad (\text{I.40})$$

$$\begin{aligned} y_i(n) &= w_i(Mn) \\ &= \sum_{l=0}^{L-1} h_i(l) r_i(Mn-l) \end{aligned} \quad (\text{I.41})$$

In the frequency domain,

$$W_i(z) = R_i(z) H_i(z) \quad (\text{I.42})$$

I: Filter Banks in Digital Communications

$$\begin{aligned}
 Y_i(z) &= \frac{1}{M} \sum_{m=0}^{M-1} W_i(z^{1/M} e^{-j2\pi m/M}) \\
 &= \frac{1}{M} \sum_{m=0}^{M-1} R_i(z^{1/M} e^{-j2\pi m/M}) H_i(z^{1/M} e^{-j2\pi m/M})
 \end{aligned}
 \tag{I.43}$$

When  $r_i(n)$  is a WSS random sequence,

$$S_{w_i}(e^{j\omega}) = S_{r_i}(e^{j\omega}) |H_i(e^{j\omega})|^2
 \tag{I.44}$$

and

$$S_{y_i}(e^{j\omega}) = \frac{1}{M} \sum_{m=0}^{M-1} S_{w_i} \left( e^{j\frac{\omega}{M}} W_M^{-m} \right)
 \tag{I.45}$$

**I.4.E. INTERLEAVING**

A set of signals  $\{x_m(n)\}_{m=0}^{M-1}$  can be interleaved into a higher symbol rate signal  $x(n)$  using a set of upsamplers and delay elements, as illustrated in Figure I.14.

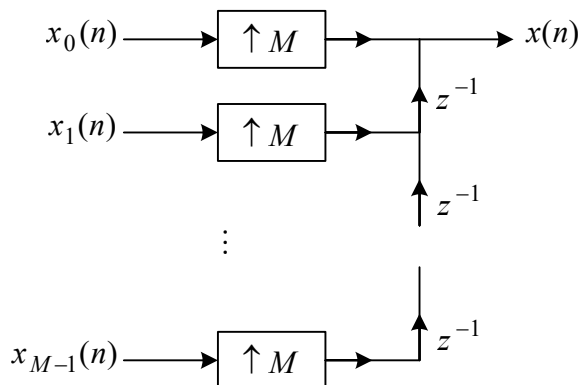


Figure I.14: Interleaving

**I.4.F. DEINTERLEAVING**

- A signal  $y(n)$  can be deinterleaved into a set of lower symbol rate signals  $\{y_m(n)\}_{m=0}^{M-1}$  using a set of downsamplers and negative delay elements, as illustrated in Figure I.15. We can regard  $y(n)$  as a time-domain multiplexed (TDM) version of the individual signals  $\{y_m(n)\}_{m=0}^{M-1}$ . This can be seen in the example in Figure I.16 for  $M = 3$ .
- $\{y_m(n)\}_{m=0}^{M-1}$  are called the polyphase components of  $y(n)$  with respect to  $M$ .

I: Filter Banks in Digital Communications

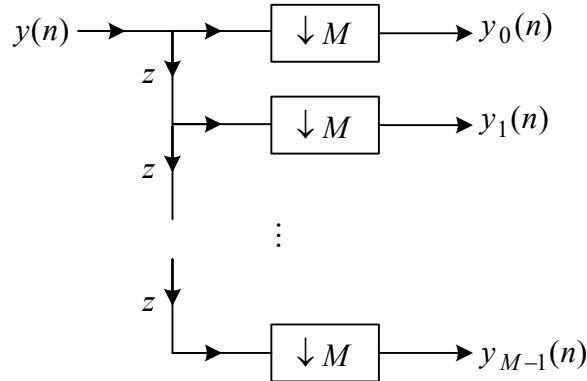


Figure I.15: Deinterleaving

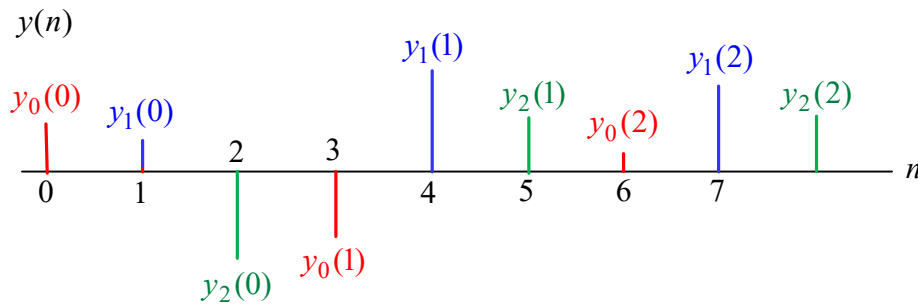


Figure I.16

**I.5. The Digital Transmultiplexer**

**I.5.A. TRANSMULTIPLEXER**

The digital transmultiplexer has been initially developed for purposes of conversion between TDM and frequency division multiplexing (FDM). However, the versatility of the transmultiplexer structure, and the many possibilities to introduce modifications into this structure, have allowed it to be used in a large number of applications. As will be seen later, multicarrier modulation (MCM) is, arguably, the most important application of transmultiplexers in digital communications.

Let's generalize the delay elements in the interleaver in Figure I.14 into a set of filters  $\{F_m(z)\}_{m=0}^{M-1}$  with corresponding impulse responses  $\{f_m\}_{m=0}^{M-1}$ . Similarly, let's generalize the advance elements in the deinterleaver in Figure I.15 into a set of filters  $\{H_l(z)\}_{l=0}^{M-1}$  with corresponding impulse responses  $\{h_l\}_{l=0}^{M-1}$ . This is illustrated in Figure I.17.

I: Filter Banks in Digital Communications

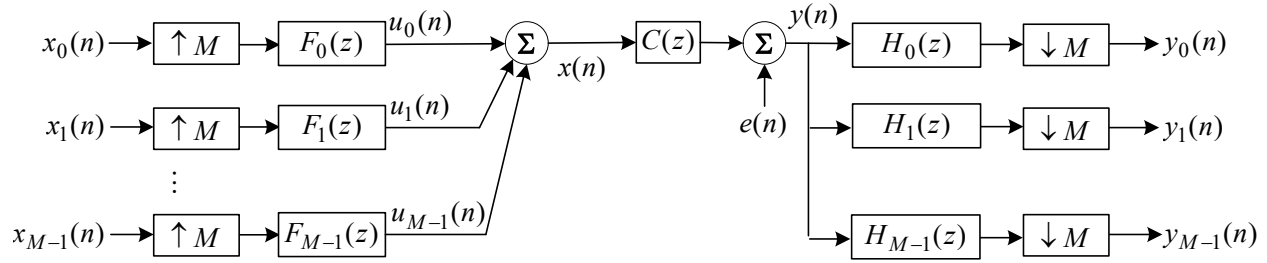


Figure I.17: Digital Transmultiplexer

The  $m$ -th transmitting filter has the output

$$u_m(n) = \sum_{\substack{i=0 \\ (n-i)/M \in \mathbb{Z}}}^{L-1} f_m(i)x_m((n-i)/M) \quad (I.46)$$

Alternatively,

$$u_m(n) = \sum_{i=-\infty}^{\infty} x_m(i)f_m(n-iM) \quad (I.47)$$

Note that

$$U_m(z) = X_m(z^M)F_m(z) \quad (I.48)$$

Equation (I.47) can be illustrated for  $F_0(z)$  as follows:

$$u_m(n) = \dots + x_m(-1)f_m(n+M) + x_m(0)f_m(n) + x_m(1)f_m(n-M) + \dots \quad (I.49)$$

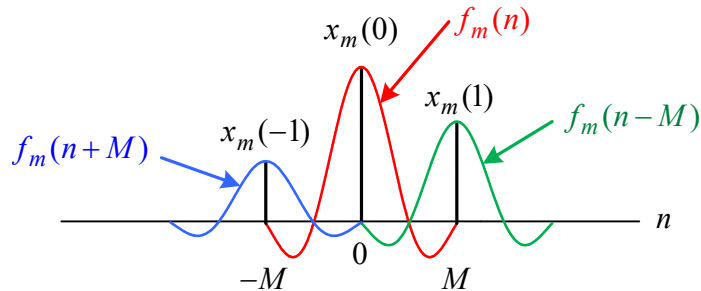


Figure I.18

$u_m(n)$  is an interpolated version of  $x_m(n)$  and has  $M$  times higher rate.

### I.5.B. FREQUENCY RESPONSES OF TRANSMITTING FILTERS

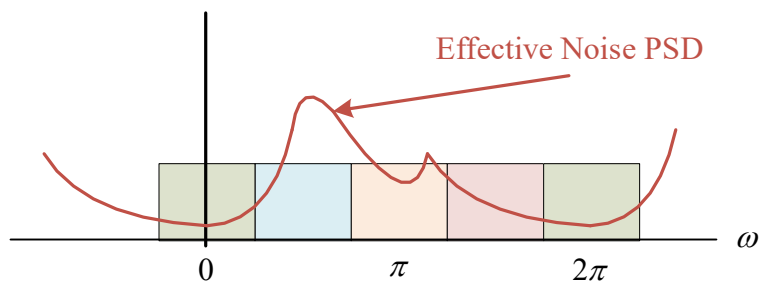


Figure I.19

Filters  $\{F_m(z)\}_{m=1}^{M-1}$  are generally bandpass, and therefore, their outputs are bandpass. Outputs of the filters  $\{F_m(z)\}_{m=0}^{M-1}$  are modulated versions of the sequences  $\{x_m(n)\}_{m=0}^{M-1}$  because they are shifted in frequency to the passbands of  $\{F_m(z)\}_{m=0}^{M-1}$ . Note that  $\{u_m(n)\}_{m=0}^{M-1}$  are combined into

$$x(n) = \sum_{m=0}^{M-1} u_m(n) \quad (I.50)$$

Note that  $x(n)$  can be seen as an FDM version of  $\{x_m(n)\}_{m=0}^{M-1}$ . This can be compared to the interleaving case in Figure I.14, where  $\{F_m(z)\}_{m=0}^{M-1}$  are mere delay elements  $\{z^{-m}\}_{m=0}^{M-1}$ , and  $x(n)$  is a TDM version of  $\{x_m(n)\}_{m=0}^{M-1}$ .

Letting  $T_s$  denote the sample spacing of  $x(n)$ , the sample spacing of  $x_m(n)$  for any  $m=0,1,\dots,M-1$  is equal to  $T = MT_s$ . This means that the sample rates of individual member sequence of  $\{x_m(n)\}_{m=0}^{M-1}$  are  $M$  times lower than that of  $x(n)$ . The filters  $\{H_m(z)\}_{m=0}^{M-1}$  separate the received signal  $y(n)$  into the set of signals  $\{y_m(n)\}_{m=0}^{M-1}$ , which are distorted and noisy versions of  $\{x_m(n)\}_{m=0}^{M-1}$ . The mismatching between corresponding values of  $\{y_m(n)\}_{m=0}^{M-1}$  and  $\{x_m(n)\}_{m=0}^{M-1}$  is a measure of the system error probability. The task at this point is to detect the symbols  $\{x_m(n)\}$  from  $\{y_m(n)\}$  with acceptable error probability. Needless to say, the error probability has to be minimized.

### I.6. Discrete Multitone Modulation (DMT)

Consider Figure I.20 below, which shows the first stage of DMT called the parsing stage. Here  $s(l)$  represents binary data to be transmitted over a channel. This data is split into nonoverlapping  $b$ -bit blocks. The  $b$  bits in each block are partitioned into  $M$  groups, the  $m$ -th group being a collection of  $b_m$  bits. Note that

I: Filter Banks in Digital Communications

$$b = \sum_{m=0}^{M-1} b_m \tag{I.51}$$

The  $b_m$  bits in the  $m$ -th group constitute the  $m$ -th symbol  $x_m$  (usually belonging to a digital modulation constellation like PAM or QAM), which can therefore be regarded as a  $b_m$ -bit number. For the  $n$ -th data block ( $n$ -th time instant), this symbol is denoted as  $x_m(n)$ . This is the modulation symbol for the  $m$ -th frequency band. The collection of symbols  $\{x_m(n)\}$  is together referred to as the DMT symbol. The sample  $x_m(n)$  is typically a PAM or a QAM symbol.

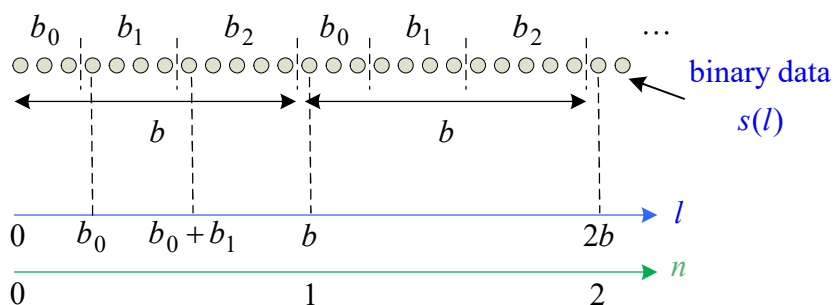


Figure I.20: DMT parsing stage

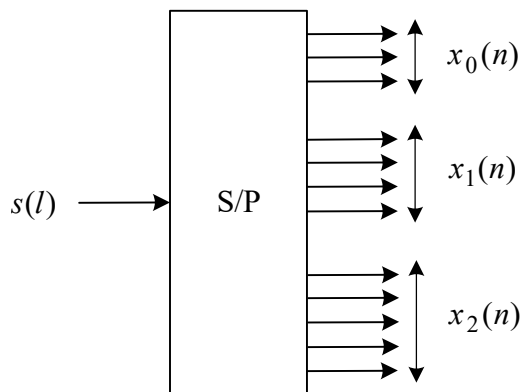


Figure I.21: DMT symbol generation

The transmitting filters  $\{f_m(n)\}$  create the  $M$ -fold higher rate signals  $\{u_m(n)\}$ , which are then added to produce the composite signal  $x(n)$ . In this way, various parts of the original binary message  $s(n)$  are packed into different frequency regions allowed by the channel.

Notice that for a given constellation, the power can be increased or decreased by scaling the distance between the constellation points. In this way the classical water-filling rule can be approximated. For a given transmitted power and probability of error, multicarrier modulation yields better bit rate than single tone modulation ( $M = 1$  case), assuming no channel coding.

**I.7. Biorthogonality and Perfect DMT Systems**

Consider the upsampler-filter-downsampler system shown below in Figure I.22.

I: Filter Banks in Digital Communications

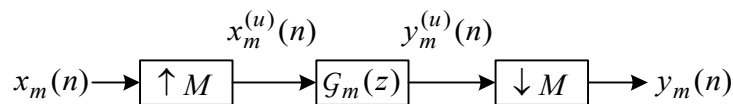


Figure I.22: Upsampler-filter-downsampler

The system in Figure I.22 can redrawn as in Figure I.23.

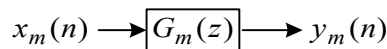


Figure I.23: Equivalent upsampler-filter-downsampler

The output of the filter  $G_m(z)$  in Figure I.22 can be expressed in the form

$$\begin{aligned} y_m^{(u)}(n) &= \sum_{i=-\infty}^{\infty} x_m^{(u)}(n)g_m(n-i) \\ &= \sum_{i=-\infty}^{\infty} x_m(i)g_m(n-iM) \end{aligned} \quad (I.52)$$

Following the downsampler the output in Figure I.22 can be found to be equal to

$$\begin{aligned} y_m(n) &= y_m^{(u)}(nM) \\ &= \sum_{i=-\infty}^{\infty} x_m(i)g_m(nM-iM) \\ &= \sum_{i=-\infty}^{\infty} x_m(i)g_m(n-i) \end{aligned} \quad (I.53)$$

where, by comparing the latter two parts of (I.53), we get the following expression for the impulse response of the filter in Figure I.23:

$$g_m(n) = g_m(nM) \quad (I.54)$$

In light of the above, the transfer function from  $x_m(n)$  to  $y_l(n)$  in the digital transmultiplexer (Figure I.17) can be seen as an  $M$ -fold downsampled version of the product-filter  $H_l(z)C(z)F_m(z)$ . Let's express this relationship in the form

$$G_{lm}(z) = [H_l(z)C(z)F_m(z)]_{\downarrow M} \quad (I.55)$$

When  $G_{lm}(z)$  is nonzero for  $l \neq m$ , then the symbol  $y_l(n)$  is affected by  $x_m(i)$  ( $i$  can be any positive or negative integer, including  $i=n$ ), resulting in interband (inter-carrier) interference. Similarly, if  $G_{mm}(z)$  is not a constant then  $y_m(n)$  is affected by  $x_m(i)$ ,  $i \neq n$ , due to the filtering effect of  $G_{mm}(z)$ . This is called intraband (intra-carrier) interference. Note that both interband interference and intraband interference lead to ISI. If both of these types of interference are eliminated, the system is ISI-free.

I: Filter Banks in Digital Communications

When filters belonging to the sets  $\{F_m(z)\}_{m=0}^{M-1}$  and  $\{H_m(z)\}_{m=0}^{M-1}$  are ideal nonoverlapping bandpass filters, interband interference cannot be present. When  $C(z)$  is completely equalized with the inverse filter  $1/C(z)$ , the system is ISI-free, and  $y_m(n) = x_m(n)$  for all  $m$  (in the absence of noise), and we have the so-called perfect symbol recovery (PR) property.

Ideal nonoverlapping filters are unrealizable, and therefore, an alternative solution that can achieve the PR property would be greatly useful. Consider the case when  $C(z) = 1$ . The PR property can be satisfied if and only if the transmitting and receiving filters satisfy the following condition:

$$[H_l(z)F_m(z)]_{\downarrow M} = \delta_{l-m} \tag{I.56}$$

Let

$$G_{lm}^{(u)}(z) = H_l(z)F_m(z) \tag{I.57}$$

Then, the impulse response  $g_{lm}^{(u)}(n)$  of the product filter  $G_{lm}^{(u)}(z)$  has the Nyquist ( $M$ ) or zero-crossing property:

$$\begin{aligned} g_{lm}^{(u)}(nM) &= 0, \quad l \neq m \\ g_{mm}^{(u)}(nM) &= \delta_n \end{aligned} \tag{I.58}$$

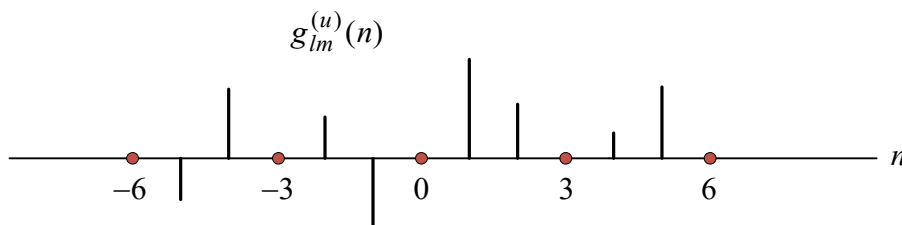


Figure I.24:  $g_{lm}^{(u)}(n)$

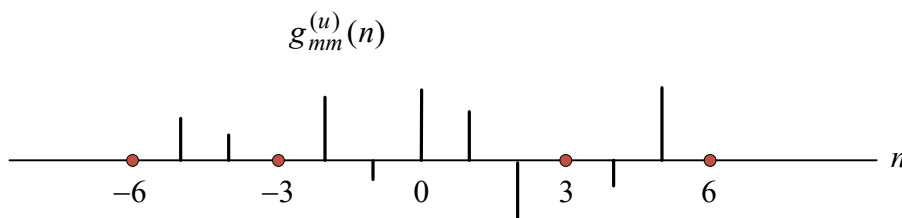


Figure I.25:  $g_{mm}^{(u)}(n)$

When a zero-forcing equalizer is employed, no interference is present, and the only signal distortion is due to the channel noise. Therefore, the received symbol can be written as:

$$y_m(n) = x_m(n) + q_m(n) \tag{I.59}$$

where  $q_m(n)$  is the channel noise after being filtered through  $H_m(z)/C(z)$  and down-sampled. The generation of  $q_m(n)$  is illustrated in Figure I.26.

I: Filter Banks in Digital Communications

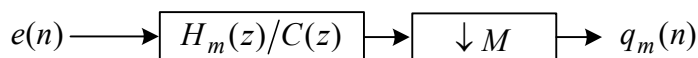


Figure I.26: Receiver noise

The variance of  $q_k(n)$  can be calculated using the equivalent circuit shown below:

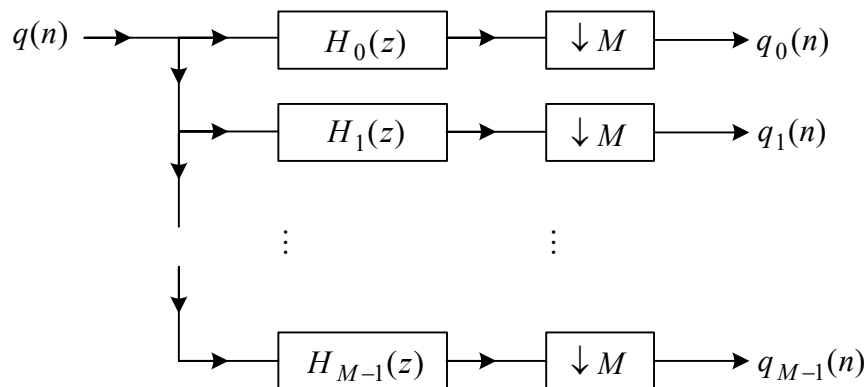


Figure I.27

**I.8. Orthonormal DMT Systems and DFT Filter Banks**

Sub-channel signals  $\{u_m(n)\}_{m=0}^{M-1}$  are the outputs of interpolation filters, and can be expressed as in (I.46). We can regard the subchannel signal  $u_m(n)$  as belonging to a subspace spanned by the basis functions  $\{\dots, f_m(n+M), f_m(n), f_m(n-M), \dots\}$ , covering the  $m$ -th frequency band. The basis function set has an infinite number of elements, each element being a filter obtained from the preceding element by a time-shift of  $M$  samples. The composite signal  $x(n)$ , which enters the channel is, therefore, a linear combination of the basis functions from all the channels.

We say that a set of  $M$  filters  $\{F_m(z)\}_{m=0}^{M-1}$  is orthonormal, if these basis functions are orthogonal to each other, and each of them is normalized to have unit energy. For perfect symbol recovery (or biorthogonality), the transmitting and receiving filters in any orthonormal filter bank are related by:

$$h_k(n) = f_k^*(-n) \tag{I.60}$$

To prove the last result, refer to (I.56) and note that,

$$\{H_k(z)F_k(z)\}_{\downarrow M} = 1 \tag{I.61}$$

This is called time reversed-conjugation. This condition means in particular that the transmitting and receiving filters have identical frequency response magnitudes. It is possible to have orthonormal filter banks where the filters are FIR.

An example is the filter bank where  $f_0(n)$  is chosen as a rectangular pulse of length  $M$  and  $\{f_m(n)\}_{m=0}^{M-1}$  are the modulated versions:

I: Filter Banks in Digital Communications

$$f_m(n) = f_0(n)e^{j\omega_m n} \tag{I.62}$$

with  $\omega_m = 2\pi m/M$  representing the  $m$ -th center-frequency. Substituting for  $\omega_m$  yields

$$f_m(n) = f_0(n)e^{j\frac{2\pi}{M}mn} \tag{I.63}$$

Therefore,

$$F_m(z) = F_0\left(ze^{-j\frac{2\pi}{M}m}\right) \tag{I.64}$$

$$F_m(e^{j\omega}) = F_0\left(e^{j\left(\omega - \frac{2\pi}{M}m\right)}\right) \tag{I.65}$$

As can be seen from (I.65), the frequency responses are uniformly shifted versions of  $F_0(e^{j\omega})$ . An example of this filter bank is shown in Figure I.28 and Figure I.29 which show the impulse response of  $F_0(z)$  and the magnitude frequency responses of  $\{F_k(z)\}_{k=1}^{M-1}$ .

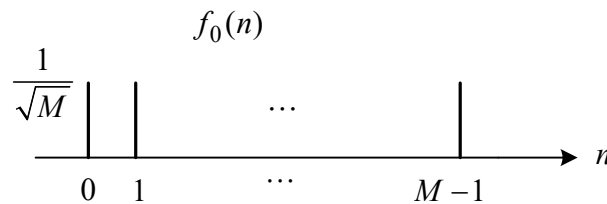


Figure I.28: Impulse response  $f_0(n)$

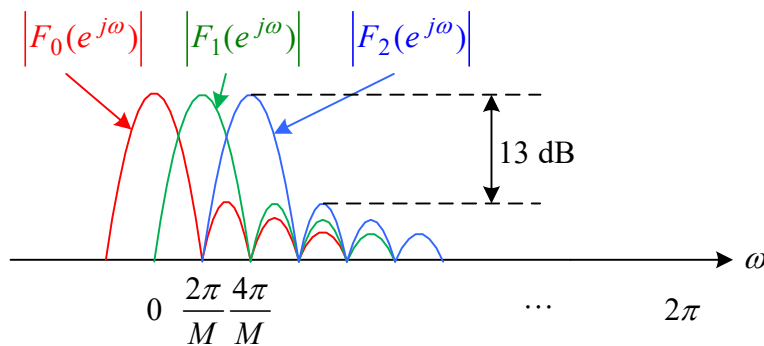


Figure I.29: Magnitude response of  $F_0(e^{j\omega})$

As can be seen from Figure I.29, the response of  $F_k(z)$  is identical to that of  $F_0(z)$  except for a frequency shift of  $2\pi k/M$ .

Note that

I: Filter Banks in Digital Communications

$$f_0(n) = \begin{cases} \frac{1}{\sqrt{M}}, & n = 0, 1, \dots, M-1 \\ 0, & \text{Otherwise} \end{cases} \quad (\text{I.66})$$

Substituting (I.66) in the defining equation of the z-transform yields

$$F_0(z) = \frac{1}{\sqrt{M}} \sum_{i=0}^{M-1} z^{-i} \quad (\text{I.67})$$

Therefore, using (I.64) results in

$$F_m(z) = \frac{1}{\sqrt{M}} \sum_{i=0}^{M-1} z^{-i} e^{j\frac{2\pi}{M}mi} \quad (\text{I.68})$$

Given that (from (I.48))

$$U_m(z) = X_m(z^M)F_m(z) \quad (\text{I.69})$$

and

$$X(z) = \sum_{m=0}^{M-1} U_m(z) \quad (\text{I.70})$$

We get

$$\begin{aligned} X(z) &= \sum_{m=0}^{M-1} X_m(z^M)F_m(z) \\ &= \frac{1}{\sqrt{M}} \sum_{m=0}^{M-1} X_m(z^M) \sum_{i=0}^{M-1} z^{-i} e^{j\frac{2\pi}{M}mi} \\ &= \sum_{i=0}^{M-1} z^{-i} \frac{1}{\sqrt{M}} \sum_{m=0}^{M-1} X_m(z^M) e^{j\frac{2\pi}{M}mi} \end{aligned} \quad (\text{I.71})$$

The last result can be rewritten in the form

$$X(z) = \sum_{i=0}^{M-1} z^{-i} V_i(z^M) \quad (\text{I.72})$$

where

$$V_i(z) = \frac{1}{\sqrt{M}} \sum_{m=0}^{M-1} X_m(z) e^{j\frac{2\pi}{M}mi} \quad (\text{I.73})$$

$$v_i(n) = \frac{1}{\sqrt{M}} \sum_{m=0}^{M-1} x_m(n) e^{j\frac{2\pi}{M}mi} \quad (\text{I.74})$$

I: Filter Banks in Digital Communications

Equation (I.74) expresses the (time domain) sequence  $\{v_i(n)\}_{i=0}^{M-1}$  as an IDFT of the (frequency domain) sequence  $\{x_m(n)\}_{m=0}^{M-1}$ . From (I.72) we have

$$X(z) = \sum_{i=0}^{M-1} z^{-i} [V_i(z)]^{\uparrow M} \quad (I.75)$$

The result in (I.75) is represented in block diagram from in the synthesis part (transmitter) of Figure I.30.

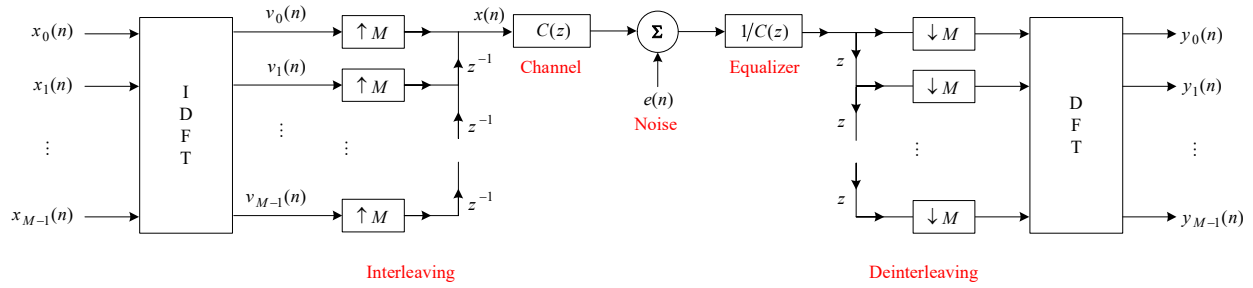


Figure I.30

This is called the DFT filter bank because it can be implemented with a DFT operation and an inverse DFT (IDFT) operation. At each instant of time  $n$ , the DMT symbol  $\{x_0(n), x_1(n), \dots, x_{M-1}(n)\}$  (considered to be in the frequency domain) is transformed into the IDFT domain (time domain). The components  $\{v_0(n), v_1(n), \dots, v_{M-1}(n)\}$  of the resulting symbol are interleaved (parallel-to-serial converted) to obtain the channel signal  $x(n)$ . At the receiver the signal is de-interleaved (serial-to-parallel converted) and a DFT is performed. The results  $\{y_m(n)\}_{m=0}^{M-1}$  are noisy versions of the transmitted symbols  $\{x_m(n)\}_{m=0}^{M-1}$ . Note that ISI is not present in  $\{y_m(n)\}_{m=0}^{M-1}$ .

Time-Domain Analysis

We have

$$u_m(n) = \sum_{i=-\infty}^{\infty} x_m(i) f_m(n - iM) \quad (I.76)$$

Note that the transmitted signal is equal to

$$x(n) = \sum_{m=0}^{M-1} u_m(n) \quad (I.77)$$

Substituting (I.76) into (I.77) yields

$$x(n) = \sum_{m=0}^{M-1} \sum_{i=-\infty}^{\infty} x_m(i) f_m(n - iM) \quad (I.78)$$

I: Filter Banks in Digital Communications

Substituting (I.62) into (I.78) yields

$$\begin{aligned} x(n) &= \sum_{m=0}^{M-1} \sum_{i=-\infty}^{\infty} x_m(i) f_0(n-iM) e^{j\frac{2\pi}{M}m(n-iM)} \\ &= \sum_{i=-\infty}^{\infty} f_0(n-iM) \sum_{m=0}^{M-1} x_m(i) e^{j\frac{2\pi}{M}mn} \end{aligned} \quad (\text{I.79})$$

Letting  $k \in \mathbb{Z}$  and  $l = 0, 1, \dots, M-1$ , the time index  $n$  can be decomposed into

$$n = kM + l \quad (\text{I.80})$$

Hence,

$$x(kM + l) = \sum_{i=-\infty}^{\infty} f_0(kM + l - iM) \sum_{m=0}^{M-1} x_m(i) e^{j\frac{2\pi}{M}ml} \quad (\text{I.81})$$

Let

$$v_l(i) = \frac{1}{\sqrt{M}} \sum_{m=0}^{M-1} x_m(i) e^{j\frac{2\pi}{M}ml} \quad (\text{I.82})$$

Note that  $v_l(i)$  is the IDFT of  $\{x_m(i)\}_{m=0}^{M-1}$  (variable  $m$  in frequency domain, variable  $l$  in time domain). This is represented in the form

$$\{v_l(i)\}_{l=0}^{M-1} = \text{IDFT} \left[ \{x_m(i)\}_{m=0}^{M-1} \right] \quad (\text{I.83})$$

Now, using (I.82) in the last row of (I.79),

$$x(kM + l) = \sqrt{M} \sum_{i=-\infty}^{\infty} f_0(kM + l - iM) v_l(i) \quad (\text{I.84})$$

Since  $f_0(n)$  has non-zero values ( $1/\sqrt{M}$ ) only when  $0 \leq n \leq M-1$ , the index of the summation in (I.84) can have values based on the inequality

$$0 \leq kM + l - iM \leq M - 1 \quad (\text{I.85})$$

Solving for  $i$  gives

$$k - 1 + \frac{l+1}{M} \leq i \leq k + \frac{l}{M} \quad (\text{I.86})$$

Since  $\frac{l}{M} < 1$  for all values of  $l$ , the only possible value of  $i$  is  $i = k$ . Hence,

I: Filter Banks in Digital Communications

$$\begin{aligned}
 x(kM+l) &= v_l(k) \\
 &= \frac{1}{\sqrt{M}} \sum_{m=0}^{M-1} x_m(k) e^{j\frac{2\pi}{M}ml}
 \end{aligned} \tag{I.87}$$

Substituting possible values of  $l$  in (I.87) verifies the transmit structure of Figure I.30, which shows a block diagram of the whole DMT system. A DMT symbol timing diagram is shown in Figure I.31.

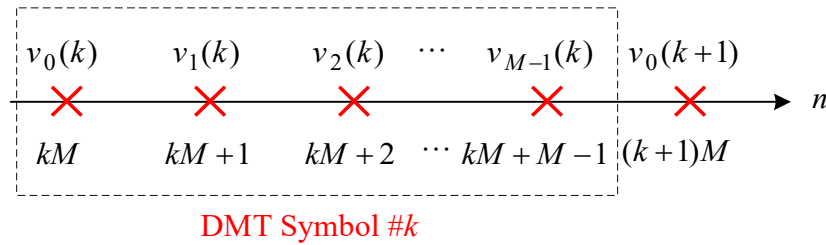


Figure I.31: OFDM Timing Diagram

D/A Conversion

After the  $M$  parallel IDFT output samples  $\{v_l(k)\}_{k=0}^{M-1}$  are converted into serial form to produce  $x(n)$ , they are D/A converted to produce the channel signal. Note that the transmitted DMT symbol has a duration  $T = MT_s$ .

Substituting  $T = MT_s$  in the exponential term in the IDFT samples in (I.82) yields

$$v_l(k) = \frac{1}{\sqrt{M}} \sum_{m=0}^{M-1} x_m(k) e^{j\frac{2\pi}{T}mlT_s} \tag{I.88}$$

Let's make the definition

$$\Delta f = \frac{1}{T} \tag{I.89}$$

Then, (I.88) becomes

$$v_l(k) = \frac{1}{\sqrt{M}} \sum_{m=0}^{M-1} x_m(k) e^{j2\pi m\Delta f l T_s} \tag{I.90}$$

Note that  $v_l(k)$  can be treated as a sampled version of the signal

$$a_k(t) = \frac{1}{\sqrt{M}} \sum_{m=0}^{M-1} x_m(k) e^{j2\pi m\Delta f t} \tag{I.91}$$

where

$$v_l(k) = a_k(lT_s) \tag{I.92}$$

I: Filter Banks in Digital Communications

Therefore the signal corresponding to the  $k$  th DMT symbol can be written in the form

$$x^{(k)}(t) = \sum_{l=0}^{M-1} a_k(t) p_{T_s}(t - kMT_s - lT_s) \quad (I.93)$$

where  $p_{T_s}(t)$  is given by

$$p_{T_s}(t) = \begin{cases} 1, & 0 \leq t < T_s \\ 0, & \text{otherwise} \end{cases} \quad (I.94)$$

Using (I.91) to substitute for  $a_k(t)$  in (I.93) results in

$$x^{(k)}(t) = \frac{1}{\sqrt{M}} \sum_{m=0}^{M-1} x_m(k) e^{j2\pi m \Delta f t} \sum_{l=0}^{M-1} p_{T_s}(t - kMT_s - lT_s) \quad (I.95)$$

Note that since  $x^{(k)}(t)$  is defined over only the interval  $kMT_s \leq t < (k+1)MT_s$ , the summation over  $l$  in (I.95) is redundant and it can be removed to give

$$x^{(k)}(t) = \frac{1}{\sqrt{M}} \sum_{m=0}^{M-1} x_m(k) e^{j2\pi m \Delta f t} \quad (I.96)$$

Finally, we have

$$x(t) = \sum_{k=-\infty}^{\infty} x^{(k)}(t) g(t - kT) \quad (I.97)$$

where  $g(t)$  is the transmit pulse shape of duration  $T$ .

**Matrix Formulation**

At each instant of time  $n$ , the DMT symbol  $\{x_0(n), x_1(n), \dots, x_{M-1}(n)\}$  is transformed into the IDFT domain. The components  $\{v_k(n)\}$  of the resulting symbol are interleaved to obtain the channel signal  $x(n)$ . At the receiver the signal is de-interleaved and a DFT is performed. The results  $\{y_k(n)\}$  are noisy versions of the transmitted symbols  $\{x_k(n)\}$ .

Let's define the two vectors

$$\underline{x}(n) = [x_0(n) \quad x_1(n) \quad \dots \quad x_{M-1}(n)]^T \quad (I.98)$$

$$\underline{v}(n) = [v_0(n) \quad v_1(n) \quad \dots \quad v_{M-1}(n)]^T \quad (I.99)$$

It can be seen from (I.82) that

I: Filter Banks in Digital Communications

$$\underline{y}(n) = \frac{1}{\sqrt{M}} \begin{bmatrix} W_M^0 & W_M^0 & W_M^0 & \cdots & W_M^0 \\ W_M^0 & W_M^1 & W_M^2 & \cdots & W_M^{M-1} \\ W_M^0 & W_M^2 & W_M^4 & \cdots & W_M^{2(M-1)} \\ W_M^0 & \vdots & \vdots & \ddots & \vdots \\ W_M^0 & W_M^{M-1} & W_M^{2(M-1)} & \cdots & W_M^{(M-1)^2} \end{bmatrix} \underline{x}(n) \quad (\text{I.100})$$

Note that

$$W_M^{l(M-1)} = W_M^{lM} W_M^{-l} = W_M^{-l} = W_M^{M-l} \quad (\text{I.101})$$

Then,

$$\underline{y}(n) = \frac{1}{\sqrt{M}} \begin{bmatrix} W_M^0 & W_M^0 & W_M^0 & \cdots & W_M^0 \\ W_M^0 & W_M^1 & W_M^2 & \cdots & W_M^{M-1} \\ W_M^0 & W_M^2 & W_M^4 & \cdots & W_M^{M-2} \\ W_M^0 & \vdots & \vdots & \ddots & \vdots \\ W_M^0 & W_M^{M-1} & W_M^{M-2} & \cdots & W_M^1 \end{bmatrix} \underline{x}(n) \quad (\text{I.102})$$

The columns of the IDFT matrix in (I.102) are orthonormal. This means the matrix is unitary. A unitary matrix  $U$  is one that has the property

$$U^{-1} = U^H \quad (\text{I.103})$$

Orthonormality of the basis functions  $\{\dots, f_k(n+M), f_k(n), f_k(n-M), \dots\}$  follows from the fact that the IDFT matrix (with proper normalization) is unitary. Note that the property in (I.103) means that the DFT matrix in the receiver has similar form to that of the matrix in (I.102), except for the Hermitian operation.

The popularity of the DFT based filter bank arises from the fact that if  $M$  is chosen as a power of two, the DFT can be implemented very efficiently using the fast Fourier transform (FFT) algorithm.

**I.9. Filter Bank Multicarrier Modulation**

A general filter bank multicarrier (FBMC) communication system is illustrated in Figure I.32. Note that the core component of the transmitter is the synthesis filter bank (SFB), while the core component of the receiver is the analysis filter bank (AFB). As in OFDM, the FFT block is present and is followed by a polyphase network (PPN), to complete the realization of a filter bank. The PPN consists of a set of digital filters whose coefficients form the impulse response of the filter bank prototype low-pass filter.

I: Filter Banks in Digital Communications

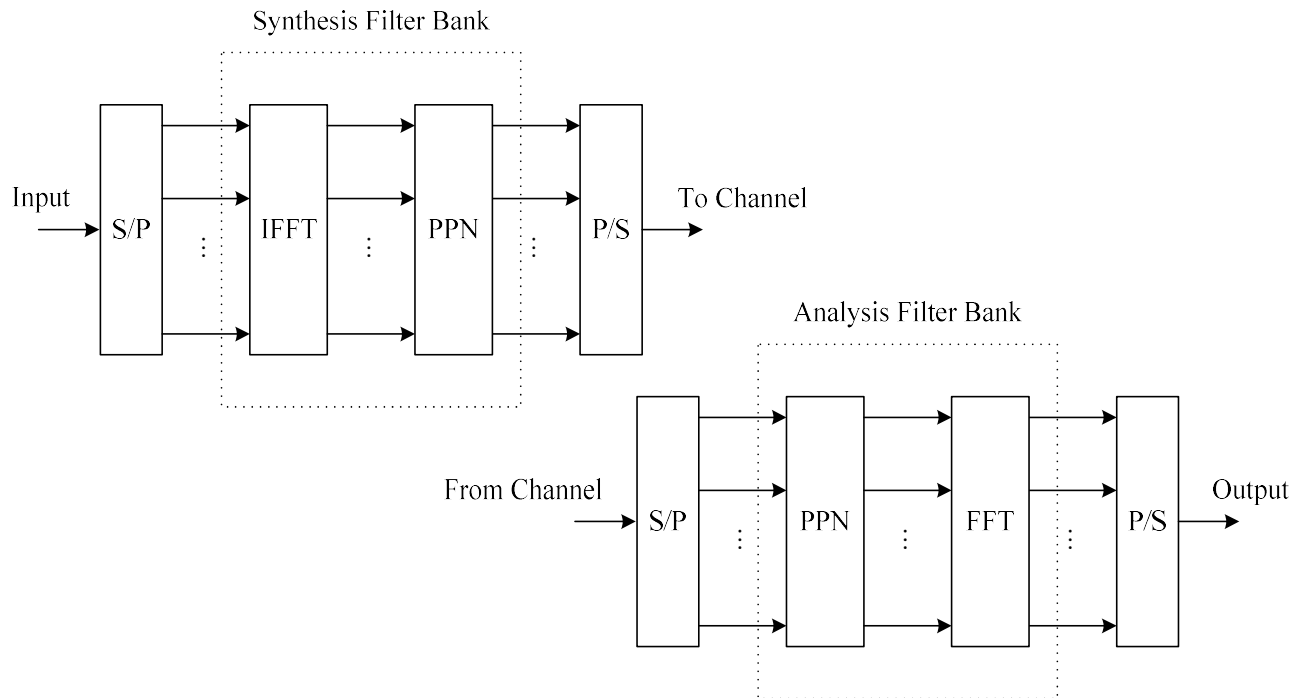


**Figure I.32: Filter Bank Multicarrier System**

The major difference between FBMC and OFDM is its improved frequency selectivity. This is illustrated in **Error! Reference source not found.**, which shows the FBMC and OFDM frequency responses, around one of the subcarriers. A well-known characteristic of OFDM that is clearly visible in **Error! Reference source not found.** is that it exhibits large ripples in the frequency domain. This is a consequence of the imposed orthogonality constraint on the subcarriers. In contrast, the filter bank frequency response has negligible response beyond the center frequency of the adjacent sub-carriers. In fact, the filter bank divides the transmission channel of the system into a set of sub-channels, such that any sub-channel overlaps only with its immediate neighbors.

The difference in the frequency responses of FBMC and OFDM has a considerable impact on the performance of wireless systems and their operational flexibility. The FBMC approach has the following features:

- No guard time, or cyclic prefix, is needed
- Full capacity of the transmission bandwidth is achieved using OQAM
- Sub-channels can be grouped into independent blocks, which is crucial for scalability and dynamic access
- With the absence of leakage in the frequency domain, high resolution spectral analysis can be achieved
- The same device can be used in cognitive radio for spectrum sensing and for reception, even simultaneously, which guaranties perfect coherence between the two functions

The analysis and synthesis filter banks are naturally the key components of the FBMC system. A basic constraint of data transmission is that the channel must satisfy the Nyquist criterion, to avoid intersymbol interference.

I: Filter Banks in Digital Communications

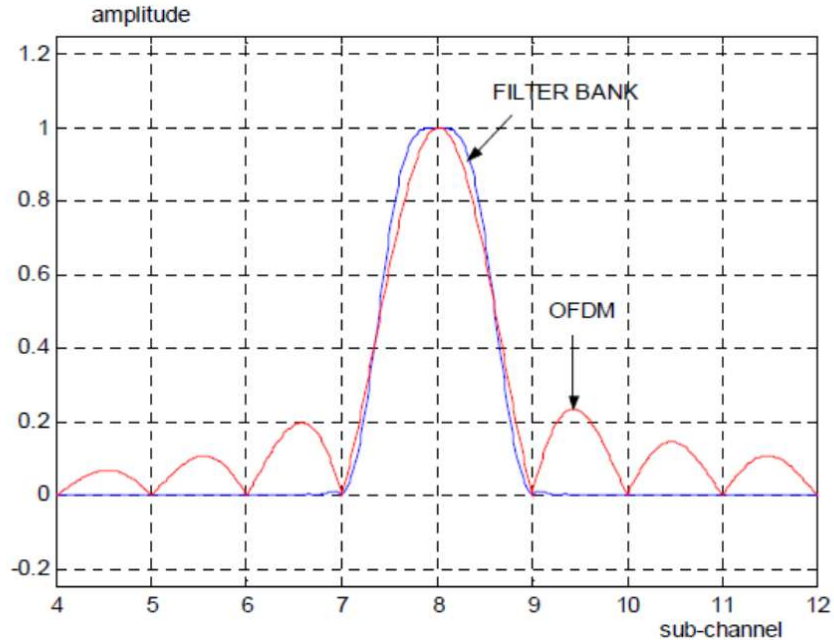


Figure I.33: Comparison of frequency responses of FBMC and OFDM

In uniform filter banks, all the sub-channels have the same bandwidth. Efficient uniform filter banks can be implemented by creating bandpass sub-channel filters from a single lowpass prototype filter, basically through frequency-shifting. There are various efficient multirate structures for the needed filter banks, including lapped transforms, lattice structures, and the polyphase structure. Common to all these structures is that they consist of a filter section, the coefficients of which are determined by the prototype filter design, and a transform section (e.g., discrete Fourier, sine or cosine transforms) implementing the modulation. In combination with the transform blocks, the structures include sampling rate conversion operations, such that the sub-channel signals operate at the basic signaling rate, whereas the synthesized wideband signal has a much higher sampling rate.

The so-called PR filter banks implement the Nyquist criterion exactly, and also without introducing any cross-talk between sub-channels in the back-to-back connection of SFB and AFB (so-called transmultiplexer). In wireless communications, the transmission channel inevitably introduces some distortion to the received sub-channel signals. Therefore, the PR condition is not essential, and it is sufficient that the cross-talk between sub-channels is small enough to be ignored in comparison to the residual interference, e.g., due to imperfect channel equalization. From the filter bank design point of view, this means that the so-called nearly perfect-reconstruction (NPR) designs are sufficient. For NPR filter banks, the polyphase structure is the natural choice, since lapped transforms and lattice structure can be used only in the PR case.

Consider a block of  $M = 2Q$  serial (generally complex-valued) QAM symbols, each having a duration  $T$ . The duration of the whole symbol block is then equal to

$$T_0 = MT \tag{I.104}$$

I: Filter Banks in Digital Communications

Note that a new parallel block of symbols is generated every  $T_0$ . We'll use integer discrete-time index  $l$  that runs at block rate, i.e.,  $l$  increases by 1 every  $T_0$ . The  $M$ -symbol block of symbols is serial-to-parallel converted to produce the simultaneous set of symbols  $\{x_m[l]\}_{m=0}^{M-1}$ , to be transmitted by the system at discrete time  $l$ .

Let each complex symbol have real and imaginary parts

$$x_m[l] = x_m^R[l] + jx_m^I[l] \quad (I.105)$$

where

$$x_m^R[l] = \text{Re}\{x_m[l]\} \quad (I.106)$$

$$x_m^I[l] = \text{Im}\{x_m[l]\} \quad (I.107)$$

Let

$$\begin{aligned} \tau &= \frac{T_0}{2} \\ &= QT \end{aligned} \quad (I.108)$$

The continuous-time transmitted signal is

$$\begin{aligned} v(t) &= \sum_{r=-\infty}^{\infty} \sum_{q=0}^{Q-1} \left[ x_{2q}^R[r]z(t-2r\tau) + jx_{2q}^I[r]z(t-(2r+1)\tau) \right] e^{j2\pi(2q)\Delta ft} \\ &+ \sum_{r=-\infty}^{\infty} \sum_{q=0}^{Q-1} \left[ jx_{2q+1}^I[r]z(t-2r\tau) + x_{2q+1}^R[r]z(t-(2r+1)\tau) \right] e^{j2\pi(2q+1)\Delta ft} \end{aligned} \quad (I.109)$$

The pulse share  $z(t)$  is an even real-valued pulse shape that generally extends for  $-\infty < t < \infty$ .

Let

$$\begin{aligned} d_{2q}[2r] &= x_{2q}^R[r] \\ d_{2q}[2r+1] &= jx_{2q}^I[r] \\ d_{2q+1}[2r] &= jx_{2q+1}^I[r] \\ d_{2q+1}[2r+1] &= x_{2q+1}^R[r] \end{aligned} \quad (I.110)$$

The operation performed in (I.110) is the first part of the pre-processing (staggering) stage, and is represented as in Figure I.34.

I: Filter Banks in Digital Communications

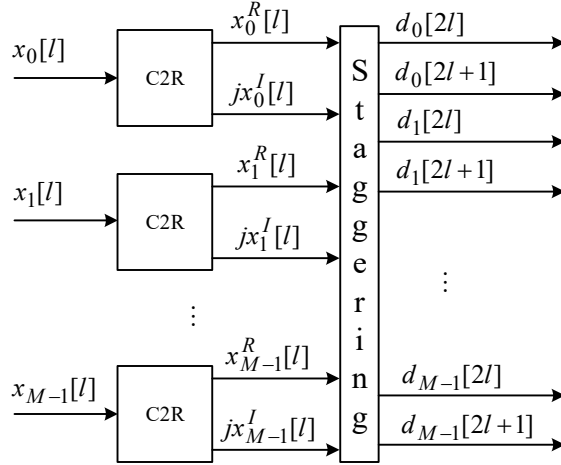


Figure I.34: First part of pre-processing operation

The symbols in (I.110) can be put in the form

$$d_m[n] = b_m[n]e^{j\varphi_m(n)} \quad (\text{I.111})$$

where

$$\varphi_m[n] = \frac{\pi}{2}(m+n)_2 \quad (\text{I.112})$$

Substituting (I.110) into (I.109) yields

$$\begin{aligned} v(t) = & \sum_{r=-\infty}^{\infty} \sum_{q=0}^{Q-1} \left[ d_{2q}[2r]z(t-2r\tau) + d_{2q}[2r+1]z(t-(2r+1)\tau) \right] e^{j2\pi(2q)\Delta ft} \\ & + \sum_{r=-\infty}^{\infty} \sum_{q=0}^{Q-1} \left[ d_{2q+1}[2r]z(t-2r\tau) + d_{2q+1}[2r+1]z(t-(2r+1)\tau) \right] e^{j2\pi(2q+1)\Delta ft} \end{aligned} \quad (\text{I.113})$$

Use  $m = 2q$  and  $m = 2q + 1$  in the summations in the first and second lines in (I.113), respectively, to get

$$\begin{aligned} v(t) = & \sum_{r=-\infty}^{\infty} \sum_{\substack{m=0 \\ m \text{ even}}}^{M-1} \left[ d_m[2r]z(t-2r\tau) + d_m[2r+1]z(t-(2r+1)\tau) \right] e^{j2\pi m\Delta ft} \\ & + \sum_{r=-\infty}^{\infty} \sum_{\substack{m=0 \\ m \text{ odd}}}^{M-1} \left[ d_m[2r]z(t-2r\tau) + d_m[2r+1]z(t-(2r+1)\tau) \right] e^{j2\pi m\Delta ft} \end{aligned} \quad (\text{I.114})$$

Noting that except for running for only even or only odd values of the index, the inner summations in the first and second lines of (I.114) are identical. Therefore, (I.114) can be simplified as follows

I: Filter Banks in Digital Communications

$$v(t) = \sum_{r=-\infty}^{\infty} \sum_{m=0}^{M-1} [d_m[2r]z(t-2r\tau) + d_m[2r+1]z(t-(2r+1)\tau)]e^{j2\pi m\Delta ft} \quad (\text{I.115})$$

Similar steps can be applied on the  $2r$  and  $2r+1$  terms in (I.115) to reach the following simplified version of the multicarrier signal

$$v(t) = \sum_{n=-\infty}^{\infty} \sum_{m=0}^{M-1} d_m[n]z(t-n\tau)e^{j2\pi m\Delta ft} \quad (\text{I.116})$$

The sequence  $d_m[n]$  in (I.116) is obtained from the outputs of Figure I.34 through the second part of the pre-processing stage, as shown in Figure I.35.

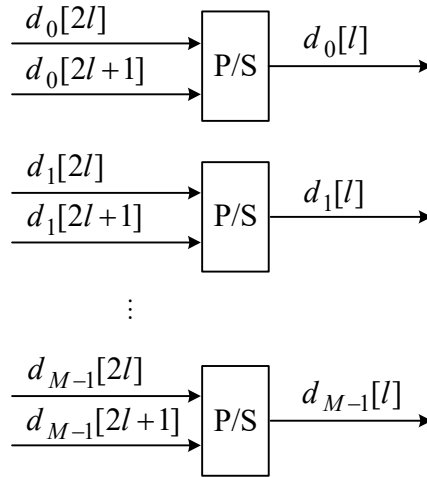


Figure I.35: Second part of pre-processing operation

The pulse shaping waveform  $z(t)$  is obviously uncausal. Let  $z(t)$  be negligibly small for  $|t| > (L-1)T/2$ , for some integer  $L$ , that is chosen such that

$$L = 2\Gamma + 1 \quad (\text{I.117})$$

where  $\Gamma = FM$  and  $F$  is an integer number. Note that with the last assumption on  $L$ ,  $z(t)$  is negligibly small for  $|t| > \Gamma T$ . Let  $z_{tr}(t)$  be a truncated version of  $z(t)$ , such that

$$z_{tr}(t) = \begin{cases} z(t), & |t| \leq \Gamma T \\ 0, & \text{otherwise} \end{cases} \quad (\text{I.118})$$

Let's define the causal waveform  $z_c(t)$ , extending for  $0 \leq t \leq 2\Gamma T$ , as follows

$$z_c(t) = z_{tr}(t - \Gamma T) \quad (\text{I.119})$$

Without loss of generality, and to simplify signal expressions that will be obtained later, we let

$$z_c(2\Gamma T) = 0 \quad (\text{I.120})$$

Let  $z_c(t)$  be sampled every  $T$ , for all  $0 \leq k \leq 2\Gamma$ , to produce the sequence  $p[k]$ , according to

I: Filter Banks in Digital Communications

$$p[k] = z_c(kT) \quad (\text{I.121})$$

Then we have

$$p[k] = z_{tr}((k - \Gamma)T) \quad (\text{I.122})$$

Note that

$$\begin{aligned} p[2\Gamma - k] &= z_c((2\Gamma - k)T) \\ &= z_{tr}((\Gamma - k)T) \end{aligned} \quad (\text{I.123})$$

From the even symmetry of  $z(t)$ , we conclude that, for all  $0 \leq k \leq 2\Gamma$ ,

$$p[2\Gamma - k] = p[k] \quad (\text{I.124})$$

From (I.120) and (I.124),

$$p[0] = p[2\Gamma] = 0 \quad (\text{I.125})$$

To create a causal discrete-time transmitted sequence, let

$$\begin{aligned} s[k] &= v((k - \Gamma)T) \\ &= \sum_{n=-\infty}^{\infty} \sum_{m=0}^{M-1} d_m[n] z((k - \Gamma)T - n\tau) e^{j2\pi m \Delta f (k - \Gamma)T} \\ &= \sum_{i=-\infty}^{\infty} \sum_{m=0}^{M-1} d_m[n] z((k - \Gamma - nQ)T) e^{j2\pi m \Delta f (k - \Gamma)T} \end{aligned} \quad (\text{I.126})$$

Note that

$$\Delta f = \frac{1}{MT} \quad (\text{I.127})$$

$$\Delta f \Gamma T = F \quad (\text{I.128})$$

Using  $z_{tr}(t)$  in place of  $z(t)$  and substituting (I.122), (I.127) and (I.128) in (I.126) yields

$$s[k] = \sum_{n=-\infty}^{\infty} \sum_{m=0}^{M-1} d_m[n] p[k - nQ] e^{j\frac{2\pi}{M}mk} \quad (\text{I.129})$$

Note that  $p[k - nQ]$  in (I.129) is non-zero only when

$$0 \leq k - nQ < 2\Gamma \quad (\text{I.130})$$

This can be rearranged into the form

$$\frac{k}{Q} - 4F < n \leq \frac{k}{Q} \quad (\text{I.131})$$

Let the high rate time index  $k$  be decomposed in terms of a lower rate time index  $l$  as follows

I: Filter Banks in Digital Communications

$$k = lQ + q \quad (\text{I.132})$$

where  $q = 0, \dots, Q-1$ .

Then

$$l - 4F + \frac{q}{Q} < n \leq l + \frac{q}{Q} \quad (\text{I.133})$$

Since  $n$  is an integer and  $0 \leq q \leq Q-1$ , the lowest possible value of  $n$  is  $l-4F$  when  $q=0$  and is  $l-4F+1$  and the largest value of  $n$  is  $l$ . Hence, we can rewrite (I.129) in the form

$$s[lQ + q] = \sum_{n=l-4F+1}^l p[(l-n)Q + q] \sum_{m=0}^{M-1} d_m[n] e^{j\frac{2\pi}{M}m(lQ+q)} \quad (\text{I.134})$$

Let's define

$$s_q[l] = s[lQ + q] \quad (\text{I.135})$$

$$p_q[n] = p[nQ + q] \quad (\text{I.136})$$

Rewriting (I.134) using (I.135) and (I.136) yields

$$s_q[l] = \sum_{n=l-4F+1}^l p_q[(l-n)] \sum_{m=0}^{M-1} d_m[n] e^{j\frac{2\pi}{M}m(lQ+q)} \quad (\text{I.137})$$

Changing variables in the outer summation in (I.137), we get

$$s_q[l] = \sum_{n=0}^{4F-1} p_q[n] \sum_{m=0}^{M-1} d_m[l-n] e^{j\frac{2\pi}{M}m(lQ+q)} \quad (\text{I.138})$$

$$s_q[l] = \sum_{n=0}^{4F-1} p_q[n] \left( \begin{array}{l} \sum_{\substack{m=0 \\ \text{even}}}^{M-1} d_m[l-n] e^{j\frac{2\pi}{M}m(lQ+q)} \\ + \sum_{\substack{m=0 \\ \text{odd}}}^{M-1} d_m[l-n] e^{j\frac{2\pi}{M}m(lQ+q)} \end{array} \right) \quad (\text{I.139})$$

$$s_q[l] = \sum_{n=0}^{4F-1} p_q[n] \left( \begin{array}{l} \sum_{m=0}^{Q-1} d_{2m}[l-n] e^{j\frac{2\pi}{M}2m(lQ+q)} \\ + \sum_{m=0}^{Q-1} d_{2m+1}[l-n] e^{j\frac{2\pi}{M}(2m+1)(lQ+q)} \end{array} \right) \quad (\text{I.140})$$

I: Filter Banks in Digital Communications

$$s_q[l] = \sum_{n=0}^{4F-1} p_q[n] \left( \begin{array}{l} \sum_{m=0}^{Q-1} d_{2m}[l-n] e^{j\frac{2\pi}{Q}m(lQ+q)} \\ + \sum_{m=0}^{Q-1} d_{2m+1}[l-n] e^{j\frac{2\pi}{M}(lQ+q)} e^{j\frac{2\pi}{Q}m(lQ+q)} \end{array} \right) \quad (\text{I.141})$$

$$s_q[l] = \sum_{n=0}^{4F-1} p_q[n] \left( \begin{array}{l} \sum_{m=0}^{Q-1} d_{2m}[l-n] e^{j\frac{2\pi}{Q}mq} \\ + e^{j\frac{2\pi}{M}(lQ+q)} \sum_{m=0}^{Q-1} d_{2m+1}[l-n] e^{j\frac{2\pi}{Q}mq} \end{array} \right) \quad (\text{I.142})$$

$$s_q[l] = \sum_{n=0}^{4F-1} p_q[n] \sum_{m=0}^{Q-1} d_{2m}[l-n] e^{j\frac{2\pi}{Q}mq} + \sum_{n=0}^{4F-1} p_q[n] e^{j\frac{2\pi}{M}(lQ+q)} \sum_{m=0}^{Q-1} d_{2m+1}[l-n] e^{j\frac{2\pi}{Q}mq} \quad (\text{I.143})$$

$$s_q[l] = \sum_{n=0}^{4F-1} p_q[n] \sum_{m=0}^{Q-1} d_{2m}[l-n] e^{j\frac{2\pi}{Q}mq} + \sum_{n=0}^{4F-1} p_q[n] e^{j\frac{2\pi}{M}(nQ+q)} e^{j\frac{2\pi}{M}(l-n)Q} \sum_{m=0}^{Q-1} d_{2m+1}[l-n] e^{j\frac{2\pi}{Q}mq} \quad (\text{I.144})$$

$$s_q[l] = \sum_{n=0}^{4F-1} p_q[n] \sum_{m=0}^{Q-1} d_{2m}[l-n] e^{j\frac{2\pi}{Q}mq} + \sum_{n=0}^{4F-1} p_q[n] e^{j\frac{2\pi}{M}(nQ+q)} \sum_{m=0}^{Q-1} d_{2m+1}[l-n] e^{j\pi(l-n)} e^{j\frac{2\pi}{Q}mq} \quad (\text{I.145})$$

Let

$$p_{q,e}[n] = p_q[n] \quad (\text{I.146})$$

$$\begin{aligned} a_{q,e}[l] &= \sum_{m=0}^{Q-1} d_{2m}[l] e^{j\frac{2\pi}{Q}mq} \\ &= \text{IFFT} \{ d_{2m}[l] \}_{m=0}^{Q-1} \end{aligned} \quad (\text{I.147})$$

The IDFT operation in (I.147) is illustrated as in Figure I.36.

I: Filter Banks in Digital Communications

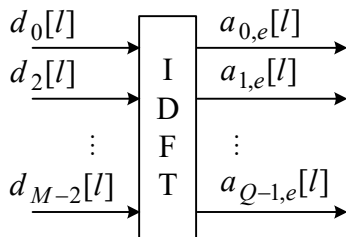


Figure I.36: Even IDFT

Let

$$p_{q,o}[n] = p_q[n] e^{j\frac{2\pi}{M}(nQ+q)} \quad (I.148)$$

$$\begin{aligned} a_{q,o}[l] &= \sum_{m=0}^{Q-1} d_{2m+1}[l] e^{j\pi l} e^{j\frac{2\pi}{Q}mq} \\ &= \text{IFFT} \left\{ d_{2m+1}[l] e^{j\pi l} \right\}_{m=0}^{Q-1} \end{aligned} \quad (I.149)$$

The IDFT operation in (I.149) is illustrated as in Figure I.37.

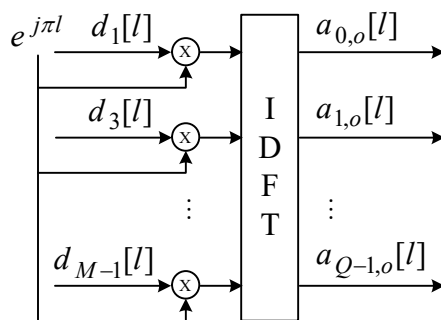


Figure I.37: Odd IDFT

Using (I.146), (I.147), (I.148) and (I.149), the signal in (I.145) can be written compactly as

$$s_q[l] = \sum_{n=0}^{4F-1} p_{q,e}[n] a_{q,e}[l-n] + \sum_{n=0}^{4F-1} p_{q,o}[n] a_{q,o}[l-n] \quad (I.150)$$

$$s_q[l] = p_{q,e}[l] * a_{q,e}[l] + p_{q,o}[l] * a_{q,o}[l] \quad (I.151)$$

The filtering of the even and odd IDFT sequences, that is performed in (I.151) is represented as in Figure I.38.

I: Filter Banks in Digital Communications

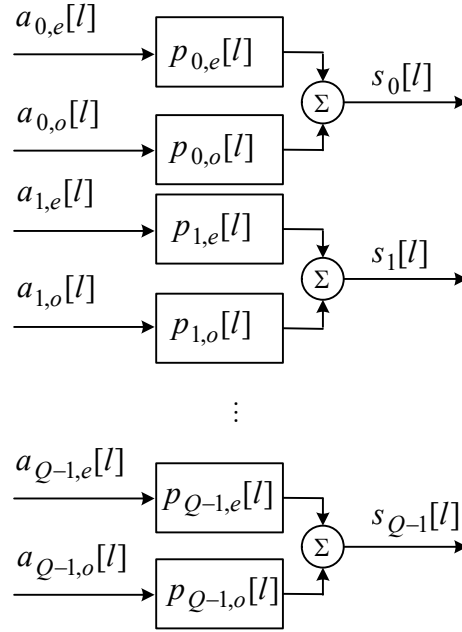


Figure I.38: Filtering of IDFT sequences

A parallel-to-serial operation is used to sequentially arrange the filtered IDFT outputs, as shown in Figure I.39.

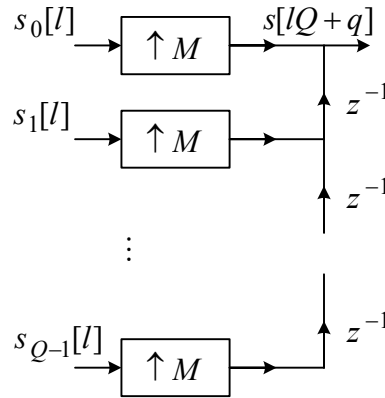


Figure I.39: Parallel-to-serial conversion

The symbols in (I.110) can be put in the form

$$d_m[n] = b_m[n]e^{j\varphi_m(n)} \tag{I.152}$$

where

$$\varphi_m[n] = \frac{\pi}{2}(m+n)_2 \tag{I.153}$$

Then we have

I: Filter Banks in Digital Communications

$$\begin{aligned}
 s[k] &= \sum_{n=-\infty}^{\infty} \sum_{m=0}^{M-1} b_m[n] e^{j\varphi_m(n)} p[k-nQ] e^{j\frac{2\pi}{M}mk} \\
 &= \sum_{n=-\infty}^{\infty} \sum_{m=0}^{M-1} b_m[n] \gamma_m[n, k]
 \end{aligned} \tag{I.154}$$

At the demodulation stage, we get an estimate of the transmitted real-valued symbol using the correlation operation

$$\begin{aligned}
 \hat{b}_m[n] &= \text{Re} \left\{ \sum_{k=-\infty}^{\infty} s[k] \gamma_m^*[n, k] \right\} \\
 &= \text{Re} \left\{ \sum_{k=-\infty}^{\infty} s[k] p[k-nQ] e^{-j\frac{2\pi}{M}mk} e^{-j\varphi_m(n)} \right\}
 \end{aligned} \tag{I.155}$$

$$\hat{b}_m[n] = \text{Re} \left\{ \sum_{i=0}^{4FQ} s[nQ+i] p[i] e^{-j\frac{2\pi}{M}m(nQ+i)} e^{-j\varphi_m(n)} \right\} \tag{I.156}$$

\*\*\*

## II. MULTICARRIER MODULATION

### II.1. Introduction

It is known that nonideal linear filter channels introduce ISI, which degrades performance compared with the ideal channel. The degree of performance degradation depends on the channel frequency response characteristics. Furthermore, the complexity of the receiver increases as the span of the ISI increases. The primary motivation for transmitting the data on multiple carriers is to reduce ISI and, thus, eliminate the performance degradation that is incurred in single carrier modulation.

The basic idea of multicarrier modulation is to divide the transmitted bit stream into many different sub-streams and send these over many different sub-channels. The data rate on each of the sub-channels is much less than the total data rate, and the corresponding sub-channel bandwidth is much less than the total system bandwidth. The reduced data rate of the sub-channels means a longer symbol duration than in single carrier systems. Typically the sub-channels are orthogonal under ideal propagation conditions.

The number of sub-streams is chosen to insure that each sub-channel has a bandwidth less than the coherence bandwidth of the channel, so the sub-channels experience relatively flat fading. Thus, the ISI on each sub-channel is small, therefore reducing the complexity of the equalizer at the receiver. To avoid fast (time selective) fading, the multicarrier symbol duration should be smaller than the coherence time of the channel. The sub-channels in multicarrier modulation need not be contiguous, so a large continuous block of spectrum is not needed for high rate multicarrier communications. Moreover, multicarrier modulation is efficiently implemented digitally.

Orthogonal frequency division multiplexing (OFDM) is based on the principle of multicarrier modulation. OFDM can be regarded both as a modulation method and a multiple-access technique. OFDM has been shown to be an effective technique to combat multipath fading in wireless communications. OFDM has been chosen as the standard for digital audio broadcasting and digital terrestrial TV broadcasting in Europe and high-speed wireless local areas networks.

OFDM is a low-complexity modulation scheme that is usually implemented using IFFT/FFT blocks in addition to other simple signal processing blocks. OFDM is used in high-bit-rate wireless applications. OFDM can overcome bit rate limitations. OFDM suffers limitations caused by the wireless environment.

Multi-carrier techniques are widely used in wireless LANs and fourth generation cellular systems. Orthogonal frequency division multiplexing (OFDM) is a widely used modulation technique in high-rate wireless systems such as IEEE 802.11a/g wireless local area network (WLAN) standard due to its robustness to frequency-selective fading. Orthogonal frequency division multiple access (OFDMA) is an extension of OFDM to accommodate multiple simultaneous users. OFDMA has been adopted for the forward channel (downlink) in Long Term Evolution (LTE) and in both the forward and reverse (uplink) channels for IEEE 802.16e Worldwide Interoperability for Microwave Access (WiMAX) standard.

OFDMA achieves multiple access by dividing the available sub-carriers into mutually exclusive sets that are assigned to distinct users for simultaneous transmission. The orthogonality of the sub-carriers ensures protection against multiple-access interference. There are three basic forms of

## II: Multicarrier Modulation

OFDMA depending on how the sub-carriers are allocated to the users. The first is clustered-carrier OFDMA (CC-OFDMA) where each user is allocated a contiguous group of sub-carriers. The second is spaced-carrier OFDMA (SC-OFDMA) where each user is assigned a group of sub-carriers that is regularly spaced across the channel bandwidth. The last is random interleaving OFDMA (RI-OFDMA) where sub-carriers are assigned in a random fashion to each user.

OFDMA has essentially the same advantages and disadvantages as OFDM when compared to single-carrier modulation schemes. It achieves robustness to frequency-selective fading by using closely spaced orthogonal sub-carriers, such that frequency domain equalization (FDE) can be employed. However, it also suffers from a high peak-to-average power ratio (PAPR) that requires the use of either PAPR reduction techniques or a highly linear power amplifier. OFDMA is attractive for use on the forward link of a cellular system, since all forward link transmissions can all use the same RF local oscillator and sample clock reference in their digital-to-analog converters (DACs). However, the use of OFDMA on the cellular reverse link is complicated considerably by the fact that waveform received at the BS from each MS will have a different carrier frequency offset, timing offset, and sampling clock offset. To overcome the difficulties of using OFDMA on the cellular reverse link, a modified form of OFDMA, called single-carrier frequency division multiple access (SC-FDMA) can be used.

### II.2. Single-Carrier Transmission

Given a particular channel characteristic, the communication system designer must decide how to efficiently utilize the available channel bandwidth in order to transmit the information reliably within the transmitter power constraint and receiver complexity constraints.

Consider a nonideal linear filter channel model. Let the time dispersion caused by the channel be much greater than the symbol duration. Therefore, ISI is assumed to result from the nonideal frequency response of the channel. Consequently, an equalizer is necessary to compensate for the channel distortion.

Consider systems that employ QAM impressed on a single carrier that is selected along with the symbol rate from a set of specified values to obtain the maximum throughput at the desired level of performance (error rate). The channel frequency-response characteristics are measured upon initial setup of the communication link, and the symbol rate and carrier frequency are selected based on this measurement.

An alternative approach to the design of a bandwidth-efficient communication system in the presence of channel distortion is to subdivide the available channel bandwidth into a number of subchannels, such that each subchannel is nearly ideal. To elaborate, suppose that  $C(f)$  is the frequency response of a nonideal, band-limited channel with a bandwidth  $W$ . Assume the power spectral density of the additive Gaussian noise is  $S_{nn}(f)$ .

A typical end-to-end configuration for a single-carrier communication system is shown in Figure II.1. Let the channel have a bandlimited impulse response  $h(t)$ , and a bandwidth  $W$ . Let the duration of a transmitted symbol  $a_n$  be  $T$  seconds. The transmission data rate is then  $R = 1/T$  symbols/s.

II: Multicarrier Modulation

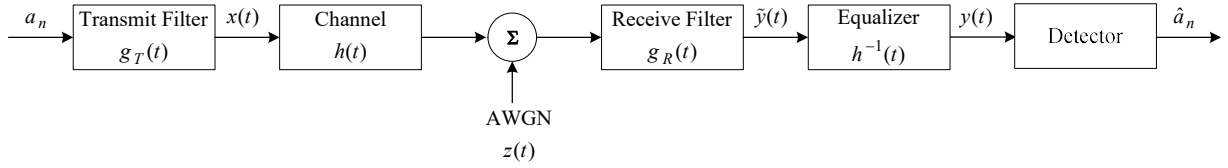


Figure II.1: Single-carrier baseband communication system model

The transmit filter has an impulse response (pulse shape)  $g_T(t)$ . At the receiver, the signal is processed by the receive filter, the equalizer, and the detector.

The output of the equalizer can be expressed as

$$y(t) = \sum_{m=-\infty}^{\infty} a_m g(t - mT) + \xi(t) \quad (\text{II.1})$$

where

$$g(t) = g_T(t) * h(t) * g_R(t) * h^{-1}(t) \quad (\text{II.2})$$

and

$$\xi(t) = z(t) * g_R(t) * h^{-1}(t) \quad (\text{II.3})$$

The sampled output signal of the equalizer can be expressed as

$$y(nT) = \sum_{m=-\infty}^{\infty} a_m g((n - m)T) + \xi(nT) \quad (\text{II.4})$$

The last result can be written in the form

$$y(nT) = a_n g(0) + \sum_{\substack{m=-\infty \\ m \neq n}}^{\infty} a_m g((n - m)T) + \xi(nT) \quad (\text{II.5})$$

Note that  $g(t)$  cannot be time-limited due to the finite channel bandwidth. The transmit and receive filters must be designed so as to minimize or eliminate the middle term in (II.5), which represents ISI.

ISI can be eliminated by satisfying the following condition on the overall impulse response:

$$g(nT) = \begin{cases} 1, & n = 0 \\ 0, & n \neq 0 \end{cases} = \delta(n) \quad (\text{II.6})$$

In the frequency domain, the no-ISI condition is:

$$\sum_{i=-\infty}^{\infty} G\left(f - \frac{i}{T}\right) = T \quad (\text{II.7})$$

II: Multicarrier Modulation

**II.3. Nyquist Criterion**

The conditions in (II.6) and (II.7) constitute the Nyquist criterion. Filters that satisfy the Nyquist criterion are known as Nyquist filters. An example Nyquist filter is an ideal LPF (Low Pass Filter), with a brick-wall frequency response, as described by

$$G_I(f) = \frac{1}{2W} \text{rect}\left(\frac{f}{2W}\right) \quad (\text{II.8})$$

where  $W = R/2$ . Note that  $W$  is the minimum required bandwidth to allow a data rate  $R$  without ISI. The ideal filter in (II.8) is not physically realizable because its impulse response is not causal.

A physically realizable Nyquist filter is the raised-cosine filter, which is specified by the following frequency response:

$$G_{RC}(f) = \begin{cases} T, & |f| \leq \frac{1-r}{2T} \\ \frac{T}{2} \left\{ 1 + \cos \frac{\pi T}{r} \left( |f| - \frac{1-r}{2T} \right) \right\}, & \frac{1-r}{2T} < |f| \leq \frac{1+r}{2T} \\ 0, & |f| > \frac{1+r}{2T} \end{cases} \quad (\text{II.9})$$

where  $0 \leq r \leq 1$  is the roll-off factor. The bandwidth of  $g_{RC}(t)$  depends on  $r$  such that  $W$  increases from  $1/2T$  when  $r = 0$  to  $1/T$  when  $r = 1$ . The flat central segment of  $G_{RC}(f)$  is largest when  $r = 0$  and is not present when  $r = 1$ . The raised cosine frequency response occupies a frequency range that is equal to (when  $r = 0$ ) or wider than (when  $r > 0$ ) the Nyquist bandwidth.

**II.4. Wireless Single-Carrier Transmission**

In order to transmit at rate of  $R$  symbols per second with no ISI, the minimum required bandwidth is the Nyquist bandwidth, which is given by  $R/2$ . This implies that a wider bandwidth is required for transmission at a higher symbol rate. Up to this point, it has been assumed that the channel is perfectly compensated by the equalizer. This is not the case in randomly time-varying wireless channels. When the signal bandwidth becomes larger than the coherence bandwidth of the wireless channel, the link suffers from multi-path fading, which generates inter-symbol interference (ISI). In general, adaptive equalizers are needed to deal with the ISI. Adaptive equalizers are implemented by finite impulse response (FIR) filters with tap coefficients that are adjusted so as to minimize the effect of ISI. More equalizer taps are required as the ISI becomes more significant, and this happens when the data rate increases.

The optimum detector for the multi-path fading channel is a maximum-likelihood sequence detector (MLSD), which bases its decisions on the observation of a sequence of received symbols over successive symbol intervals, in favor of maximizing the posteriori probability. The complexity of the MLSD detector depends on the modulation order  $M$  and the size of the channel memory  $L$ . When  $M$  and  $L$  are large, suboptimum equalizers, such as MMSE or LS equalizers, can be used. However, the complexity of these suboptimum equalizers can still be too enormous to be implemented at high data rates. This particular situation can be explained by the fact that the

## II: Multicarrier Modulation

inverse function (frequency-domain response of equalizer) becomes sharper as the frequency-selectivity of the channel increases. In conclusion, a high data rate single-carrier transmission may not be feasible due to too much complexity of the equalizer in the receiver.

### II.5. Multi-Carrier Transmission

An MCM signal consists of the superposition of a number of sinusoidal subcarriers, a process through which the total signal bandwidth is divided into many narrowband sub-channels to be transmitted simultaneously. In other words, an MCM signal is the result of splitting up a wideband signal having a high symbol rate into several lower rate signals, each one occupying a narrower bandwidth. MCM signals are known to be robust to multipath fading. This is why MCM signals are usually used when transmission is performed over frequency selective fading channels. The bandwidths of MCM sub-channels are chosen so that they are lower than the coherence bandwidth of the communication channel.

Therefore, even though the overall communication channel may be frequency selective, the sub-channels can be made frequency flat. An important feature of MCM systems is the ability to use the IFFT to generate the signals in the transmitter, and the FFT to perform the demodulation at the receiver. The advantages of multicarrier modulation over a classical single carrier system are the following:

- In a single carrier system, a single fade or interferer can cause the entire link to fail, but in a multicarrier system, only a small percentage of subcarriers will be affected. Error correction coding can then be used to correct the few erroneous subcarriers.
- Adaptation of the data rates of sub-channels based on the possible variations of the channel characteristics. In that sense, multicarrier systems overcome problems introduced by the inherent colored nature of the channel noise in wide-band transmission systems. This technique is also known as “adaptive loading”.
- Combining different coding schemes including block (e.g., Reed–Solomon) and trellis-based modulation in order to increase the system’s robustness toward transmission errors. MCM allows a given symbol to be transmitted at a precise location in the time–frequency plane. Thus, it is easier for the system designer to scatter in the time–frequency plane all elements of the channel coder in such a way that they are seldom statistically impaired by selective fading at the same time.

The basic structure of a multi-carrier transmission system is shown in Figure II.2.

II: Multicarrier Modulation

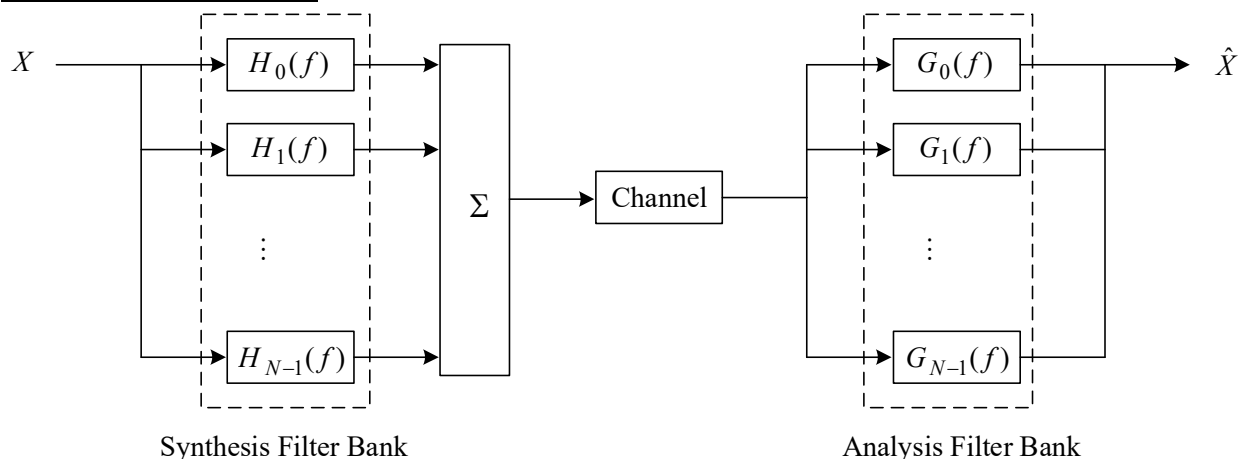


Figure II.2: Structure of a multicarrier system

**II.6. Orthogonal Frequency Division Multiplexing**

**II.6.A. CYCLIC PREFIX**

Consider an orthogonal frequency division multiplexing (OFDM) system where the number of sub-carriers  $M$  is chosen to be large enough so that the channel transfer function  $C(t, f)$  is essentially constant across sub-bands of width  $1/T$ . Let

$$T(t, k) \doteq T(t, k\Delta f), \quad k\Delta f - \frac{1}{2T} \leq f \leq k\Delta f + \frac{1}{2T} \quad (II.10)$$

For transmissions over this sub-channel, no equalization is necessary because the ISI is negligible. If  $M$  is chosen so that  $M \gg L$ , where  $L$  is the length of the discrete-time channel impulse response, then the ISI will only affect a small fraction of the symbol transmitted on each sub-carrier. Assume a guard interval, in the form of a length- $G$  cyclic prefix or cyclic suffix, is attached to each IDFT output vector

$$\begin{aligned} \underline{x}_k &= [x(kM) \quad x(kM + 1) \quad \cdots \quad x(kM + M - 1)]^T \\ &= [x_{k,0} \quad x_{k,1} \quad \cdots \quad x_{k,M-1}]^T \end{aligned} \quad (II.11)$$

Note that  $\underline{x}_k \in \mathbb{C}^{M \times 1}$ . If the discrete-time channel impulse response has duration  $L \leq G$ , then the guard interval can completely remove the ISI in a very efficient fashion.

Note that

$$x_{k,m} = x(kM + m) \quad (II.12)$$

Let  $\underline{x}_k^g \in \mathbb{C}^{(M+G) \times 1}$  be defined such that

$$\underline{x}_k^g = [x_{k,0}^g \quad x_{k,1}^g \quad \cdots \quad x_{k,M+G-1}^g]^T \quad (II.13)$$

II: Multicarrier Modulation

Similar to (II.12), we can define

$$x_{k,m}^g = x^g(k(M + G) + m) \quad (II.14)$$

To make the guard interval attachment cyclic, let

$$x_{k,m}^g = x_{k,(m)_M}, m = 0, 1, \dots, M + G - 1 \quad (II.15)$$

where  $(.)_M$  means modulo  $M$ .

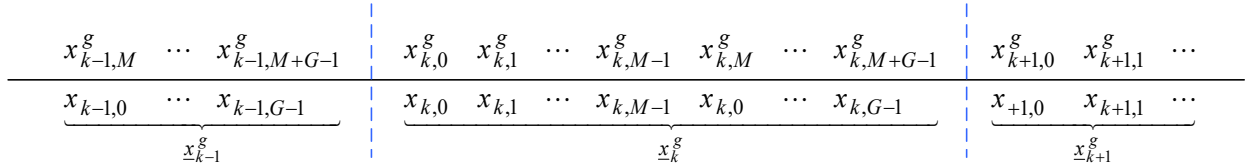


Figure II.3: Cyclic prefix

Note that

$$\begin{aligned} x_{k,m} &= v_m(k) \\ &= \frac{1}{\sqrt{M}} \sum_{l=0}^{M-1} x_l(k) e^{j \frac{2\pi}{M} lm} \end{aligned} \quad (II.16)$$

Therefore,

$$\begin{aligned} x_{k,m}^g &= \frac{1}{\sqrt{M}} \sum_{l=0}^{M-1} x_l(k) e^{j \frac{2\pi}{M} l(m)_M} \\ &= \frac{1}{\sqrt{M}} \sum_{l=0}^{M-1} x_l(k) e^{j \frac{2\pi}{M} lm} \end{aligned}, m = 0, 1, \dots, M + G - 1 \quad (II.17)$$

Note the original symbol rate is equal to

$$R = \frac{1}{T} \quad (II.18)$$

The symbol rate after inserting the CP becomes

$$R^g = \frac{1}{T^g} \quad (II.19)$$

The new symbol duration  $T_g$  can be determined from

$$(M + G)T^g = MT \quad (II.20)$$

Solving for  $T_g$ ,

II: Multicarrier Modulation

$$T^g = \frac{M}{M+G}T \quad (\text{II.21})$$

Therefore,

$$R^g = \frac{M+G}{M}R \quad (\text{II.22})$$

Consider a linear time-invariant ISI channel with an equivalent discrete-time FIR filter impulse response sequence

$$\underline{g} = [g_0 \quad g_1 \quad \cdots \quad g_L]^T \quad (\text{II.23})$$

Convolving the transmitted signal  $\underline{x}_k^g$  (of length  $M+G$ ) with the channel response  $\underline{g}$  (of length  $L+1$ ) produces the discrete-time received sequence

$$\underline{r}_k^g = [r_{k,0}^g \quad r_{k,1}^g \quad \cdots \quad r_{k,M+G-1}^g]^T \quad (\text{II.24})$$

where

$$r_{k,m}^g = \begin{cases} \sum_{i=0}^m g_i x_{k,m-i}^g + \sum_{i=m+1}^L g_i x_{k-1,M+G+m-i}^g + n_{k,m}, & 0 \leq m < L \\ \sum_{i=0}^L g_i x_{k,m-i}^g + n_{k,m}, & L \leq m \leq M+G-1 \end{cases} \quad (\text{II.25})$$

To see the above result, note that

$$\begin{aligned} r_{k,m}^g &= r^g(k(M+G)+m) \\ &= \sum_{i=0}^L g_i x^g(k(M+G)+m-i) \\ &= \sum_{i=0}^L g_i x^g(kM+kG+m-i) \end{aligned} \quad (\text{II.26})$$

Note that the first  $L$  received symbols contain ISI from the symbol at  $k-1$ . Therefore, the first  $G$  symbols ( $G \geq L$ ) are replaced by the last  $G$  symbols. Note that in the transmitted sequence the first and last  $G$  symbols are the same. After removing the CP, we have

$$\begin{aligned} r_{k,m} &= r_{k,G+(m-G)}^g \\ &= \sum_{i=0}^L g_i x_{k,(m-i)}^g + n_{k,m}, \quad 0 \leq m \leq M-1 \end{aligned} \quad (\text{II.27})$$

II: Multicarrier Modulation

Note that the first term in (II.27) represents a circular convolution of the transmitted sequence  $\underline{x}_k$  with the discrete-time channel response  $\underline{g}$ .

**Exercise II.1**

Apply the DFT to  $\underline{r}_k$  to obtain the demodulated samples.

**II.7. Effect of Multipath Channel on OFDM Symbols**

Consider the OFDM signal transmitted in the interval  $lT_{sym} \leq t < (l+1)T_{sym}$ , as given by

$$x_l(t) = \sum_{k=0}^{N-1} X_l(k) e^{j2\pi f_k(t-lT_{sym})} \tag{II.28}$$

For a channel with an impulse response  $h_l(t)$ , the received signal is given as

$$\begin{aligned} y_l(t) &= x_l(t) * h_l(t) + z_l(t) \\ &= \int_0^{\infty} h_l(\alpha) x_l(t-\alpha) d\alpha + z_l(t), \quad lT_{sym} \leq t < (l+1)T_{sym} \end{aligned} \tag{II.29}$$

where  $z_l(t)$  is the additive white Gaussian noise (AWGN) process. Taking samples at  $t = nT_s$ , (II.29) can be represented in a discrete time as follows:

$$\begin{aligned} y_l[n] &= x_l[n] * h_l[n] + z_l[n] \\ &= \sum_{m=0}^{\infty} h_l[m] x_l[n-m] + z_l[n] \end{aligned} \tag{II.30}$$

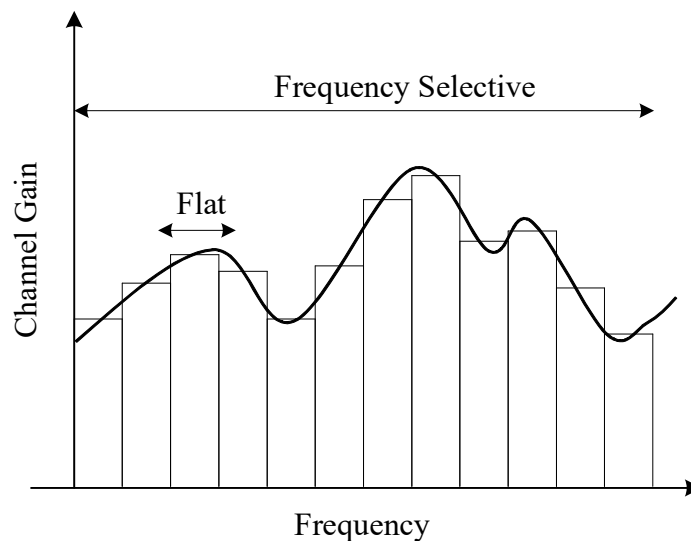


**Figure II.4: Frequency selective channel gain**

II: Multicarrier Modulation

If the delay spread of the channel is  $\tau$ , such that  $(P-1)T_s \leq \tau < PT_s$ , where integer  $P > 0$ , then ISI will take place. In order to understand an ISI effect of the multipath channel, we consider the illustrative examples for the discrete-time channel in Figure II.5 and Figure II.6, where two impulse responses with different lengths are shown along with their frequency responses.

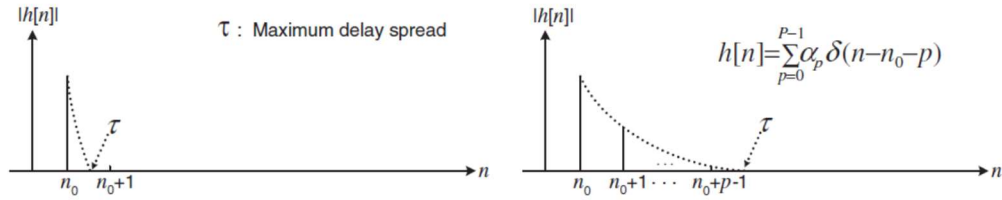


Figure II.5: Channel impulse response

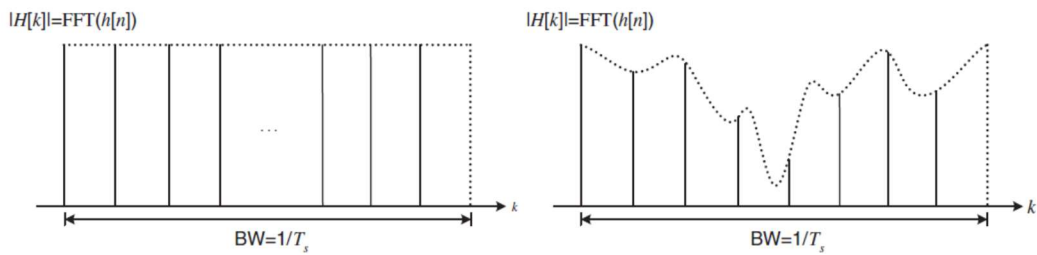


Figure II.6: Channel frequency response

Figure II.7 illustrates an ISI effect of the multipath channel over two consecutive OFDM symbols. Let's denote the duration of the effective OFDM symbol without guard interval by

$$\begin{aligned}
 T_{sub} &= NT_s \\
 &= \frac{1}{\Delta f}
 \end{aligned}
 \tag{II.31}$$

By extending the symbol duration, the effect of the multipath fading channel is greatly reduced on the OFDM symbol. However, its effect still remains as a harmful factor that may break the orthogonality among the subcarriers in the OFDM scheme.

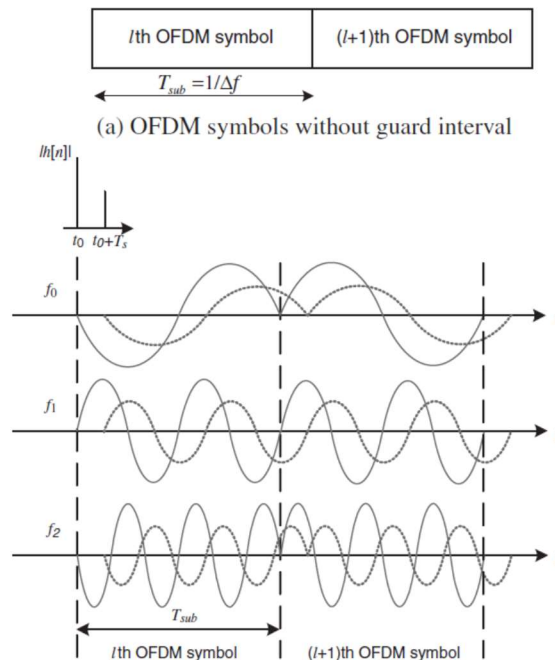


Figure II.7: ISI effect of a multipath channel on the received signal

The first received symbol in Figure II.7 (plotted in a solid line) is mixed up with the second received symbol (plotted in a dotted line), which incurs the ISI. It is obvious that all subcarriers are no longer orthogonal over the duration of each OFDM symbol. To warrant a performance of OFDM, there must be some means of dealing with the ISI effect over the multipath channel. As discussed in the sequel, a guard interval between two consecutive OFDM symbols will be essential.

### II.7.A. CYCLIC PREFIX (CP)

Cyclic prefix (CP) is done by extending the OFDM symbol by copying the last samples of the OFDM symbol into its front. Let  $T_G$  denote the length of CP in terms of samples. Then, the extended OFDM symbols have the duration

$$T_{sym} = T_{sub} + T_G \quad (II.32)$$

Figure II.8 shows two consecutive OFDM symbols, each of which has a CP of length  $T_G$ , while illustrating the OFDM symbol of length as in (II.32).

II: Multicarrier Modulation

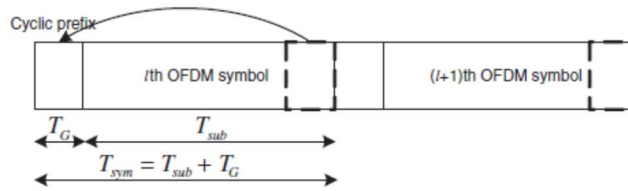


Figure II.8: OFDM symbols with CP

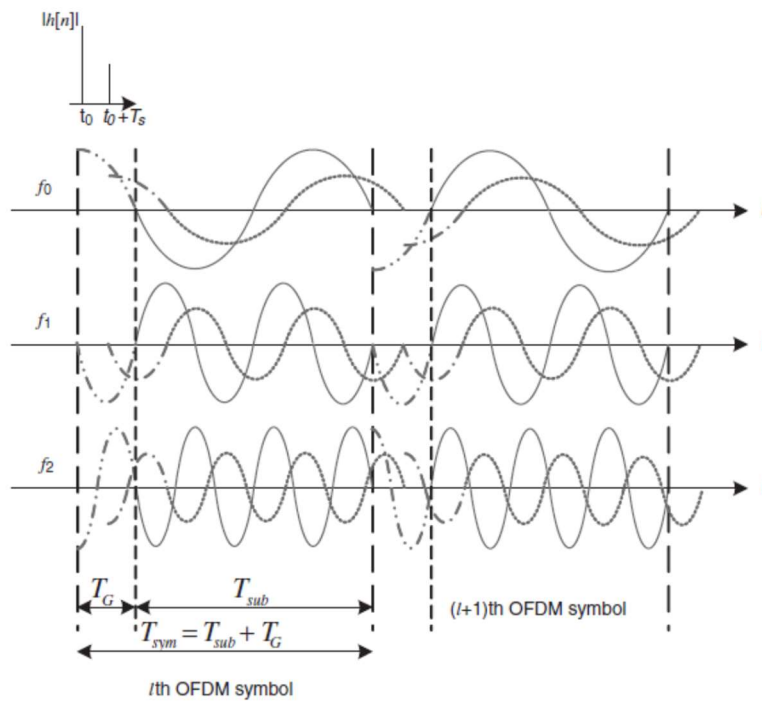


Figure II.9: ISI effect of a multipath channel for each subcarrier

Figure II.9 shows the ISI effects of a multipath channel on some subcarriers of the OFDM symbol. It can be seen from this figure that if the length of the guard interval (CP) is set longer than or equal to the maximum delay of a multipath channel, the ISI effect of an OFDM symbol (plotted in a dotted line) on the next symbol is confined within the guard interval so that it may not affect the FFT of the next OFDM symbol, taken for the duration of  $T_{sub}$ . This implies that the guard interval longer than the maximum delay of the multipath channel allows for maintaining the orthogonality among the subcarriers. As the continuity of each delayed subcarrier has been warranted by the CP, its orthogonality with all other subcarriers is maintained over  $T_{sub}$ .

Figure II.10 shows that if the length of the guard interval (CP) is set shorter than the maximum delay of a multipath channel, the tail part of an OFDM symbol (denoted by a quarter circle) affects the head part of the next symbol, resulting in ISI. In practice, symbol timing offset (STO) may occur, which keeps the head of an OFDM symbol from coinciding with the FFT window start point.

II: Multicarrier Modulation

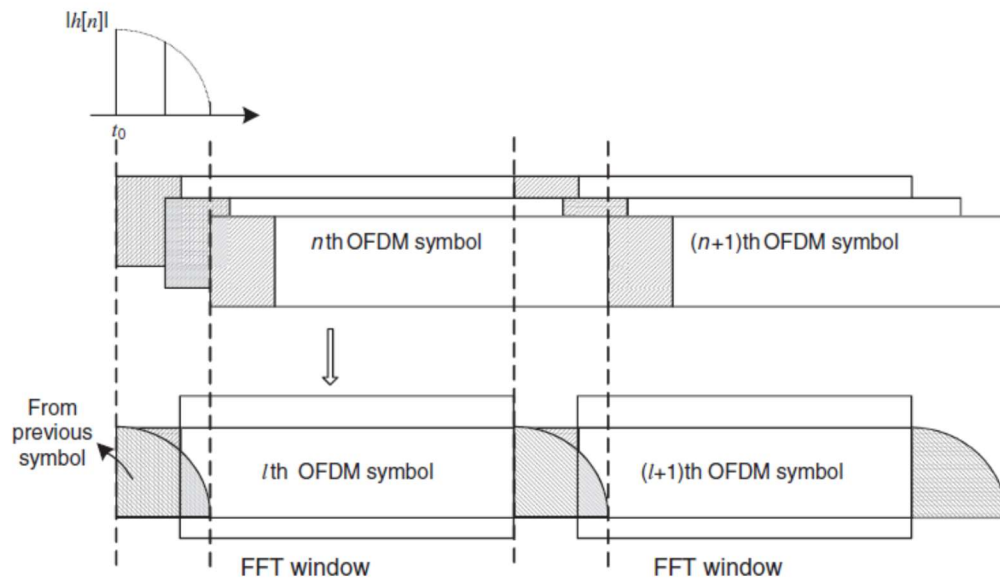


Figure II.10: ISI effect of a multipath channel on OFDM symbols with CP length shorter than the maximum delay of the channel

Figure II.11 shows that even if the length of CP is set longer than the maximum delay of the multipath channel, ISI and/or ICI may occur depending on the timing of the FFT window start point. More specifically, if the FFT window start point is earlier than the lagged end of the previous symbol, ISI occurs; if it is later than the beginning of a symbol, not only ISI (caused by the next symbol), but ICI also occurs.

Now we suppose that the CP length is set not shorter than the maximum delay of the channel and the FFT window start point of an OFDM symbol is determined within its CP interval (i.e., unaffected by the previous symbol). Then the OFDM receiver takes the FFT of the received samples  $\{y_l[n]\}_{n=0}^{N-1}$  yielding

$$Y_l[k] = \sum_{n=0}^{N-1} y_l[n] e^{-j \frac{2\pi}{N} kn} \quad (II.33)$$

II: Multicarrier Modulation

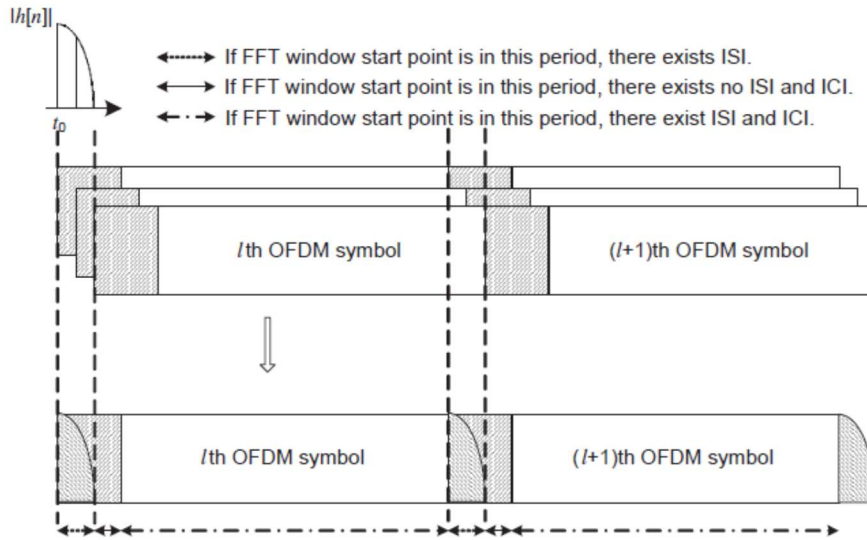


Figure II.11: ISI/ICI effect depending on the FFT window start point

Substituting (II.30) into (II.33),

$$\begin{aligned}
 Y_l[k] &= \sum_{n=0}^{N-1} \left\{ \sum_{m=0}^{\infty} h_l[m] x_l[n-m] + z_l[n] \right\} \\
 &= H_l[k] X_l[k] + Z_l[k]
 \end{aligned}
 \tag{II.34}$$

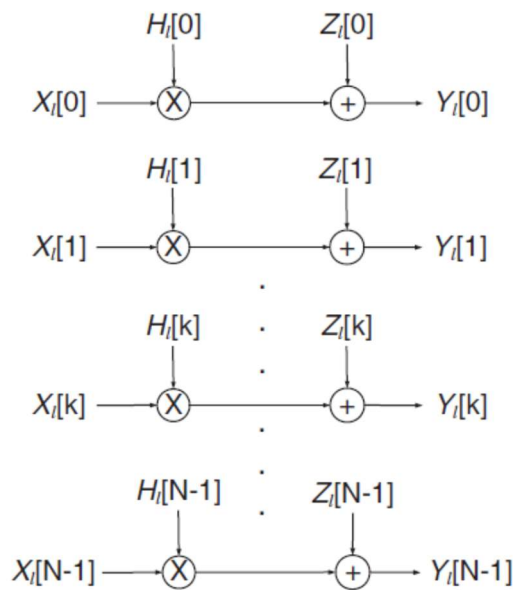


Figure II.12: Frequency-domain equivalent model of OFDM system

II: Multicarrier Modulation

Since  $Y_l[k] = H_l[k]X_l[k]$  under no noise condition, the transmitted symbol can be detected by one-tap equalization, which simply divides the received symbol by the channel gain.

Note that  $Y_l[k] \neq H_l[k]X_l[k]$  without CP, since  $DFT\{y_l[n]\} \neq DFT\{h_l[n]\}DFT\{x_l[n]\}$  when  $y_l[n] = x_l[n]*h_l[n]$  (i.e., using the convolution operation). In fact,  $Y_l[k] = H_l[k]X_l[k]$  when  $y_l[n] = x_l[n] \otimes h_l[n]$  (i.e., using the circular convolution operation). In other words, insertion of CP in the transmitter makes the transmit samples circularly-convolved with the channel samples, which yields  $Y_l[k] = H_l[k]X_l[k]$  as desired in the receiver.

**II.8. OFDMA: Multiple Access Extension of OFDM**

In general, OFDM is a transmission technique in which all subcarriers are used for transmitting the symbols of a single user. In other words, OFDM is not a multiple access technique by itself, but it can be combined with existing multiple access techniques such as TDMA (Time Division Multiple Access), FDMA (Frequency Division Multiple Access), and CDMA (Code Division Multiple Access) for a multi-user system. As depicted in Figure II.13, all subcarriers can be shared by multiple users in the forms of OFDM-TDMA, OFDMA (OFDM-FDMA), or MC-CDMA (OFDM-CDMA).

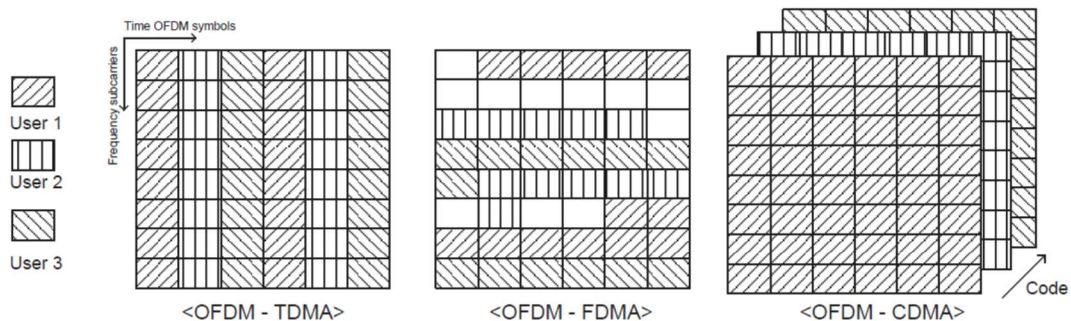


Figure II.13: Multiple access techniques used in OFDM systems

The OFDM-TDMA system allocates all subcarriers only to a single user for the duration of several OFDM symbols, where the number of OFDM symbols per user can be adaptively changed in each frame. In this case, the resource allocation among the users is orthogonal in time.

The OFDMA system assigns a subset of subcarriers (not all subcarriers in each OFDM symbol) to each user, where the number of subcarriers for a specific user can be adaptively varied in each frame. In other words, the subcarriers in each OFDM symbol are orthogonally divided among the multiple users.

An OFDM-CDMA system allows for sharing both time and subcarriers among all users (not in an orthogonal manner) where a subset of orthogonal codes is assigned to each user and the information symbols are spread in the frequency domain.

Among these multiple access techniques associated with OFDM, OFDMA is one of the most useful approaches in the mobile cellular system. As users in the same cell may have different signal-to-noise and interference ratios (SINRs), it would be more efficient to allow multiple users

II: Multicarrier Modulation

to select their own subset of subcarriers with better channel conditions, rather than selecting a single user that uses all the subcarriers at the same time. In other words, there may be one or more users with significantly better channel conditions, especially when the number of users increases. Improvement in the bandwidth efficiency, achieved by selecting multiple users with better channel conditions, is referred to as multi-user diversity gain. OFDMA is a technique that can fully leverage the multi-user diversity gain inherent to the multi-carrier system.

The amount of physical resources (i.e., time slots, subcarrier, and spreading codes, assigned to each user in these techniques) depends not only on the required data rate of each user, but also on the multi-user diversity gain among the users. Note that the aforementioned multiple access techniques associated with OFDM systems differ from each other in many aspects (e.g., flexibility and multiple access interference (MAI)), as compared in Table II.1.

**Table II.1: Multiple access techniques associated with OFDM**

Attributes		TDMA	FDMA	CDMA
Method		One user/subset of time slots/ all subcarriers	Multiple users/same time/subset of subcarriers	All users/same time/all subcarriers
Flexibility		Variable number of time slots	Variable number of subcarriers	Variable number of spreading code
MAI	Intra-cell	None	None	Present
	Inter-cell	Present	Present	Present
MAI suppression		Interference avoidance (low frequency reuse factor)	Interference avoidance Interference averaging	Multi-user detection Interference averaging
Others		Small FFT size Isolated cell (wireless LAN)	Large FFT size Cellular system Multi-user diversity Power concentration	Inherent frequency diversity

**II.9. MC-CDMA**

**II.9.A. SIGNAL STRUCTURE**

Figure II.14 shows multi-carrier spectrum spreading of one complex-valued data symbol  $d^{(k)}$  assigned to user  $k$ . The rate of the serial data symbols is  $1/T_d$ . For brevity, but without loss of generality, the MC-CDMA signal generation is described for a single data symbol per user as far as possible, such that the data symbol index can be omitted. In the transmitter, the complex-valued data symbol  $d^{(k)}$  is multiplied with the user specific spreading  $L$ -chip code given as

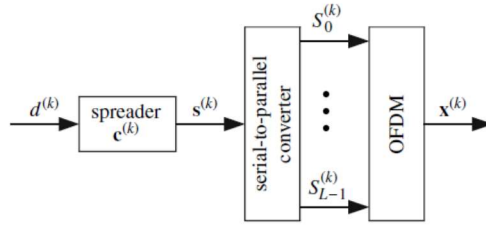


Figure II.14: Multi-carrier spread spectrum signal generation

$$\underline{c}^{(k)} = (c_0^{(k)}, c_1^{(k)}, \dots, c_{L-1}^{(k)})^T \quad (\text{II.35})$$

A chip duration is denoted as  $T_c = T_d/L$ . The chip rate of the serial spreading code before serial-to-parallel conversion is

$$\begin{aligned} R_c &= \frac{1}{T_c} \\ &= \frac{L}{T_d} \end{aligned} \quad (\text{II.36})$$

The complex-valued sequence obtained after spreading is given in vector notations by

$$\begin{aligned} \underline{s}^{(k)} &= d^{(k)} \underline{c}^{(k)} \\ &= (S_0^{(k)}, S_1^{(k)}, \dots, S_{L-1}^{(k)})^T \end{aligned} \quad (\text{II.37})$$

A multi-carrier spread spectrum signal is obtained after modulating the components  $\{S_l^{(k)}\}_{l=0}^{L-1}$ , in parallel onto  $L$  sub-carriers. With multi-carrier spread spectrum, each data symbol is spread over  $L$  sub-carriers. In cases where the number of sub-carriers  $N_c$  of one OFDM symbol is equal to the spreading code length  $L$ , the OFDM symbol duration with multi-carrier spread spectrum including a guard interval results in

$$T'_s = T_g + LT_c \quad (\text{II.38})$$

In this case one data symbol per user is transmitted in one OFDM symbol.

### II.9.B. DOWNLINK SIGNAL

In the synchronous downlink, it is computationally efficient to add the spread signals of the  $K$  users before the OFDM operation as depicted in Figure II.15. The superposition of the  $K$  sequences  $\underline{s}^{(k)}$  results in the sequence

$$\begin{aligned} \underline{s} &= \sum_{k=0}^{K-1} \underline{s}^{(k)} \\ &= (S_0, S_1, \dots, S_{L-1})^T \end{aligned} \quad (\text{II.39})$$

II: Multicarrier Modulation

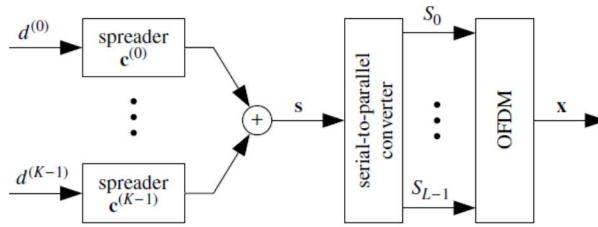


Figure II.15: MC-CDMA downlink transmitter

An equivalent representation for  $\underline{s}$  in the downlink is

$$\underline{s} = C\underline{d} \quad (II.40)$$

where

$$\underline{d} = \left( d^{(0)}, d^{(1)}, \dots, d^{(K-1)} \right)^T \quad (II.41)$$

is the vector with the transmitted data symbols of the  $K$  active users and  $C$  is the spreading matrix given by

$$C = \left( \underline{c}^{(0)}, \underline{c}^{(1)}, \dots, \underline{c}^{(K-1)} \right) \quad (II.42)$$

By assuming that the guard time is long enough to remove all multipath, the received vector of the transmitted sequence  $\underline{s}$  after inverse OFDM and frequency deinterleaving is given by

$$\begin{aligned} \underline{r} &= H\underline{s} + \underline{n} \\ &= (R_0, R_1, \dots, R_{L-1})^T \end{aligned} \quad (II.43)$$

where  $H$  is the  $L \times L$  channel matrix and  $\underline{n}$  is the noise vector of length  $L$ . The vector  $\underline{r}$  is fed to the data detector in order to get an estimate of the transmitted data. For the description of the multiuser detection techniques, an equivalent notation for the received vector  $\underline{r}$  is introduced,

$$\begin{aligned} \underline{r} &= A\underline{d} + \underline{n} \\ &= (R_0, R_1, \dots, R_{L-1})^T \end{aligned} \quad (II.44)$$

The system matrix  $A$  for the downlink is defined as

$$A = HC \quad (II.45)$$

**II.9.C. UPLINK SIGNAL**

In the uplink, the MC-CDMA signal is obtained directly after processing the sequence  $\underline{s}^{(k)}$  of user  $k$  in the OFDM block. After inverse OFDM and frequency deinterleaving, the received vector of the transmitted sequences  $\underline{s}^{(k)}$  is given by

II: Multicarrier Modulation

$$\begin{aligned} \underline{r} &= \sum_{k=0}^{K-1} H^{(k)} \underline{s}^{(k)} + \underline{n} \\ &= (R_0, R_1, \dots, R_{L-1})^T \end{aligned} \quad (\text{II.46})$$

where  $H^{(k)}$  contains the coefficients of the sub-channels assigned to user  $k$ . The uplink is assumed to be synchronous in order to achieve the high spectral efficiency of OFDM. The vector  $\underline{r}$  is fed to the data detector in order to get an estimate of the transmitted data. The system matrix

$$A = (\underline{a}^{(0)}, \underline{a}^{(1)}, \dots, \underline{a}^{(K-1)}) \quad (\text{II.47})$$

comprises  $K$  user-specific vectors, as given by

$$\begin{aligned} \underline{a}^{(k)} &= H^{(k)} \underline{c}^{(k)} \\ &= \left( H_{0,0}^{(k)} c_0^{(k)}, H_{1,1}^{(k)} c_1^{(k)}, \dots, H_{L-1,L-1}^{(k)} c_{L-1}^{(k)} \right)^T \end{aligned} \quad (\text{II.48})$$

**II.9.D. SPREADING TECHNIQUES**

The spreading techniques in MC-CDMA schemes differ in the selection of the spreading code and the type of spreading. As well as a variety of spreading codes, different strategies exist to map the spreading codes in time and frequency direction with MC-CDMA. Finally, the constellation points of the transmitted signal can be improved by modifying the phase of the symbols to be distinguished by the spreading codes.

Spreading Codes

Various spreading codes exist which can be distinguished with respect to orthogonality, correlation properties, implementation complexity and peak-to-average power ratio (PAPR). The selection of the spreading code depends on the scenario. In the synchronous downlink, orthogonal spreading codes are of advantage, since they reduce the multiple access interference compared to non-orthogonal sequences. However, in the uplink, the orthogonality between the spreading codes gets lost due to different distortions of the individual codes. Thus, simple PN sequences can be chosen for spreading in the uplink. If the transmission is asynchronous, Gold codes have good cross-correlation properties. In cases where pre-equalization is applied in the uplink, orthogonality can be achieved at the receiver antenna, such that in the uplink orthogonal spreading codes can also be of advantage.

Walsh-Hadamard Codes

Orthogonal Walsh–Hadamard codes are simple to generate recursively by using the following Hadamard matrix generation,

$$C_L = \begin{bmatrix} C_{L/2} & C_{L/2} \\ C_{L/2} & -C_{L/2} \end{bmatrix}, \quad \forall L = 2^m, m \geq 1, C_1 = 1 \quad (\text{II.49})$$

The maximum number of available orthogonal spreading codes is  $L$  which determines the maximum number of active users  $K$ .

II: Multicarrier Modulation

Fourier Codes

The columns of an FFT matrix can also be considered as spreading codes, which are orthogonal to each other. The chips are defined as

$$c_l^{(k)} = e^{-j\frac{2\pi}{L}lk} \quad (\text{II.50})$$

Thus, if Fourier spreading is applied in MC-CDMA systems, the FFT for spreading and the IFFT for the OFDM operation cancels out if the FFT and IFFT are the same size, i.e., the spreading is performed over all sub-carriers. Thus, the resulting scheme is a single-carrier system with cyclic extension and frequency domain equalizer. This scheme has a dynamic range of single-carrier systems. The computationally efficient implementation of the more general case where the FFT spreading is performed over groups of sub-carriers which are interleaved equidistantly is described in. A comparison of the amplitude distributions between Hadamard codes and Fourier codes shows that Fourier codes result in an equal or lower peak-to-average power ratio.

Pseudo Noise (PN) Spreading Codes

The property of a PN sequence is that the sequence appears to be noise-like if the construction is not known at the receiver. They are typically generated by using shift registers. Often used PN sequences are maximum-length shift register sequences, known as  $m$ -sequences. A sequence has a length of

$$n = 2^m - 1 \quad (\text{II.51})$$

bits and is generated by a shift register of length  $m$  with linear feedback. The sequence has a period length of  $n$  and each period contains  $2^{m-1}$  ones and  $2^{m-1} - 1$  zeros, i.e., it is a balanced sequence.

Gold Codes

PN sequences with better cross-correlation properties than  $m$ -sequences are the so-called Gold sequences. A set of  $n$  Gold sequences is derived from a preferred pair of  $m$ -sequences of length  $L = 2^n - 1$  by taking the modulo-2 sum of the first preferred  $m$ -sequence with the  $n$  cyclically shifted versions of the second preferred  $m$ -sequence. By including the two preferred  $m$ -sequences, a family of  $n+2$  Gold codes is obtained. Gold codes have a three-valued cross correlation function with values  $\{-1, -t(m), t(m) - 2\}$  where

$$t(m) = \begin{cases} 2^{(m+1)/2} + 1, & \text{when } m \text{ is odd} \\ 2^{(m+2)/2} + 1, & \text{when } m \text{ is even} \end{cases} \quad (\text{II.52})$$

Golay Codes

Orthogonal Golay complementary codes can recursively be obtained by

$$C_L = \begin{bmatrix} C_{L/2} & \bar{C}_{L/2} \\ C_{L/2} & -\bar{C}_{L/2} \end{bmatrix}, \quad \forall L = 2^m, m \geq 1, C_1 = 1 \quad (\text{II.53})$$

II: Multicarrier Modulation

where the complementary matrix  $\bar{C}_L$  is defined by reverting the original matrix  $C_L$ . If

$$C_L = [A_L \quad B_L] \quad (II.54)$$

and  $A_L$  and  $B_L$  are  $L \times L/2$  matrices, then

$$\bar{C}_L = [A_L \quad -B_L] \quad (II.55)$$

**II.10. MC-DS-CDMA**

**II.10.A. SIGNAL STRUCTURE**

The MC-DS-CDMA signal is generated by serial-to-parallel converting data symbols into  $N_c$  sub-streams and applying DS-CDMA on each individual sub-stream. Thus, with MC-DS-CDMA, each data symbol is spread in bandwidth within its sub-channel, but in contrast to MC-CDMA or DS-CDMA not over the whole transmission bandwidth for  $N_c > 1$ . An MC-DS-CDMA system with one sub-carrier is identical to a single-carrier DS-CDMA system. MC-DS-CDMA systems can be distinguished in systems where the sub-channels are narrowband and the fading per sub-channel appears flat and in systems with broadband sub-channels where the fading is frequency-selective per sub-channel. The fading over the whole transmission bandwidth can be frequency-selective in both cases. The complexity of the receiver with flat fading per sub-channel is comparable to that of an MC-CDMA receiver, when OFDM is assumed for multi-carrier modulation. As soon as the fading per sub-channel is frequency-selective and ISI occurs, more complex detectors have to be applied. MC-DS-CDMA is of special interest for the asynchronous uplink of mobile radio systems, due to its close relation to asynchronous single-carrier DS-CDMA systems. On one hand, a synchronization of users can be avoided, however, on the other hand, the spectral efficiency of the system decreases due to asynchronism.

Figure II.16 shows the generation of a multi-carrier direct sequence spread spectrum signal. The data symbol rate is  $1/T_d$ . A sequence of  $N_c$  complex-valued data symbols  $\{d_n^{(k)}\}_{n=0}^{N_c-1}$  of user  $k$  is serial-to-parallel converted onto  $N_c$  sub-streams. The data symbol rate on each sub-stream becomes  $1/(N_c T_d)$ . Within a single sub-stream, a data symbol is spread with the user-specific spreading code of length  $L$ :

$$c^{(k)}(t) = \sum_{l=0}^{L-1} c_l^{(k)} p_{T_c}(t - lT_c) \quad (II.56)$$

The duration of a chip within a sub-stream is

$$T_c = \frac{N_c T_d}{L} \quad (II.57)$$

With MC-DS-CDMA, each data symbol is spread over  $L$  multi-carrier symbols, each of duration  $T_c$ . The complex-valued sequence obtained after spreading is given by

II: Multicarrier Modulation

$$x^{(k)}(t) = \sum_{n=0}^{N_c-1} d_n^{(k)} c^{(k)}(t) e^{j2\pi f_n t}, \quad 0 \leq t < LT_c \quad (\text{II.58})$$

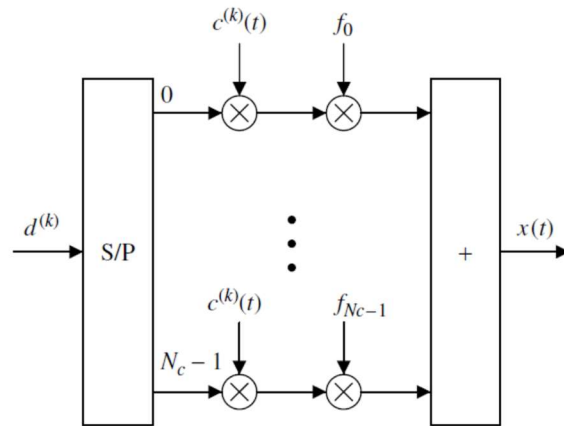


Figure II.16: MC-DS-CDMA transmitter

\*\*\*

### III. MULTIPLE-INPUT MULTIPLE OUTPUT (MIMO) SYSTEMS

Multiple-input multiple-output (MIMO) channel models (vector channels), can be used as a general channel description in a wide range of applications. SISO (Single-Input Single-Output), MISO (Multiple-Input Single-Output), and SIMO (Single-Input Multiple-Output) models are the four possible special cases. MIMO channels are often restricted to systems with multiple antennas at the transmitted and/or the receiver.

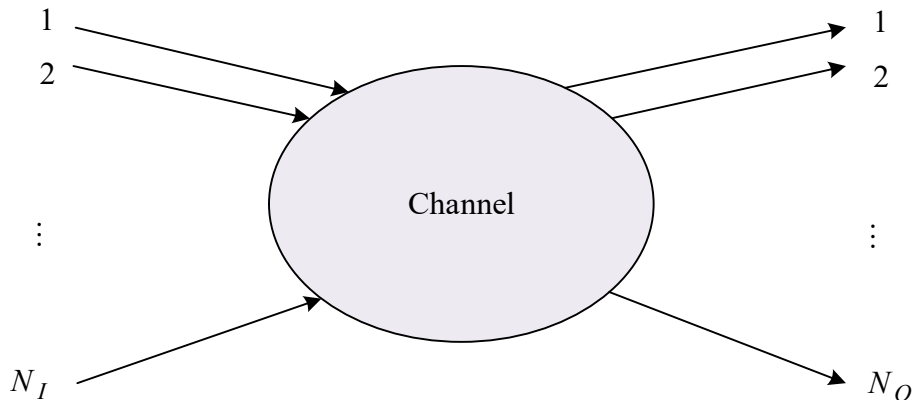


Figure III.1: MIMO channel

The demand for higher network capacity and for higher performance of wireless networks is not breakable. MIMO Systems are able to improve the spectral efficiency significantly, and consequently MIMO plays a key role in many future wireless communication systems. Several options like higher bandwidth, optimized modulation or even code-multiplexing systems offer practically limited potential to increase the spectral efficiency. MIMO systems utilize space-multiplexing by using antenna arrays to enhance the efficiency in the used bandwidth. Figure III.2 shows the basic setup of a MIMO communication system.

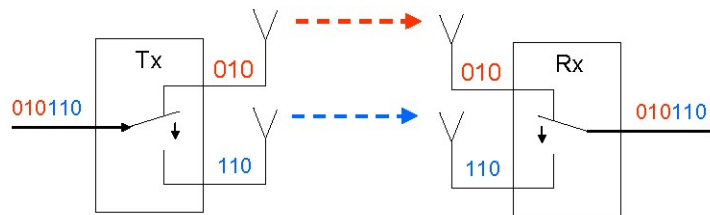


Figure III.2

MIMO systems use multiple inputs and multiple outputs into and out of a single physical channel. These systems are designed to provide spatial diversity and spatial multiplexing. Spatial diversity enables the receiver to utilize more than one version of the transmitted signal; to increase robustness (to symbol decision errors) in the operation of the receiver. With spatial multiplexing the system is able to carry more than one spatial data stream over one frequency simultaneously. MIMO was established in IEEE 802.11n, 802.16-2004 and 802.16e as well as in 3GPP. Further

### III: Multiple-Input Multiple Output (MIMO) Systems

standards which include MIMO are IEEE 802.20 (Mobile Broadband Wireless Access<sup>1</sup>) and 802.22 (Wireless Regional Area Network<sup>2</sup>).

MIMO techniques improve the link reliability, that is, the error probability or the outage probability are reduced. This can be accomplished by enhancing the instantaneous signal-to-noise ratio (SNR) (beamforming) or by decreasing the variations of the SNR (diversity). If multiple access or cochannel interference in cellular networks disturbs the transmission, interferers that are separable in space can be suppressed with multiple antennas, resulting in an improved signal to interference plus noise ratio (SINR).

MIMO techniques multiply the data rate by transmitting several data streams simultaneously over different antennas. This approach is denoted as space division multiple access (SDMA) and can certainly be combined with other multiple access schemes. Since bandwidth became a very valuable and expensive resource, using the space for increasing data rates without expanding the bandwidth is very attractive. The potential capacity gain of multiple antenna systems is much larger than the gain obtained by simply increasing the transmit power.

#### III.1. Baseband Channel Representation

SISO channels represent an important building block of vector channels. Using a representation in the equivalent baseband is beneficial for simulation purposes; because the carrier whose frequency is generally much higher than the signal bandwidth needs not to be explicitly considered. Input  $x(k)$  is a sequence of generally complex-valued symbols of duration  $T_s$  according to some finite symbol alphabet  $\mathcal{X}$ . The output sequence  $y(k)$  has the same rate  $1/T_s$  and its symbols are distributed within the complex plane  $\mathcal{C}$ . The input is first transformed by the transmit filter  $g_T(t)$  of bandwidth  $B$  into a time-continuous, band limited signal given by:

$$x(t) = T_s \sum_k x(k) g_T(t - kT_s) \quad (\text{III.1})$$

This is called the complex envelope. Let's Denote the symbols of the alphabet  $\mathcal{X}$  by  $X_\mu$ . Let's assume that the energy of the transmit filter impulse response is defined to be

$$\int_{-\infty}^{\infty} |g_T(t)|^2 dt = \frac{1}{T_s} \quad (\text{III.2})$$

A single symbol  $T_s x(k) g_T(t - kT_s)$  has the energy

---

<sup>1</sup> MBWA is a specification by the standard association of the IEEE for mobile wireless Internet access networks. MBWA is no longer being actively developed.

<sup>2</sup> The development of the IEEE 802.22 WRAN standard is aimed at using cognitive radio (CR) techniques to allow sharing of geographically unused spectrum allocated to the television broadcast service, on a non-interfering basis, to bring broadband access to hard-to-reach, low population density areas, typical of rural environments. It is the first worldwide effort to define a standardized air interface based on CR techniques for the opportunistic use of TV bands on a non-interfering basis.

III: Multiple-Input Multiple Output (MIMO) Systems

$$\begin{aligned}
 E_s &= T_s^2 \mathbb{E} \left[ |X_\mu|^2 \right] \int_{-\infty}^{\infty} |g_T(t)|^2 dt \\
 &= T_s \mathbb{E} \left[ |X_\mu|^2 \right]
 \end{aligned}
 \tag{III.3}$$

The average power is, thus, equal to:

$$\begin{aligned}
 \sigma_x^2 &= \frac{E_s}{T_s} \\
 &= \mathbb{E} \left[ |X_\mu|^2 \right]
 \end{aligned}
 \tag{III.4}$$

For zero-mean and independent identically distributed (i.i.d.) symbols  $x(k)$ , the average spectral density of  $x(t)$  is

$$\begin{aligned}
 \Phi_{xx}(j\omega) &= T_s |G_T(j\omega)|^2 \mathbb{E} \left[ |X_\mu|^2 \right] \\
 &= E_s |G_T(j\omega)|^2
 \end{aligned}
 \tag{III.5}$$

Obviously, it largely depends on the spectral shape of the transmit filter  $g_T(t)$ , and not on the kind of modulation scheme. The real-valued bandpass transmitted signal is given by:

$$\begin{aligned}
 x_{BP}(t) &= \sqrt{2} \operatorname{Re} \left\{ x(t) e^{j\omega_0 t} \right\} \\
 &= \sqrt{2} \left[ x'(t) \cos(\omega_0 t) - x''(t) \sin(\omega_0 t) \right]
 \end{aligned}
 \tag{III.6}$$

The average spectral density of  $x_{BP}(t)$  has the form

$$\Phi_{x_{BP}x_{BP}}(j\omega) = \frac{E_s}{2} \left[ |G_T(j\omega - j\omega_0)|^2 + |G_T(j\omega + j\omega_0)|^2 \right]
 \tag{III.7}$$

Now,  $x_{BP}(t)$  is transmitted over the mobile radio channel, which is generally represented by its time-variant impulse response  $h_{BP}(t, \tau)$  and an additive noise term  $n_{BP}(t)$  with spectral density  $N_0/2$ . The channel output is given by:

$$\begin{aligned}
 y_{BP}(t) &= h_{BP}(t, \tau) * x_{BP}(t) + n_{BP}(t) \\
 &= \int_0^{\infty} h_{BP}(t, \tau) x_{BP}(t - \tau) d\tau + n_{BP}(t)
 \end{aligned}
 \tag{III.8}$$

The lowpass equivalent channel output is given by:

$$\begin{aligned}
 y(t) &= g_R(t) * h(t, \tau) * x(t) + n(t) \\
 &= T_s \sum_k x(k) \left[ g_R(t) * h(t, \tau) * g_T(t - kT_s) \right] + n(t)
 \end{aligned}
 \tag{III.9}$$

Let

III: Multiple-Input Multiple Output (MIMO) Systems

$$\tilde{h}(t, kT_s) = g_R(t) * h(t, \tau) * g_T(t - kT_s) \quad (III.10)$$

Then,

$$y(t) = T_s \sum_k x(k) \tilde{h}(t, kT_s) + n(t) \quad (III.11)$$

$\tilde{h}(t, kT_s)$  represents the response of a time-discrete channel to an impulse transmitted at time instant  $kT_s$ . The optimum receive filter  $g_R(t)$  that maximizes the SNR at its sampled output has to be matched to the concatenation of channel impulse response and the transmit filter, i.e.,

$$g_R(t) = f^*(-t) \quad (III.12)$$

$$f(t) = g_T(t) * h(t, \tau) \quad (III.13)$$

In order to avoid interference between successive symbols, the transmit and receive filters are generally chosen such that their convolution fulfills the first Nyquist criterion. This criterion also ensures that the filtered and sampled noise remains white, and a symbol-wise detection is still optimum. However, even if  $g_T(t) * g_R(t)$  fulfills the first Nyquist criterion, the channel impulse response  $h(t, \tau)$  between them destroys this property and the background noise  $n(t)$  is colored. Therefore, a pre-whitening filter  $g_w(k)$  working at the sampling rate  $1/T_s$  and decorrelating the noise samples  $n(t)|_{t=kT_s}$  is required. This procedure involves sampling  $y(t)$  at rate  $1/T_s$  and filtering it with  $g_w(k)$ . We assume  $g_T(t)$  to be a perfect lowpass filter of bandwidth  $B = 1/2T_s$ . With  $g_R(t)$  matched to  $g_T(t) * h(t, \tau)$ , and a perfect prewhitening filter, the received signal  $y(k)$  has the form

$$y(k) = \sum_{\kappa=0}^{L_t} h(k, \kappa) x(k - \kappa) + n(k) \quad (III.14)$$

where  $L_t$  denotes the total filter length of the time-discrete channel model  $h(k, \kappa)$ .

Non-MIMO Systems are linked over multiple channels by several frequencies. The MIMO channel has multiple links and operates on the same frequency. While coding and signal processing are key elements to successful implementation of a MIMO system, the communication channel represents a major component that determines system performance. A considerable volume of work has been performed to characterize communication channels for general wireless applications. However, because MIMO systems operate at an unprecedented level of complexity to exploit the channel space-time resources, a new level of understanding of the channel space-time characteristics is required to assess the potential performance of practical multi-antenna links.

The manner in which multiple antennas should be used depends on the properties of the channel, especially on the rank the channel impulse response covariance matrix. As an example, correlation among the sub-channels reduces the diversity gain. In the case of a strong line-of-sight component (Rice fading), diversity is also not an appropriate means because fading is not a severe problem. If we can exploit other sources of diversity, for example, frequency diversity with the Rake

III: Multiple-Input Multiple Output (MIMO) Systems

receiver or time diversity due to coding over time-varying channels, we are probably already close to the additive white Gaussian Noise (AWGN) performance and little can be gained by a further increase of the diversity degree. In each of these cases, multiple antennas should be used in a different way.

For spatial multiplexing, a channel should have a rank that is larger than one. Otherwise, we cannot reliably transmit parallel data streams. Hence, for highly correlated channels with a unity rank, beamforming that exploits only the strongest eigenmode of a channel would be an appropriate choice instead of multilayer transmission. Therefore, the manner in which multiple antennas are used has to be properly adapted to the general propagation conditions.

In Figure III.3, a stream of  $Q \times 1$  vector input symbols  $\underline{b}^{(k)}$ , where  $k$  is a time index, are fed into a space-time encoder, generating a stream of  $N_T \times 1$  complex vectors  $\underline{x}^{(k)}$ , where  $N_T$  represents the number of transmit antennas. Pulse shaping filters transform each element of the vector to create an  $N_T \times 1$  time-domain signal vector  $\underline{x}(t)$ , which is up-converted to a suitable transmission carrier. The resulting signal vector  $\underline{x}_A(t)$  drives the transmit transducer array, which in turn radiates energy into the propagation environment.

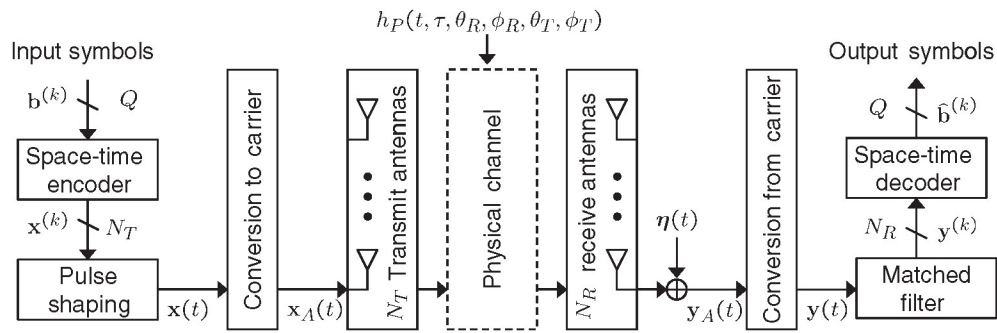


Figure III.3

The function  $h_P(t, \tau, \theta_R, \theta_T, \phi_R, \phi_T)$  represents the impulse response relating field radiated by the transmit array to the field incident on the receive array. The dependence on time suggests that this impulse response is time variant because of motion of scatterers within the propagation environment or motion of the transmitter and receiver. The variable  $\tau$  represents the time delay relative to the excitation time  $t$ . We assume a finite impulse response, so that  $h_P(t, \tau, \theta_R, \theta_T, \phi_R, \phi_T) = 0$  for  $\tau > \tau_0$ . We also assume that  $h_P(t, \tau, \theta_R, \theta_T, \phi_R, \phi_T)$  remains constant over a time interval  $t_0$  so that over a single transmission, the physical channel can be treated as a linear, time-invariant system.

The  $N_R$ -element receive array then generates the  $N_R \times 1$  signal vector  $\underline{y}_A(t)$  at the array terminals. Interference is generated in the physical propagation channel, while thermal noise is generated by the receiver front-end electronics. To simplify the discussion, we will lump all additive noise into a single contribution represented by the  $N_R \times 1$  vector  $\underline{\eta}(t)$  that is injected at the receive antenna terminals. The resulting signal plus noise vector  $\underline{y}_A(t)$  is then down-converted

III: Multiple-Input Multiple Output (MIMO) Systems

to produce the  $N_R \times 1$  baseband output vector  $\underline{y}(t)$ . Finally,  $\underline{y}(t)$  is passed through a matched filter whose output is sampled once per symbol to produce  $\underline{y}^{(k)}$ , after which the space-time decoder produces estimates  $\hat{\underline{b}}^{(k)}$  of the originally transmitted symbols.

III.2. The MIMO Channel

A common assumption will be that all scattering in the propagation channel is in the far field and that a discrete number of propagation paths connect the transmit and receive arrays. Under this assumption, the physical channel response for  $L$  paths may be written as:

$$h_P(t, \tau, \theta_R, \theta_T, \varphi_R, \varphi_T) = \sum_{l=1}^L A_l \delta(\tau - \tau_l) \delta(\theta_T - \theta_{T,l}) \times \delta(\varphi_T - \varphi_{T,l}) \delta(\theta_R - \theta_{R,l}) \delta(\varphi_R - \varphi_{R,l}) \tag{III.15}$$

where  $A_l$  is the gain of the  $l$ th path with angle of departure (AOD)  $(\theta_{T,l}, \varphi_{T,l})$ , angle of arrival (AOA)  $(\theta_{R,l}, \varphi_{R,l})$ , and time of arrival (TOA)  $\tau_l$ . The time variation of the channel is included by making the parameters of the multipaths  $(L, A_l, \tau_l, \theta_{T,l}, \dots)$  time dependent. To use this response to relate  $\underline{x}_A(t)$  to  $\underline{y}_A(t)$ , it is easier to proceed in the frequency domain. This results in

$$\tilde{\underline{y}}_A(\omega) = H_P(\omega) \tilde{\underline{x}}(\omega) + \tilde{\underline{\eta}}(\omega) \tag{III.16}$$

where  $H_P(\omega)$  is the channel transfer matrix or simply channel matrix. This representation uses the antenna properties in constructing the channel matrix, and therefore facilitates examination of a variety of antenna configurations for a single physical propagation channel. Also, because it is based on the physical channel impulse response, it is appropriate for wideband or frequency selective channels for which the elements of  $H_P(\omega)$  vary significantly over the bandwidth of interest.

While the physical channel model in (III.16) is useful for certain cases, in most signal processing analyses the channel is taken to relate the input to the pulse shaping block  $\underline{x}^{(k)}$  to the output of the matched filter  $\underline{y}^{(k)}$ . This model is typically used for cases where the frequency domain channel transfer function remains approximately constant over the bandwidth of the transmitted waveform, often referred to as the frequency nonselective or flat fading scenario. In this case, the frequency domain transfer functions can be treated as complex constants that simply scale the complex input symbols. We can therefore write the input/output relationship as:

$$\underline{y}^{(k)} = H^{(k)} \underline{x}^{(k)} + \underline{\eta}^{(k)} \tag{III.17}$$

where  $\underline{\eta}^{(k)}$  denotes the noise that has passed through the receiver and has been sampled at the matched-filter output. The term  $H^{(k)}$  represents the channel matrix for the  $k$ th transmitted symbol, with the superscript explicitly indicating that the channel can change over time.

### III.3. Channel Normalization

Consider the channel model in (III.17) where the noise  $\underline{\eta}^{(k)}$  is assumed to be a random vector with zero-mean complex normal entries and covariance  $\sigma_\eta^2 I$ , where  $I$  is the identity matrix. The average noise power in each receiver is therefore given by the variance  $\sigma_\eta^2$  of the complex random variables. The signal power averaged in time as well as over all receive ports is given as:

$$\begin{aligned} P_R &= \frac{1}{N_R} \mathbb{E} \left[ \underline{x}^{(k)H} H^{(k)H} H^{(k)} \underline{x}^{(k)} \right] \\ &= \frac{1}{N_R} \text{Tr} \left( \mathbb{E} \left[ \underline{x}^{(k)} \underline{x}^{(k)H} \right] \mathbb{E} \left[ H^{(k)H} H^{(k)} \right] \right) \end{aligned} \quad (\text{III.18})$$

We have used the statistical independence of the signal  $\underline{x}^{(k)}$  and channel matrix  $H^{(k)}$  to manipulate this expression. If the transmitter divides the total transmit power  $P_T$  equally across statistically independent streams on the multiple antennas, then

$$\mathbb{E} \left[ \underline{x}^{(k)} \underline{x}^{(k)H} \right] = \frac{P_T}{N_T} I \quad (\text{III.19})$$

If the expectation  $\mathbb{E} \left[ H^{(k)H} H^{(k)} \right]$  is approximated using a sample mean over a series  $1 \leq k \leq K$ , the average received signal power is

$$P_R = \frac{P_T}{N_T N_R} \frac{1}{K} \sum_{k=1}^K \|H^{(k)}\|_F^2 \quad (\text{III.20})$$

where  $\|\cdot\|_F$  is the Frobenius norm, given by:

$$\|A\|_F = \sqrt{\text{Tr}(A^H A)} \quad (\text{III.21})$$

The signal-to-noise ratio  $SNR$  averaged in time as well as over all receive ports is therefore

$$SNR = \frac{P_T}{\sigma_\eta^2} \underbrace{\frac{1}{N_T N_R} \frac{1}{K} \sum_{k=1}^K \|H^{(k)}\|_F^2}_\Upsilon \quad (\text{III.22})$$

We recognize that  $\Upsilon$  represents the average of the power gains between each pair of transmit and receive antennas. The resulting  $SNR$  is equivalent to what would be obtained if the power were transmitted between a single pair of antennas with a channel power gain  $\Upsilon$ . We therefore refer to (III.22) as the single-input single-output (SISO)  $SNR$ .

When performing simulations and analyses using channel matrices obtained from measurements or models, it is often useful to properly scale  $H^{(k)}$  to achieve a specified average  $SNR$ . We

**III: Multiple-Input Multiple Output (MIMO) Systems**

therefore define a new set of channel matrices  $H_0^{(k)} = \Psi H^{(k)}$ , where  $\Psi$  is a normalizing constant. To achieve a given average SNR,  $\Psi$  should be chosen according to

$$\Psi^2 = SNR \frac{\sigma_n^2}{P_T} \frac{N_T N_R K}{\sum_{k=1}^K \|H^{(k)}\|_F^2} \tag{III.23}$$

If  $K = 1$ , then this implies that each individual channel matrix is normalized to have the specified SNR. If  $K > 1$ , the average SNR over the group of  $K$  matrices will be as specified, although the SNR for each individual matrix will fluctuate about this mean value. This allows investigation of the relative variations in received signal strength over an ensemble of measurements or simulations.

**III.3.A. NOISE-LIMITED MIMO FADING CHANNELS**

A MIMO channel with  $T$  transmit antennas and  $R$  receive antennas can be modeled by:

$$\underline{y} = H\underline{x} + \underline{n} \tag{III.24}$$

where  $\underline{x} \in C^T$ ,  $\underline{y} \in C^R$ ,  $\underline{n} \in C^R$  and  $H \in C^{R \times T}$  with  $\{H\}_{i,j}$  being the complex channel coefficient between the  $j$ -th transmit antenna and the  $i$ -th receive antenna. The input vector has the power constraint

$$\text{Tr} \left( E \left[ \underline{x} \underline{x}^H \right] \right) \leq \Omega \tag{III.25}$$

The noise vector has a zero mean and a covariance matrix  $\sigma_n^2 I_R$ .

We usually consider MIMO channels that are subject to frequency-flat fading. Therefore,  $H$  is a random matrix that is often assumed to be complex Gaussian.

**III.3.B. MIMO CHANNELS WITH COCHANNEL INTERFERENCE**

In a MIMO channel with  $T$  antennas at the transmitter,  $R$  antennas at the receiver and  $L$  interfering users each equipped with  $T_i$  transmit antenna elements,  $i = 1, 2, \dots, L$ , the  $R \times 1$  vector at the desired user's receiver can be modeled as

$$\underline{y} = H_D \underline{x}_D + \sum_{i=1}^L \sqrt{\Omega_i} H_i \underline{x}_i + \underline{n} \tag{III.26}$$

where the  $R \times T$  matrix  $H_D$  and the  $T \times 1$  vector  $\underline{x}_D$  are, respectively, the normalized channel matrix and the transmitted data vector of the desired user.  $\Omega_i$  is the short-term average power of the  $i$ -th cochannel interferer. The  $R \times T_i$  matrix  $H_i$  and the  $T_i \times 1$  vector  $\underline{x}_i$  are, respectively, the normalized channel matrix and the normalized transmitted data vector of the  $i$ -th cochannel interferer. We further assume that all transmitted symbols are from complex Gaussian code books.

III: Multiple-Input Multiple Output (MIMO) Systems

The interference-plus-noise  $\sum_{i=1}^L \sqrt{\Omega_i} H_i \underline{x}_i + \underline{n}$ , conditioned on  $H_i$  is a complex Gaussian vector with zero mean and covariance matrix

$$B_I = \sum_{i=1}^L \Omega_i H_i K_i H_i^H + \sigma_n^2 I_R \quad (\text{III.27})$$

where

$$K_i = E \left[ \underline{x}_i \underline{x}_i^H \right] \quad (\text{III.28})$$

Given a total transmitting power constraint  $\Omega_D$ , we have

$$\text{Tr}(K_i) \leq \Omega_D \quad (\text{III.29})$$

Similar to the noise-limited case, we assume that fading is frequency-flat. We further assume that CCI users are subject to Rayleigh fading. The interfering channel matrices  $\{H_i\}$  are complex Gaussian matrices with zero mean and independent rows, but we allow the columns to be correlated (i.e., the receiver antennas are uncorrelated but the transmitter antennas are possibly correlated).

Let us assume that  $\{H_i\}$  are zero mean complex Gaussian matrices with i.i.d. rows, but the columns are possibly correlated with a  $T_i \times T_i$  covariance matrix  $A_i$  (semi-correlated Rayleigh faded interferers). Then  $H_i$  can be represented as  $H_i = Z_i A_i^{1/2}$ , where the  $R \times T_i$  matrix  $Z_i$  is complex Gaussian with i.i.d. entries that have zero means and unity variances. In this case, the term  $H_i K_i H_i^H$  in (III.27) can be written as  $Z_i \left( A_i^{1/2} K_i A_i^{1/2} \right) Z_i^H$ , that is, this interferer can be viewed to be subject to i.i.d. Rayleigh fading but with the “effective” signal covariance  $A_i^{1/2} K_i A_i^{1/2}$ . This means that the correlations among the transmitter antenna elements of each interferer do not change the problem if we properly adjust  $K_i$ . One exception to this argument is when interferers have perfect channel state information (CSI) at both the transmitter and the receiver and their signals are designed to exploit this CSI, for example, when interferers are transmitting on the basis of the water-filling principle with CSI at both transmitter and receiver. Therefore, it is sufficient to study the case when  $\{H_i\}$  are uncorrelated and each has i.i.d. complex Gaussian entries with zero mean and unity variance, even if interferers’ transmit antennas are correlated and/or interferers are correlated.

III.4. Frequency Selective MIMO Channel

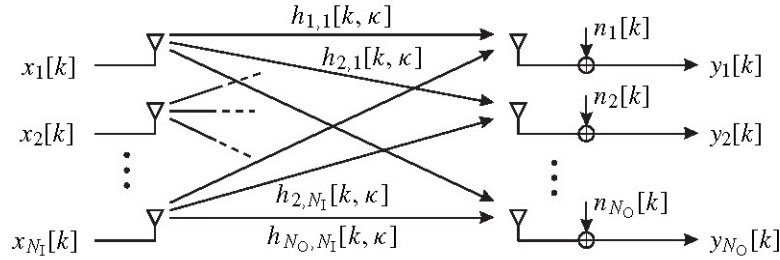


Figure III.4

The output of a frequency-selective SISO channel can be described by:

$$y(k) = \sum_{\kappa=0}^{L-1} h(k, \kappa)x(k - \kappa) + n(k) \quad (III.30)$$

As a consequence,  $N_I$  signals  $\{x_\mu(k)\}_{\mu=1}^{N_I}$  form the input of the system at each time instant  $k$  and we obtain  $N_O$  output signals  $\{y_\nu(k)\}_{\nu=1}^{N_O}$ . Each pair  $(\mu, \nu)$  of inputs and outputs is connected by a channel impulse response  $h_{\nu, \mu}(k, \kappa)$ . Therefore, the  $\nu$ -th output at time instant  $k$  can be expressed as:

$$y_\nu(k) = \sum_{\mu=1}^{N_I} \sum_{\kappa=0}^{L_t-1} h_{\nu, \mu}(k, \kappa)x_\mu(k - \kappa) + n_\nu(k) \quad (III.31)$$

where  $L_t$  denotes the largest number of taps among all the contributing channels. Exploiting vector notations by comprising all the output signals  $y_\nu(k)$  into a column vector  $\underline{y}(k)$  and all the input signals  $x_\mu(k)$  into a column vector  $\underline{x}(k)$ , (III.31) becomes

$$\underline{y}(k) = \sum_{\kappa=0}^{L_t-1} H(k, \kappa)\underline{x}(k - \kappa) + \underline{n}(k) \quad (III.32)$$

The channel matrix has the form

$$H(k, \kappa) = \begin{bmatrix} h_{1,1}(k, \kappa) & \cdots & h_{1,N_I}(k, \kappa) \\ \vdots & \ddots & \vdots \\ h_{N_O,1}(k, \kappa) & \cdots & h_{N_O,N_I}(k, \kappa) \end{bmatrix} \quad (III.33)$$

Finally, we can combine the  $L_t$  channel matrices  $H(k, \kappa)$  to obtain a single matrix

$$\underline{H}(k) = [H(k, 0) \quad \cdots \quad H(k, L_t - 1)] \quad (III.34)$$

With the new input vector

III: Multiple-Input Multiple Output (MIMO) Systems

$$\underline{x}_{L_t}(k) = \left[ \underline{x}^T(k) \quad \dots \quad \underline{x}^T(k - L_t + 1) \right]^T \quad (III.35)$$

we obtain

$$\underline{y}(k) = \underline{H}(k)\underline{x}_{L_t}(k) + \underline{n}(k) \quad (III.36)$$

In order to simplify notation, we restrict ourselves to frequency-nonselctive channels. Hence, the impulse response  $h_{\nu,\mu}(k,\kappa)$  reduces to  $h_{\nu,\mu}(k)$  and the channel matrix in (III.33) becomes  $H(k) = H(k, 0)$ . Figure III.5 illustrates the resulting structure of the communication system. The received signal can be described by:

$$\underline{y}(k) = H(k)\underline{x}(k) + \underline{n}(k) \quad (III.37)$$

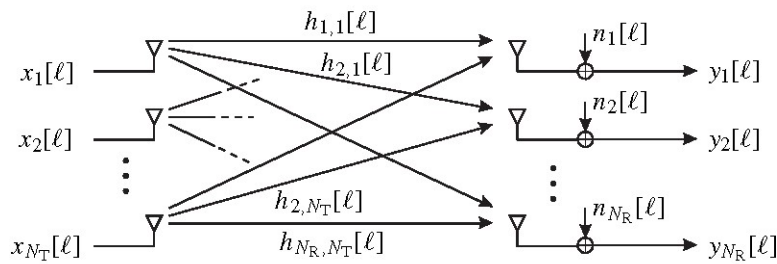


Figure III.5

**III.5. Spatial Diversity Concepts**

Only frequency-nonselctive channels are considered for notational as well as conceptual simplicity. Another reason is that spatial diversity concepts achieve the highest gains for channels that do not provide diversity in other dimensions such as frequency or time. Moreover, only Rayleigh fading channels without a line-of-sight component are considered. Since we know that correlations among the contributing channels reduce the diversity gain, we further assume that the channels are totally uncorrelated.

Uncorrelated channels can be achieved by an appropriate antenna spacing depending on the spatial channel characteristics, for example, the angle spread. Assuming a uniform linear array with equidistantly arranged antennas and an isotropic scattering environment where signals impinge from all directions with the same probability, a small distance  $d = \lambda/2$  between neighboring elements may be sufficient. The parameter  $\lambda$  denotes the wavelength. On the contrary,  $d \gg \lambda/2$  must hold in scenarios with small angle spread and  $d$  can take values up to  $10\lambda$ . This obviously requires a device large enough to host several antennas with appropriate distances.

**III.5.A. RECEIVE DIVERSITY**

The simplest method to achieve spatial diversity is to use multiple antennas at the receiver. The structure of the system is depicted in Figure III.6. It can be mathematically described with:

$$\underline{y}(l) = \underline{h}(l)x(l) + \underline{n}(l) \quad (III.38)$$

III: Multiple-Input Multiple Output (MIMO) Systems

where  $\underline{h}(l) = [h_1(l) \ \cdots \ h_{N_R}(l)]^T$  comprises all contributing channel coefficients.

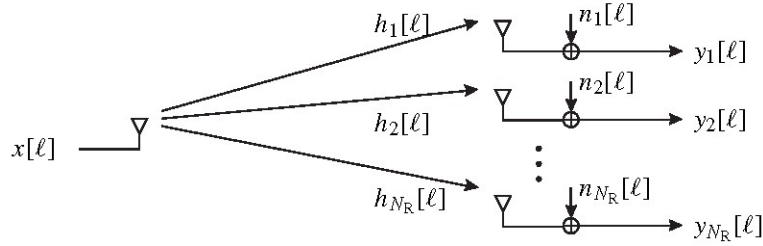


Figure III.6

Since there is no interference, a simple matched filter performing maximum ratio combining represents the optimum receiver and we obtain

$$\begin{aligned} r(l) &= \frac{\underline{h}^H(l)}{\|\underline{h}(l)\|^2} y(l) \\ &= x(l) + \tilde{n}(l) \end{aligned} \tag{III.39}$$

where  $\tilde{n}(l)$  denotes the noise at the matched filter output, and is given by:

$$\tilde{n}(l) = \frac{\underline{h}^H(l)}{\|\underline{h}(l)\|^2} \underline{n}(l) \tag{III.40}$$

From (III.39), we recognize that the full diversity degree  $D = N_R$  is achieved as long as the channel coefficients remain uncorrelated. Receive diversity is an efficient and simple possibility to increase the link reliability. However, its applicability becomes immediately limited if the size of the receiving terminal is very small. Cell phones for mobile radio communications have become smaller and smaller in recent years so that it is a difficult task to place several antennas on such small devices. Even if we succeed, it is questionable whether the spacing would be large enough to guarantee uncorrelated channels. Although different polarizations represent a further dimension to obtain diversity, the decoupling is generally imperfect, leading to cross talk. In this situation, the question arises whether diversity can also be exploited with multiple antennas at the transmitter.

**III.5.B. SPACE-TIME CODES**

In this subsection, the general concept of space-time transmit diversity is addressed, that is, using multiple antennas at the transmitter. A straightforward implementation where a signal  $x(l)$  is transmitted simultaneously over several antennas will not provide the desired diversity gain. Looking at the received signal

$$y(l) = \frac{1}{N_T} x(l) \sum_{v=1}^{N_T} h_v + n(l) \tag{III.41}$$

III: Multiple-Input Multiple Output (MIMO) Systems

we see that an incoherent superposition is obtained, resulting in a Rayleigh-distributed channel. Hence, the equivalent SISO channel still has SNR variations as large as the original single-input single-output system and no diversity has been gained.

To overcome this dilemma, appropriate coding is required at the transmitter. This coding is performed in the dimensions space and time leading to the name space–time codes. The general structure of the considered system is depicted in Figure III.7.

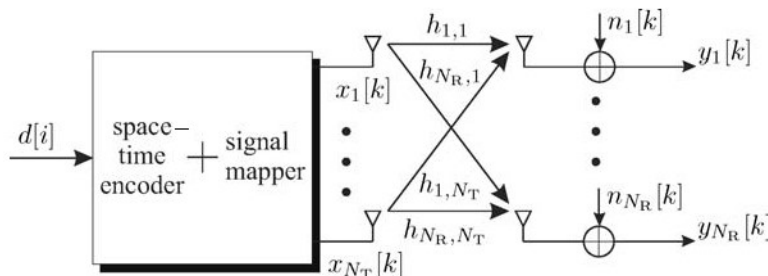


Figure III.7

The data bits  $d(i)$  are fed into the space–time encoder that outputs  $L$  vectors  $\underline{x}(0), \underline{x}(1), \dots, \underline{x}(L-1)$ , each of length  $N_T$ . We can write

$$\underline{x}(k) = [x_1(k) \quad x_2(k) \quad \dots \quad x_{N_T}(k)]^T \tag{III.42}$$

The signal vectors are transmitted over a MIMO channel according to (III.37). The channel coefficients  $h_{\mu,\nu}(k) = h_{\mu,\nu}$  are assumed to be constant during one encoded frame so that the received signal becomes

$$\underline{y}(k) = H\underline{x}(k) + \underline{n}(k) \tag{III.43}$$

Note that  $H(k)$  has been replaced by  $H$ . Combining all  $L$  vectors  $\underline{x}(k), \underline{y}(k)$ , and  $\underline{n}(k)$  within one coded frame as column vectors into the matrices  $X, Y$  and  $N$ , respectively, results in

$$Y = HX + N \tag{III.44}$$

where the  $N_T \times L$  matrix

$$X = [\underline{x}(0) \quad \underline{x}(1) \quad \dots \quad \underline{x}(L-1)] = \begin{bmatrix} x_1(0) & x_1(1) & \dots & x_1(L-1) \\ x_2(0) & x_2(1) & \dots & x_2(L-1) \\ \vdots & \vdots & \ddots & \vdots \\ x_{N_T}(0) & x_{N_T}(1) & \dots & x_{N_T}(L-1) \end{bmatrix} \tag{III.45}$$

denotes the entire data frame encoded in space and time. The code comprising all possible code matrices is termed  $\mathcal{X}$ . The matrices  $N$  and  $Y$  have the dimensions  $N_R \times L$ .

Next, we derive some general results concerning the achievable diversity and coding gains that can be used for the code design. An optimum maximum likelihood decision and a perfectly known

III: Multiple-Input Multiple Output (MIMO) Systems

channel matrix  $H$  are assumed at the receiver. We start with the pairwise error probability between two competing code words  $X$  and  $\tilde{X}$ . Note that we receive a mixture of all transmit signals at each receive antenna. Therefore, we have to look at the squared Frobenius norm of the noiseless received signals  $\|HX - H\tilde{X}\|_F^2$  of both code words. The conditional pairwise error probability is

$$\Pr\{X \rightarrow \tilde{X} | H\} = \frac{1}{2} \operatorname{erfc} \left( \sqrt{\frac{\|HX - H\tilde{X}\|_F^2}{4\sigma_N^2}} \right) \quad (\text{III.46})$$

We now normalize the space-time code words to  $B = X/\sqrt{E_s/T_s}$  and  $\tilde{B} = \tilde{X}/\sqrt{E_s/T_s}$ . This changes the squared Euclidean distance to

$$\|H(X - \tilde{X})\|_F^2 = \|H(B - \tilde{B})\|_F^2 \frac{E_s}{T_s} \quad (\text{III.47})$$

Now, (III.46) becomes with  $\sigma_N^2 = N_0/T_s$  for complex-valued signals

$$\Pr\{X \rightarrow \tilde{X} | H\} = \frac{1}{2} \operatorname{erfc} \left( \sqrt{\|H(B - \tilde{B})\|_F^2 \frac{E_s}{4N_0}} \right) \quad (\text{III.48})$$

The complementary error function can be upper bounded by  $\operatorname{erfc}(x) < e^{-x}$ . Denoting the  $\mu$ -th row of  $H$  with  $h_\mu$  leads to an upper bound

$$\begin{aligned} \Pr\{B \rightarrow \tilde{B} | H\} &\leq \frac{1}{2} \exp \left( -\|H(B - \tilde{B})\|_F^2 \frac{E_s}{4N_0} \right) \\ &\leq \frac{1}{2} \exp \left( -\sum_{\mu=1}^{N_R} \|h_\mu(B - \tilde{B})\|_F^2 \frac{E_s}{4N_0} \right) \\ &\leq \frac{1}{2} \prod_{\mu=1}^{N_R} \exp \left( -h_\mu(B - \tilde{B})(B - \tilde{B})^H h_\mu^H \frac{E_s}{4N_0} \right) \end{aligned} \quad (\text{III.49})$$

Obviously, the matrix  $A = (B - \tilde{B})(B - \tilde{B})^H$  is Hermitian and its rank  $r$  equals that of  $(B - \tilde{B})$ . Moreover, it is positive semidefinite and its  $r$  nonzero eigenvalues  $\lambda_\nu$ , obtained by an eigenvalue decomposition  $A = U\Lambda U^H$  are real and positive. The pairwise error probability can now be expressed as

III: Multiple-Input Multiple Output (MIMO) Systems

$$\begin{aligned} \Pr\{B \rightarrow \tilde{B} | H\} &\leq \frac{1}{2} \prod_{\mu=1}^{N_R} \exp\left(-\underline{h}_\mu U \Lambda U^H \underline{h}_\mu^H \frac{E_s}{4N_0}\right) \\ &\leq \frac{1}{2} \prod_{\mu=1}^{N_R} \exp\left(-\underline{\beta}_\mu \Lambda \underline{\beta}_\mu^H \frac{E_s}{4N_0}\right) \end{aligned} \quad (\text{III.50})$$

The new row vectors  $\underline{\beta}_\mu = \underline{h}_\mu U = [\beta_{\mu,1} \ \beta_{\mu,2} \ \cdots \ \beta_{\mu,N_T}]$  still consist of complex rotationally invariant Gaussian distributed random variables  $\beta_{\mu,\nu}$  because  $U$  is unitary. Hence, the squared magnitudes of their elements are chi-squared distributed with two degrees of freedom. In order to obtain a pairwise error probability that is independent of the instantaneous channel matrix  $H$ , we have to calculate the expectation of (III.50) with respect to  $H$ . This results in

$$\begin{aligned} \Pr\{B \rightarrow \tilde{B}\} &= E_H \left[ \Pr\{B \rightarrow \tilde{B} | H\} \right] \\ &\leq \frac{1}{2} \left( \prod_{\nu=1}^r \frac{1}{1 + \lambda_\nu E_s / 4N_0} \right)^{N_R} \end{aligned} \quad (\text{III.51})$$

A further upper bound that is tight for large SNRs is obtained by dropping the +1 in the denominator, leading to the expression

$$\Pr\{B \rightarrow \tilde{B}\} \leq \frac{1}{2} \left( \frac{E_s}{4N_0} \left( \prod_{\nu=1}^r \lambda_\nu \right)^{1/r} \right)^{-rN_R} \quad (\text{III.52})$$

The exponent  $rN_R$  is called the diversity gain. From (III.52), the following conclusions can be drawn. In order to achieve the maximum possible diversity degree, the minimum rank  $r$  among all pairwise differences  $B - \tilde{B}$  should be maximized, leading to the diversity gain

$$g_d = N_R \min_{(B, \tilde{B})} \left\{ \text{rank}(B - \tilde{B}) \right\} \quad (\text{III.53})$$

On the other hand, the coding gain leading to a horizontal shift of the error rate curves can be described by

$$g_c = \min_{(B, \tilde{B})} \left\{ \left( \prod_{\nu=1}^r \lambda_\nu \right)^{1/r} \right\} \quad (\text{III.54})$$

If the code design ensures full-rank differences with  $r = \text{rank}(A) = N_T$ , the product of the eigenvalues equals the determinant  $\det(A)$ , leading to

$$g_c = \min_{(B, \tilde{B})} \left\{ \left( \prod_{\nu=1}^{N_T} \lambda_\nu \right)^{1/N_T} \right\} = \min_{(B, \tilde{B})} \left\{ \left( \det(B - \tilde{B}) \right)^{1/N_T} \right\} \quad (\text{III.55})$$

III: Multiple-Input Multiple Output (MIMO) Systems

We obtain the code design criteria according to

- Rank Criterion: In order to obtain the maximum diversity gain, the first design goal is to maximize the minimum rank  $r$  of all matrices  $X - \tilde{X}$ . The diversity degree equals; its maximum is  $N_T N_R$ .
- Determinant Criterion: For a diversity gain of  $r N_R$ , the coding gain is maximized if the

$$\text{minimum of } \left( \prod_{v=1}^r \lambda_v \right)^{1/r} \text{ is maximized over all code word pairs.}$$

A code optimization according to these criteria cannot be performed analytically but has to be carried out as a computer-based code search. Orthogonal STBCs are presented next. Since their code words are obtained by orthogonal matrix design, the determinant is constant and no coding gain is obtained. However, full diversity gains are achievable and the receiver structures are very simple. Second, space-time trellis codes are briefly described, providing additional coding gains at the expense of much higher decoding complexity.

**III.5.C. ORTHOGONAL SPACE-TIME BLOCK CODES**

Figure III.8 shows the principle structure of a space-time block coding system for  $N_R = 1$  receive antenna. The subsequent derivation includes more generally the application of an arbitrary number of receive antennas. As a variation from the general concept of space-time coding depicted in Figure III.7, the signal mapper and space-time encoder are separated. First, the data bits are mapped onto symbols  $a(l)$  that are elements of a finite signal constellation. Next, the space-time block encoder collects a block of  $K$  successive symbols  $a(l)$  and maps them onto a sequence of  $L$  consecutive vectors  $\underline{x}(k) = [x_1(k) \ x_2(k) \ \dots \ x_{N_T}(k)]^T$  for  $k = 0, 1, \dots, L-1$ . Hence, the generated symbols  $a(l)$  are encoded in two dimensions, namely, in space and time explaining the name space-time coding. The code rate amounts to

$$R_c = \frac{K}{L} \tag{III.56}$$

The system can certainly be improved by an outer forward error correction (FEC) coding scheme. In the following part, we make the widely used assumption that the channel remains constant during one coding block. Therefore, we can drop the time indices of the channel coefficients (assuming  $h_\mu(k) = h_\mu$ ) in subsequent derivations.

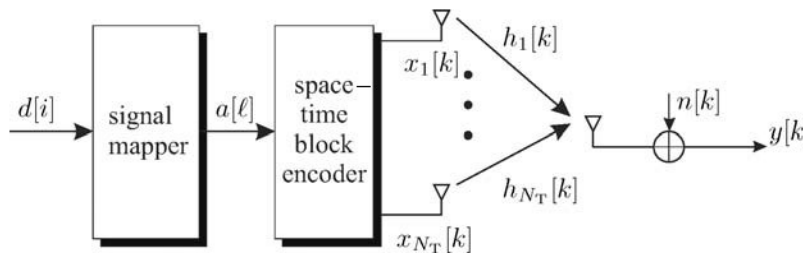


Figure III.8

III: Multiple-Input Multiple Output (MIMO) Systems

Alamouti Scheme

In order to illustrate how oSTBCs work, a simple example introduced by Alamouti (1998) is used. Originally, it employs  $N_T = 2$  transmit antennas and  $N_R = 1$  receive antenna. However, it can be easily extended to more receive antennas. To be precise, we have to consider blocks of  $K = 2$  consecutive symbols, say  $a_1 = a(2l)$  and  $a_2 = a(2l+1)$ . These two symbols are now encoded in the following way. At time instant  $2k = 2l$ , symbol  $x_1(2k) = a_1/\sqrt{2}$  is transmitted at the first antenna and  $x_2(2k) = a_2/\sqrt{2}$  at the second antenna. At the next time instant  $2k+1$ , the symbols are flipped and  $x_1(2k+1) = -a_2^*/\sqrt{2}$  as well as  $x_2(2k+1) = a_1^*/\sqrt{2}$  hold. The whole codeword arranged in space and time can be described using vector notations

$$\begin{aligned} X_2 &= [\underline{x}(2k) \quad \underline{x}(2k+1)] \\ &= \frac{1}{\sqrt{2}} \begin{bmatrix} a_1 & -a_2^* \\ a_2 & a_1^* \end{bmatrix} \end{aligned} \quad (III.57)$$

where the factor  $1/\sqrt{2}$  ensures that the total average transmit power per symbol equals  $E_s/T_s$ . The columns comprise the symbols transmitted at a certain time instant, while the rows represent the symbols transmitted over a certain antenna. Since  $K = 2$  symbols  $a_1$  and  $a_2$  are transmitted during  $L = 2$  time instants, the rate of this code is equal to 1. It is important to mention that the columns are orthogonal and so Alamouti scheme does not provide a coding gain.

The corresponding two received symbols can be expressed by

$$y(2k) = \frac{1}{\sqrt{2}}(h_1 a_1 + h_2 a_2) + n(2k) \quad (III.58)$$

$$y(2k+1) = \frac{1}{\sqrt{2}}(-h_1 a_2^* + h_2 a_1^*) + n(2k+1) \quad (III.59)$$

Using vector notations, we can combine the two received symbols and the two noise samples into vectors  $\underline{y} = [y(2k) \quad y(2k+1)]^T$  and  $\underline{n} = [n(2k) \quad n(2k+1)]^T$ , respectively. This yields the compact description

$$\begin{aligned} \underline{y} &= \begin{bmatrix} y_1 \\ y_2 \end{bmatrix} = \frac{1}{\sqrt{2}} \begin{bmatrix} a_1 & a_2 \\ -a_2^* & a_1^* \end{bmatrix} \begin{bmatrix} h_1 \\ h_2 \end{bmatrix} + \begin{bmatrix} n_1 \\ n_2 \end{bmatrix} \\ &= X_2 \underline{h} + \underline{n} \end{aligned} \quad (III.60)$$

Rewriting (III.60) by taking the conjugate complex of the second line, we obtain

$$\tilde{\underline{y}} = \begin{bmatrix} y_1 \\ y_2^* \end{bmatrix} = \frac{1}{\sqrt{2}} \begin{bmatrix} h_1 & h_2 \\ h_2^* & -h_1^* \end{bmatrix} \begin{bmatrix} a_1 \\ a_2 \end{bmatrix} + \begin{bmatrix} n_1 \\ n_2^* \end{bmatrix} = \frac{1}{\sqrt{2}} H(X_2) \underline{a} + \tilde{\underline{n}} \quad (III.61)$$

III: Multiple-Input Multiple Output (MIMO) Systems

With this slight modification, we have transformed the multiple-input single-output (MISO) channel  $\underline{h}$  into an equivalent MIMO channel  $H(X_2)$ . The matrix describing this equivalent channel has orthogonal columns. In this case, we already know that the matched filter represents the optimum detector according to the maximum likelihood principle. The matched filter output becomes

$$\begin{aligned} \tilde{\underline{r}} &= H^H(X_2)\tilde{\underline{y}} \\ &= \frac{1}{\sqrt{2}} \begin{bmatrix} |h_1|^2 + |h_2|^2 & 0 \\ 0 & |h_1|^2 + |h_2|^2 \end{bmatrix} \underline{a} + H^H(X_2)\tilde{\underline{n}} \end{aligned} \quad (III.62)$$

Looking at the diagonal elements that equal the squared norm of the contributing channel coefficients, we observe that the Alamouti scheme provides the full diversity degree  $D = N_T = 2$  that can be achieved with two transmit antennas. Moreover, no interference between  $a_1$  and  $a_2$  disturbs the transmission because  $H^H(X_2)H(X_2)$  is a diagonal matrix. Owing to this reason and the fact that the noise remains white when multiplied by a matrix consisting of orthogonal columns, the ML decision with respect to the vector  $\underline{a}$  can be split into element-wise decisions

$$\hat{a}_\mu = \arg \min_{\tilde{a}} \left\{ \left| \tilde{r}_\mu - (|h_1|^2 + |h_2|^2) \tilde{a} \right|^2 \right\} \quad (III.63)$$

Like all space-time coding schemes, the Alamouti scheme can be easily combined with multiple receive antennas. According to (III.61), we obtain a vector

$$\tilde{\underline{y}}_\mu = H_\mu(X_2)\underline{a} + \tilde{\underline{n}}_\mu \quad (III.64)$$

containing two successive symbols at each receive antenna  $\mu = 1, 2, \dots, N_R$ . They are now included in the vector

$$\tilde{\underline{y}} = \left[ \tilde{\underline{y}}_1^T \quad \tilde{\underline{y}}_2^T \quad \dots \quad \tilde{\underline{y}}_{N_R}^T \right]^T \quad (III.65)$$

Consequently, the equivalent channel matrix  $\underline{H}(X_2)$  also has to be extended. Following the notation in (III.61) it becomes

III: Multiple-Input Multiple Output (MIMO) Systems

$$\underline{H}(X_2) = \begin{bmatrix} H_1(X_2) \\ H_2(X_2) \\ \vdots \\ H_{N_R}(X_2) \end{bmatrix} = \begin{bmatrix} \boxed{h_{1,1}} & \boxed{h_{1,2}} \\ \boxed{h_{1,2}^*} & \boxed{-h_{1,1}^*} \\ \boxed{h_{2,1}} & \boxed{h_{2,1}} \\ \boxed{h_{2,2}^*} & \boxed{h_{2,2}^*} \\ \vdots & \vdots \\ \boxed{h_{N_R,1}} & \boxed{h_{N_R,1}} \\ \boxed{h_{N_R,2}^*} & \boxed{h_{N_R,2}^*} \end{bmatrix} \quad (\text{III.66})$$

The receiver now consists of a bank of matched filters, one for each receive antenna. Their outputs are simply summed, yielding

$$\begin{aligned} \tilde{\underline{r}} &= \underline{H}^H(X_2)\tilde{\underline{y}} \\ &= \frac{1}{\sqrt{2}} \sum_{\mu=1}^{N_R} \left( |h_{\mu,1}|^2 + |h_{\mu,2}|^2 \right) \underline{a} + \underline{H}^H(X_2)\tilde{\underline{n}} \end{aligned} \quad (\text{III.67})$$

As long as all channels remain uncorrelated, a maximum diversity degree of  $D = 2N_R$  can be achieved.

Extension to More than Two Transmit Antennas

Using some basic results from matrix theory, one can show that Alamouti's scheme is the only orthogonal space-time code with rate 1. For more than two transmit antennas, several orthogonal codes have been found with lower rates, so that spectral efficiency is lost. The code matrix  $X_{N_T}$  generally consists of  $N_T$  rows and  $L$  columns and contains the symbols  $a_1, \dots, a_K$  as well as the conjugate complex counterparts  $a_1^*, \dots, a_K^*$ . The construction of  $X_{N_T}$  has to be performed such that it has orthogonal rows, that is,

$$X_{N_T} X_{N_T}^H = P I_{N_T} \quad (\text{III.68})$$

where  $P$  is a constant depending on the symbol powers that will be discussed later. In the following part, all codeword matrices are presented without normalization.

Tarokh *et al.* have shown that there exist half-rate codes for an arbitrary number of transmit antennas. The code matrices for  $N_T = 3$  and  $N_T = 4$  are presented as examples. For  $N_T = 3$ , we obtain

$$X_3 = \begin{bmatrix} a_1 & -a_2 & -a_3 & -a_4 & a_1^* & -a_2^* & -a_3^* & -a_4^* \\ a_2 & a_1 & a_4 & -a_3 & a_2^* & a_1^* & a_4^* & -a_3^* \\ a_3 & -a_4 & a_1 & a_2 & a_3^* & -a_4^* & a_1^* & a_2^* \end{bmatrix} \quad (\text{III.69})$$

III: Multiple-Input Multiple Output (MIMO) Systems

This provides a diversity degree of  $D = N_T = 3$ . Obviously,  $X_3$  consists of  $L = 8$  columns and  $K = 4$  different symbols  $a_1, \dots, a_4$  are encoded, leading to the rate  $R_c = K/L = 1/2$ . Each symbol  $a_\mu$  occurs six times with full energy in  $X$ . From (III.69), we can write the received vector as

$$\underline{y} = \begin{bmatrix} h_1 & h_2 & h_3 & 0 & 0 & 0 & 0 & 0 \\ h_2 & -h_1 & 0 & -h_3 & 0 & 0 & 0 & 0 \\ h_3 & 0 & -h_1 & h_2 & 0 & 0 & 0 & 0 \\ 0 & h_3 & -h_2 & -h_1 & 0 & 0 & 0 & 0 \\ 0 & 0 & 0 & 0 & h_1 & h_2 & h_3 & 0 \\ 0 & 0 & 0 & 0 & h_2 & -h_1 & 0 & -h_3 \\ 0 & 0 & 0 & 0 & h_3 & 0 & -h_1 & h_2 \\ 0 & 0 & 0 & 0 & 0 & h_3 & -h_2 & -h_1 \end{bmatrix} \begin{bmatrix} a_1 \\ a_2 \\ a_3 \\ a_4 \\ a_1^* \\ a_2^* \\ a_3^* \\ a_4^* \end{bmatrix} + \underline{n} \quad (III.70)$$

We observe in (III.70) that the last four symbols in  $y$  only depend on the conjugate complex transmit symbols. Hence, conjugating the last four rows similar to the procedure for Alamouti's scheme results in

$$\begin{bmatrix} y_1 \\ y_2 \\ y_3 \\ y_4 \\ y_5^* \\ y_6^* \\ y_7^* \\ y_8^* \end{bmatrix} = \begin{bmatrix} h_1 & h_2 & h_3 & 0 \\ h_2 & -h_1 & 0 & -h_3 \\ h_3 & 0 & -h_1 & h_2 \\ 0 & h_3 & -h_2 & -h_1 \\ h_1^* & h_2^* & h_3^* & 0 \\ h_2^* & -h_1^* & 0 & -h_3^* \\ h_3^* & 0 & -h_1^* & h_2^* \\ 0 & h_3^* & -h_2^* & -h_1^* \end{bmatrix} \begin{bmatrix} a_1 \\ a_2 \\ a_3 \\ a_4 \end{bmatrix} + \begin{bmatrix} n_1 \\ n_2 \\ n_3 \\ n_4 \\ n_5^* \\ n_6^* \\ n_7^* \\ n_8^* \end{bmatrix} \quad (III.71)$$

$$\underline{\tilde{y}} = H[\mathbb{X}_3] \underline{a} + \underline{\tilde{n}} \quad (III.72)$$

Obviously, (III.71) uses only the original symbols  $\underline{a} = [a_1 \ a_2 \ a_3 \ a_4]^T$  and not their conjugate complex versions. Moreover, the columns in  $H[\mathbb{X}_3]$  are orthogonal so that

$$\begin{aligned} H^H[\mathbb{X}_3] H[\mathbb{X}_3] &= 2 \sum_{\mu=1}^{N_T} |h_\mu|^2 I_4 \\ &= 2(|h_1|^2 + |h_2|^2 + |h_3|^2) I_4 \end{aligned} \quad (III.73)$$

III: Multiple-Input Multiple Output (MIMO) Systems

Therefore, the optimum receiver is again a matched filter that multiplies the modified received vector  $\tilde{\underline{y}}$  with  $H^H[\mathbb{X}_3]$ . In the case of multi-amplitude modulation, an appropriate scaling prior to the hard decision is necessary.

For  $N_T = 4$ , a diversity gain of  $D = N_T = 4$  is achieved with the code matrix

$$X_4 = \begin{bmatrix} a_1 & -a_2 & -a_3 & -a_4 & a_1^* & -a_2^* & -a_3^* & -a_4^* \\ a_2 & a_1 & a_4 & -a_3 & a_2^* & a_1^* & a_4^* & -a_3^* \\ a_3 & -a_4 & a_1 & a_2 & a_3^* & -a_4^* & a_1^* & a_2^* \\ a_4 & a_3 & -a_2 & a_1 & a_4^* & a_3^* & -a_2^* & a_1^* \end{bmatrix} \quad (\text{III.74})$$

Equivalent to the case of  $N_T = 3$ , we obtain a received vector  $\underline{y}$  according to

$$\underline{y} = \begin{bmatrix} h_1 & h_2 & h_3 & h_4 & 0 & 0 & 0 & 0 \\ h_2 & -h_1 & h_4 & -h_3 & 0 & 0 & 0 & 0 \\ h_3 & -h_4 & -h_1 & h_2 & 0 & 0 & 0 & 0 \\ h_4 & h_3 & -h_2 & -h_1 & 0 & 0 & 0 & 0 \\ 0 & 0 & 0 & 0 & h_1 & h_2 & h_3 & h_4 \\ 0 & 0 & 0 & 0 & h_2 & -h_1 & h_4 & -h_3 \\ 0 & 0 & 0 & 0 & h_3 & -h_4 & -h_1 & h_2 \\ 0 & 0 & 0 & 0 & h_4 & h_3 & -h_2 & -h_1 \end{bmatrix} \begin{bmatrix} a_1 \\ a_2 \\ a_3 \\ a_4 \\ a_1^* \\ a_2^* \\ a_3^* \\ a_4^* \end{bmatrix} + \underline{n} \quad (\text{III.75})$$

Complex conjugation of the last four elements in  $\underline{y}$  leads to  $\tilde{\underline{y}} = H[\mathbb{X}_4]\underline{a} + \tilde{\underline{n}}$  with

$$H[\mathbb{X}_4] = \begin{bmatrix} h_1 & h_2 & h_3 & h_4 \\ h_2 & -h_1 & h_4 & -h_3 \\ h_3 & -h_4 & -h_1 & h_2 \\ h_4 & h_3 & -h_2 & -h_1 \\ h_1^* & h_2^* & h_3^* & h_4^* \\ h_2^* & -h_1^* & h_4^* & -h_3^* \\ h_3^* & -h_4^* & -h_1^* & h_2^* \\ h_4^* & h_3^* & -h_2^* & -h_1^* \end{bmatrix} \quad (\text{III.76})$$

Again, the columns of  $H[\mathbb{X}_4]$  are mutually orthogonal and estimates  $\hat{\underline{a}}$  are obtained by multiplying  $\tilde{\underline{y}}$  with  $H^H[\mathbb{X}_4]$  and appropriate scaling.

III: Multiple-Input Multiple Output (MIMO) Systems

Looking at higher spectral efficiencies, only two codes with  $N_T = 3$  and  $N_T = 4$  have been found for  $R_c > 1/2$ .

**III.6. Multilayer Transmission**

**III.6.A. CHANNEL KNOWLEDGE AT THE TRANSMITTER AND RECEIVER**

The diversity techniques discussed so far improve the link reliability, mainly by using multiple antennas at the transmitter and one or more receive antennas. On the contrary, we now try to enhance the data rate by transmitting parallel data streams termed layers over the antennas and, thus, perform spatial multiplexing. Hence, we remember the general MIMO concept with the channel output  $\underline{y} = H\underline{x} + \underline{n}$ .

First, we focus on the case where the transmitter and receiver both have perfect channel knowledge. Let the  $N_R \times N_T$  channel matrix have rank  $r$ . Let the columns of  $N_R \times N_R$  matrix  $U$  contain the eigenvectors of  $HH^H$ . Let the columns of  $N_T \times N_T$  matrix  $V$  contain the eigenvectors of  $H^H H$ . Let  $N_R \times N_T$  diagonal matrix  $\Sigma$  contain nonnegative, real-valued elements  $\sigma_k$  on its diagonal.

Matrix  $H$  can be decomposed in the form

$$H = U\Sigma V^H \tag{III.77}$$